Research Article

The Journal of Comparative Neurology
Research in Systems Neuroscience
DOI 10.1002/cne.24289

High diversity in neuropeptide immunoreactivity patterns among three closely related species of Dinophilidae (Annelida)

Alexandra Kerbl[1*], Markus Conzelmann[2], Gáspár Jékely[2] & Katrine Worsaae[1*]

[1]Marine Biology Section - Department of Biology, Faculty of Science, University of Copenhagen, 2100 Copenhagen, Denmark

[2]Max Planck Institute for Developmental Biology, 72076 Tübingen, Germany

Running head: NEUROPEPTIDE PATTERN OF DINOPHILID BRAINS

Name of editor to whom this manuscript is submitted: Dr. PAUL TAGHERT

Key words: Neuroanatomy, meiofauna, neurotransmitter, nervous system, regionalization, neuropeptide, interspecies variation, brain organization, RRID: AB_477585, RRID: AB_10603594, RRID: AB_477522, RRID: AB_572232

Corresponding authors:

Katrine Worsaae, Marine Biological Section, Department of Biology, University of Copenhagen, Universitetsparken 4, 2100 Copenhagen, Denmark. Email address: kworsaae@bio.ku.dk

Alexandra Kerbl, Marine Biological Section, Department of Biology, University of Copenhagen, Universitetsparken 4, 2100 Copenhagen, Denmark. Email address: alexandra.kerbl@bio.ku.dk

Received: Jan 10, 2017; Revised: Jun 23, 2017; Accepted: Jul 07, 2017

Grant information: This work was supported by the Villum Foundation (grant Nr. 1025442 to K. Worsaae).

Abstract

Neuropeptides are conserved metazoan signaling molecules, and represent useful markers for comparative investigations on the morphology and function of the nervous system. However, little is known about the variation of neuropeptide expression patterns across closely related species in invertebrate groups other than insects. In this study, we compare the immunoreactivity patterns of 14 neuropeptides in three closely related microscopic dinophilid annelids (*Dinophilus gyrociliatus*, *D. taeniatus* and *Trilobodrilus axi*).

The brains of all three species were found to consist of around 700 somata, surrounding a central neuropil with 3-5 ventral and 2-5 dorsal commissures. Neuropeptide immunoreactivity was detected in the brain, the ventral cords, stomatogastric nervous system, and additional nerves. Different neuropeptides are expressed in specific, non-overlapping cells in the brain in all three species. FMRFamide, MLD/pedal peptide, allatotropin, RNamide, excitatory peptide and FVRIamide showed a broad localization within the brain, while calcitonin, SIFamide, vasotocin, RGWamide, DLamide, FLamide, FVamide, MIP and serotonin were present in fewer cells in demarcated regions.

The different markers did not reveal ganglionic subdivisions or physical compartmentalization in any of these microscopic brains. The non-overlapping expression of different neuropeptides may indicate that the regionalization in these uniform, small brains is realized by individual cells, rather than cell clusters, representing an alternative to the lobular organization observed in several macroscopic annelids. Furthermore, despite the similar gross brain morphology, we found an unexpectedly high variation in the expression patterns of neuropeptides across species. This suggests that neuropeptide expression evolves faster than morphology, representing a possible mechanism for the evolutionary divergence of behaviors.

1. Background

Studies on the annelid brain and major nerves conducted by serial sectioning and TEM-studies go back several decades (Windoffer and Westheide, 1988a; b; Purschke, 1993; Orrhage and Müller, 2005). The advancements in immunocytochemistry in combination with CLSM facilitated new neural descriptions in a broad range of invertebrates and has proven especially well-suited for studies on microscopic representatives (e.g. meiofaunal taxa or temporary meiofauna such as embryos, larvae and juveniles of macroscopic species), where not only the nervous system but also its intricate relation to musculature and ciliated structures can be exposed (e.g., Hay-Schmidt, 1992; Müller and Sterrer, 2004; Wanninger et al., 2005; McDougall et al., 2006; Worsaae and Rouse, 2008; Nielsen and Worsaae, 2010; Worsaae and Rouse, 2010; Schwaha and Wanninger, 2012; Worsaae et al., 2012; Kerbl et al., 2015; Schmidt-Rhaesa et al., 2015; Bekkouche and Worsaae, 2016a; b; Worsaae et al., 2016; Kerbl et al., 2016a; Gasiorowski et al., 2017; Henne et al., 2017a; b). Yet, few studies have taken advantage of the small-sized meiofauna for studying the distribution of the numerous and proposedly highly conserved neuropeptides in adult nervous systems, using immunocytochemistry to identify putative morphological or functional regionalizations in their small and compact brain and nervous system.

Recent studies on invertebrates have shown that proneuropeptides (larger biologically inactive precursor proteins, which get cleaved and converted into neuropeptides) are conserved and orthologous peptides with only slight alternations, which can be identified across most protostomes (Jekely, 2013). Furthermore, the immunoreactivity patterns of several neuropeptides could be shown to be rather similar among spiralian larvae of e.g. annelids and molluscs (Conzelmann and Jekely, 2012), suggesting that patterns of a more comprehensive range of neuropeptides may inform on deep homologies and ancestral

functionalities in the nervous system (Conzelmann and Jekely, 2012). However, we lack detailed comparative analyses of a broader range of neuropeptide markers in closely related species to inform on homology vs. homoplasticity of specific expression patterns (Verleyen et al., 2004; Henne et al., 2017a; b). Complementary analyses of adult microscopic brains would be relevant due to their comparably low cell number, which makes the examination of the adult brain anatomy and neurotransmitter immunoreactivity among closely related species more comprehensible. Furthermore, the relevance of microscopic animals for spiralian phylogenies was recently emphasized, with these branching off as early lineages within Spiralia, Ecdysozoa and Bilateria (Andrade et al., 2015; Laumer et al., 2015; Struck et al., 2015; Cannon et al. 2016).

Many brains of macroscopic invertebrates (prime examples being cephalopods and insects, but also annelids such as *Nereis*) show structural compartmentalization in the form of lobes or ganglia (Young, 1971; Uyeno and Kier, 2005; Heuer and Loesel, 2007; Wollesen et al., 2009; Cardona et al., 2010; Lam et al., 2010; Heuer et al., 2010a; Aso et al., 2014). These subregions of the brain include cells with common function to either directly process sensory input or serve as higher organization/integration centers (Uyeno and Kier, 2005; Williamson and Chrachri, 2007). Many small annelids, however, have seemingly uniform brains without any obvious ganglionic substructure (Müller and Westheide, 2002; Worsaae and Rouse, 2008; Meyer and Seaver, 2009b; a; Kerbl et al., 2016a). This raises the question of whether (and how) these brains are regionalized and whether neurons are multifunctional and thereby less specific for individual neurotransmitters.

Within annelids, *Platynereis dumerilii* (Audouin & Milne-Edwards, 1834) and to some extend also *Capitella teleta* Blake, Grassle & Eckelbarger, 2009 have been established as

model animals, and their neurogenesis and detailed anatomy have been reconstructed (Meyer and Seaver, 2009a; Fischer et al., 2010; Meyer et al., 2015) as well as the neural circuits related to e.g., vision and feeding (Conzelmann et al., 2013b; Randel et al., 2015; Williams et al., 2015). These neural circuits are repeatedly shown to feature cells with specific neuropeptide profile (Wilgren et al., 1986; Pape et al., 2010; Conzelmann et al., 2013b; Randel et al., 2014; Schoofs and Beets, 2016), thereby indicating that these molecules and their interactions play a major role in orchestrating behavior (Argiolas, 1999; Kristan et al., 2005; Nylander and Roman, 2012; Giulianini and Edomi, 2016).

Neuropeptides have very specific effects on behavior, which may vary between species and is mostly studied in insects, crustaceans and nematodes, all members of the large group Ecdysozoa (Verleyen et al., 2004; Johnston et al., 2010; Suska et al., 2011; Bargmann, 2012; Giulianini and Edomi, 2016). Fewer members of the invertebrate sister group, Spiralia, are studied for the detailed functions of individual neuropeptides (Stent et al., 1979; Lloyd et al., 1984; Sweedler et al., 2002; Zhen and Samuel, 2015). Expression of neuropeptides such as the myoinhibitory protein (MIP) (e.g. Conzelmann et al., 2013b, Williams et al., 2015) seems to be limited to clearly defined regions in the nervous system of the tested Spiralians, whereby the inclusion of more specific neural markers for the characterization of nervous systems may complement the patterns observed with broadly expressed neurotransmitter markers such as FMRFamide (Diaz-Miranda et al., 1991; Orchard and Lange, 2013) or serotonin (Miron and Anctil, 1988; Barlow and Truman, 1992; Kerbl et al., 2015; Schwaha and Wanninger, 2015; Bekkouche and Worsaae, 2016a; Kerbl et al., 2016a).

The entirely meiofaunal family Dinophilidae (Annelida) contains 16 marine species inhabiting the interstitial environment of intertidal to sublittoral shores (Korschelt, 1887;

Jägersten, 1951; Westheide, 1967; Donworth, 1985). Dinophilidae comprises the genera *Dinophilus* and *Trilobodrilus*, with *Dinophilus* showing two morphotypes: one being *hyaline* and strongly dimorphic (e.g. *D. gyrociliatus* Schmidt, 1857 (Schmidt, 1858), and one being yellow-orange pigmented, monomorphic, and with a prolonged life cycle including an encystment stage (such as *D. taeniatus* Harmer, 1889 (Harmer, 1889)). *Trilobodrilus axi* Westheide, 1967, a representative of the other genus within Dinophilidae, is hyaline, but lacks the otherwise characteristic transverse ciliary bands on the trunk, does not have dwarf males, and does not have an encystment stage (Westheide, 1967; 1985). While previous studies based on morphology proposed all *Dinophilus*-species to form a sister group to members of the genus *Trilobodrilus* (Westheide, 2008), more recent molecular analyses proposed a closer relationship of monomorphic species of *Dinophilus* and *Trilobodrilus*, which are then sister group to the sexually dimorphic species of *Dinophilus* (Worsaae unpubl.). The nervous systems of all species, but especially of *D. gyrociliatus*, have been studied previously (Kotikova, 1973; Windoffer and Westheide, 1988a; Beniash et al., 1992; Müller and Westheide, 1997; 2002; Fofanova and Voronezhskaya, 2012; Fofanova et al., 2014). Furthermore, the recently created detailed atlas of neuromuscular development in two *Dinophilus*-species (Kerbl et al., 2016a) provides the foundation for a detailed comparative analysis of neurotransmitter patterns in this taxon. Dinophilidae therefore offer a comprehensive system to investigate i) conservation vs. variation of immunoreactivity patterns of specific neurotransmitters and ii) possible compartmentalization and/or functional regionalization of a superficially uniform brain.

Here we describe and compare the commissures and arrangement of neural somata in the brains of the three dinophilid species *D. gyrociliatus*, *D. taeniatus* and *T. axi*, which allows us to test for conservation of the neural gross anatomy. Onto the anatomical templates of brain

and central nervous system we furthermore map the immunoreactivity patterns of 15 neurotransmitters (using 13 non-commercial neuropeptide antibodies and the commonly used neural markers anti-FMRFamide and anti-serotonin) in order to compare their distribution and variation among three closely related species..

2. Materials and Methods

2.1. Specimens

Cultures of *Dinophilus gyrociliatus* are kept at the Marine Biology Section, University of Copenhagen, Denmark, in seawater with salinity 28 per mille at 18°C in the dark. Water was exchanged and the animals were fed with spinach and fish food (TetraMin flakes for Aquarium fish) once a month. Females were sampled and starved for two days prior to fixation. Due to the strongly altered morphology of the dwarf males, only females were used in this comparative study and only females are considered in the text when referring to *D. gyrociliatus*.

Adult specimens of *D. taeniatus* were collected in the area of Kaldbak, Faroe Islands, from filamentous algae on the sublittoral sandy beach. These animals were anesthetized and fixed directly after extracting them from the algae and sediment samples.

Adult *Trilobodrilus axi* were collected in the sandy intertidal beach in the region of Königshafen in List, Sylt, Germany, from extractions of clean sand. These animals were treated similar to *D. taeniatus* described above.

2.2. Scanning electron microscopy

Samples of all three species were fixed in trialdehyde and stored in 0.1M sodium cacodylate buffer, were postfixed in an aqueous 2% OsO_4-solution for 1h at room temperature (RT) and subsequently rinsed in demineralized water. Following dehydration via an ascending ethanol

series and transfer to acetone, samples were critical-point-dried (using an Autosamdri 815-machine at the Natural History Museum of Denmark, University of Copenhagen) and mounted on aluminum stubs. A high-resolution sputter coater (JFC-2300HR) applied an approximately 80-90 nm layer of platinum/palladium-mixture onto the samples prior to examination using a JEOL JSM-6335F field emission scanning electron microscope at the Natural History Museum of Denmark, University of Copenhagen.

2.3. Identification of neuropeptides in *Dinophilus gyrociliatus*

Proneuropeptides (pNPs) were first identified in the *D. gyrociliatus*-transcriptome (SRX2030658, Kerbl et al., (2016b)), by BLAST searches using a large curated set of metazoan pNP query sequences (Conzelmann et al., 2013a). The resulting sequences were examined for the presence of a signal peptide cleavage region (SP), for cleavage sites, conserved peptide motifs, and other hallmarks of bioactive peptides and their processing (e.g. amidation signature C-terminal Gly, pyroglutamination signature N-terminal Gln, Cys-containing stretches, mono- or dibasic cleavage sites). Subsequently, the transcriptomes of *D. taeniatus* (SRX1025580, Andrade et al. (2015)) and *T. axi* (SRR2014693, Struck et al. 2015)) were searched employing BLAST using the sequences of *P. dumerilii* and *D. gyrociliatus*.

This search identified more than 23 neuropeptides within the transcriptomes, with several neuropeptides not present in all tested dinophilid species (Table 1). Several absences of neuropeptides from the transcriptomes of *D. taeniatus* and *T. axi* nicely coincide with our results of absent immunoreactivity to the respective antibody (e.g. RGWamide-LIR and vasotocin-LIR). The presence of immunoreactivity patterns of neuropeptides absent from the transcriptome (such as allatotropin-LIR) however also indicates that the quality of these two latter transcriptomes might be too low for a comprehensive search of neuropeptide precursors.

2.4. Immunohistochemistry

2.4.1. Fixation and preparation of samples

Specimens were anesthetized with isotonic $MgCl_2$ prior to fixation with 3.7% paraformaldehyde in phosphate buffered saline (PBS) at room temperature (RT) for 1 hour, followed by several rinses with PBS and storage in PBS rinsing buffer + 0.05% NaN_3 at +4°C. Specimens fixed with a modified 3.7% paraformaldehyde/ 0,05% glutaraldehyde-mixture at RT for 1 hour (for blocking reactive aldehyde groups prior to staining with anti-MLD/pedal peptide antibody), and were additionally blocked with glycine-solution (2mg/ml in PBS) for 1 hour, followed by several rinses in PBS. Additional specimens were rinsed with 0.1% PTw (PBS + 0.1% Tween-20), transferred (via two rinses in deionized water) and stored in 100% methanol at -20°C. Both treatments lead to the same immunoreactivity (IR) patterns.

2.4.2. Antibody generation and specificity

The antibodies used in this study were provided by G. Jékely and M. Conzelmann, and the generation of the polyclonal antibodies against peptides of *Platynereis dumerilii* is described in Conzelmann and Jekely (2012), using immunization in rabbits and affinity-purification with Sulfo-Link resin (Thermo Scientific, Rockford, USA). More detailed information can be found in Table 2 and in Conzelmann and Jekely (2012).

The specificity of these antibodies against allatotropin, FVamide, and MIP was tested by morpholino gene knockdown in larvae of *P. dumerilii* (Shahidi et al., 2015; Williams et al., 2015), and the specificity of antibodies against calcitonin, DLamide, excitatory peptide, FLamide, FVamide, FVRIamide, MLD/pedal peptide, RGWamide, RNamide/sCAP, SIFamide and vasotocin was tested by whole mount in situ hybridization in larvae (Tables 1,

2, Jekely, 2008; Conzelmann et al., 2011; Asadulina et al., 2012; Conzelmann and Jekely, 2012; Shahidi et al., 2015; Williams et al., 2015,; Williams et al., 2017).

2.4.3. Antibody labeling

Quadruple labeling was applied to investigate characters in the nervous system and correlate its architecture to ciliation and/or musculature. These stainings included F-actin staining (Alexa Fluor 488-labeled phalloidin, A12379, INVITROGEN, Carlsbad, USA), DNA-staining (405nm fluorescent DAPI, included in Vectashield) and immunostaining against tubulin antibodies (monoclonal mouse anti-acetylated α-tubulin (T6793, SIGMA, St. Louis, USA, RRID:AB_477585) or polyclonal chicken anti acetylated α-tubulin (SAB3500023-100UG, SIGMA, RRID:AB_10603594)) in all species. The specific neurotransmitters tested in this study were labeled by polyclonal rabbit anti-FMRFamide (20091, IMMUNOSTAR, Hudson, USA, RRID:AB_572232), monoclonal rabbit anti-serotonin (5-HT, S5545, SIGMA, RRID:AB_477522) and polyclonal antibodies raised in rabbits against specific neuropeptides originally designed after *P. dumerilii* sequences (Conzelmann et al., 2013a). These were partly found in the transcriptomes of *D. gyrociliatus*, *D. taeniatus* and *T. axi* (Table 1). Antibodies against Synapsin I (3C11, DSHB, Iowa, USA) and Synapsin II (ADI-VAS-SV061-E, ENZO Life Sciences, Farmingdale, New York, USA) did not reveal any positive IR in *Dinophilus gyrociliatus* and were therefore not considered. Prior to adding the primary antibody-mix, the samples were preincubated in PTA (PBS with 0.1% Triton-X, 0.05% NaN3, 0.25% BSA, 10% sucrose) for 2 hours. Specimens were incubated for up to 24 hours at RT in the 1-2 primary antibodies diluted to 1 □g/ml. This incubation solution was removed by several rinses in PBS and PTA. Subsequently, specimens were incubated with the appropriate secondary antibodies conjugated with fluorophores (mixed 1:1, in a final concentration of 1:400, goat anti-mouse conjugated with CY5 (115-175-062, JACKSON

IMMUNO-RESEARCH, West Grove, USA), goat anti-chicken conjugated with Dylight 649 (103-495-1550, JACKSON IMMUNO RESEARCH) and goat anti-rabbit conjugated with TRITC (T5268, SIGMA)) for up to 48 hours at RT. This step was followed by incubation for 1 hour in Alexa Fluor 488-labeled phalloidin solution (0.17M phalloidin in PTA). Thereafter, specimens were rinsed in PBS and finally mounted in Vectashield (including DAPI, VECTOR LABORATORIES, Burlingame, USA). Specificity of primary antibody binding was tested by treating specimens only with secondary antibodies, but otherwise using the same protocol. The reproducibility of the results was checked by replicating the incubations.

2.4.4. Imaging

The prepared slides were examined using an OLYMPUS IX 8 inverted microscope in combination with a Fluoview FV-1000 confocal unit of K. Worsaae at the Marine Biology Section at the University of Copenhagen. Acquired z-stacks were either projected into 2-dimensional images or exported as stacks to the IMARIS 7.0 software package (BITPLANE SCIENTIFIC SOFTWARE, Zürich, Switzerland) to conduct further three-dimensional investigations and surface reconstructions.

At least three specimens of both *D. gyrociliatus* and *T. axi* and one to two specimens of *D. taeniatus* (depending on availability of material) have been analyzed in detail for each neuropeptide. Due to the sometimes weak labeling and strong background signal, respectively, some to all immunoreactive somata are highlighted by “irc” in Figures 7-21. These “irc” have been confirmed by simultaneous DAPI-labeling of nuclei in all cases.

2.5. Manual image registration and template creation

The steps described in the following were conducted for all three species investigated in this study, but are only described in detail for *D. gyrociliatus*. These examinations revealed little

or no variation in nerve cell number in the brains, which allowed for establishment of a brain template and subsequent mapping of specific neuropeptide-like immunoreacitvity onto this.

2.5.1. Establishing the overall morphology and conserved arrangement of the brain

The number of cells in the brains and their arrangement between several specimens had to be assessed to allow for the creation of a model based on the cellular arrangement in one animal. Therefore, the detailed confocal image stacks focusing on the head of *D. gyrociliatus* (including DAPI-labeling of the nuclei, one neuropeptide marker (the respective neurotransmitter) and one reference structure (musculature (phalloidin-labeling) and tubulin-like immunoreactive structures (acetylated αstubulin-labeling), exported as .oib-files from the Fluoview Viewer software version 4.2 (Olympus, Tokyo, Japan)) were imported into the software package IMARIS 7.0 equipped with the *Measurement Pro*-plugin (Bitplane Scientific Software, Zürich, Switzerland). The *Spot*-tool provided by this plugin was used to automatically detect the spherical and/or ellipsoid DAPI-signal after setting the region of interest (ROI, extending anteriorly, dorsally, ventrally and laterally to the epidermis of the animals and posteriorly to approximately the middle of the mouth opening), the respective channel (DAPI), and the minimal diameter of the round or oval structures to be recognized (1.0µm, after measurements of at least 20 nuclei in *Slice*-view (ranging between 1.25-3.2µm – the recognizing distance is set smaller to account for all cells in the brain) and possible double-labeling (one oval cell being recognized as two by the programme) had to be corrected by hand. These settings labeled all nuclei in the predefined region, including nuclei of nerve cells, epithelial cells, gland cells, etc. and created up to 2970 spots in their respective centres. These spots are formed as *Surface*-element in IMARIS and can therefore be activated and deactivated independent from the *Volume*-element (which is the 3D-representation of the entire stack). Two *Surface*-elements also can be merged, which was used for mapping

specific neuropeptidergic cells. All spots representing nuclei not directly associated with the brain had to be manually deleted. For this, the IMARIS *ObiqueSlicer*-tool was used to scroll through the entire stack section by section with all channels activated (and therefore all labeled structures visible) overlaying the surface with the created spots and deleting non-brain somata. The remaining nuclei were automatically counted by the *Statistics*-tool in IMARIS (with *Measurement Pro*-plugin). Thereby, a number of 639-720 cells remained, which are from now on referred to as somata. This procedure was repeated on ten confocal stacks from the prostomium of ten different specimens. The approximate number of nerve cells forming the brain is 650 (639-655), with only one in ten experiments differing remarkably by having 720 cells. Based on the little variation in these numbers as well as in the arrangement of the nuclei, we assumed the number and arrangement to be sufficiently conserved for using one as a representative for constructing a brain template. The immunoreactive channels showing nerve- and muscle staining are still present in the same file as this surface reconstructed brain template and later aid to the positioning of the immunoreactive somata in the template (see below).

2.5.2. Manually registering neuropeptidergic somata onto the template of brain nuclei

All neuropeptide patterns are based on quadruple labeling experiments, including the specific neuropeptide, DAPI (cell nuclei), acetylated alpha-tubulin (tubulinergic structures = ciliary structures and nerve bundles) and phalloidin (actin-filaments, musculature). All labeled structures are used to position the somata within the brain through their relative location to distinctive muscular bifurcations, crossings, emerging nerves, specific nerve fiber bundles, specific nuclear accumulations, etc. (see results-section). These structures were already identified in the previously generated brain nuclei map.

Once a nucleus of an immunoreactive cell was positively positioned in the template, the spot

representing this specific nucleus was marked (with a slightly bigger diameter of 1.5µm to facilitate differentiation from other brain nuclei), and a total model of this neuropeptide signal was created. This procedure was repeated for each neuropeptide in at least three specimens (except for *D. taeniatus*, where specimens were occasionally limited to 1-2), and the three models were compared and always found to be congruent. To test the accuracy of the assigned spots, each of these was initially enlarged to a 4µm sphere (about 2 cell-widths), which still could rarely be misidentified with other spots, and only showed limited overlap with other immunoreactive cells. The number of cells per respective neuropeptide immunoreactivity was both counted manually and by using the *Statistics*-tool in IMARIS.

2.6. Image preparation

Brightness, saturation and contrast adjustment was conducted in Adobe Photoshop CC 2016 (ADOBE Systems Inc., San Jose, USA) prior to assembling figure plates in Adobe Illustrator CC 2016, where the schematic drawings were also created. Magenta-green converted copies of all figures are available in the supplementary materials of this article.

For the 3D-templates of the three dinophilid brains showing the location of specific immunoreactivities of the neuropeptides, the individual patterns ("*Surface*") were exported as VRML-files from IMARIS and imported one after the other using the ADOBE 3D Toolkit, where each surface-file gets assigned to a specific material. After merging the individual patterns, the file was exported as U3D-file and imported into ADOBE Acrobat Pro DC (Version 2015), where the "*Rich Media*"-tool was used to import 3D-templates and export them as PDF-files. By using ADOBE Reader, the models can be activated by clicking on them, allowing for a 3-dimensional investigation of the datasets.

3. Results

3.1. Gross architecture of the nervous system in three dinophilid species

The nervous system in all three dinophilid species shows a similar organization into i) a central nervous system comprising a dorsoanterior brain (br, Figures 1-3, Tables 3, 4) connected through the circumesophageal connectives (cec) to a pentaneural ganglionated ventral cord (Figure 4), ii) a stomatogastric nervous system including nerve rings around esophagus and midgut-hindgut transition as well as intestinal nerve net and iii) additional peripheral nerves, e.g., longitudinal dorsal, dorsolateral and ventrolateral nerves as well as circumferential nerves emerging from the ventral cords (Figure 4, Table 3).

3.1.2. Brain (Figures 1-3)

The brain consists of a central neuropil with a dense neural plexus and multiple condensed fiber bundles (commissures) connecting the circumesophageal connectives (cec, Figures 1-3, Table 3). Ventrally, an anterior (acvr) and a posterior (pcvd) commissure of the ventral root of the circumesophageal connective are found in *Trilobodrilus axi* (Figure 1a6-8, c, e, Table 3). The two dinophilid species *Dinophilus gyrociliatus* and *D. taeniatus* also have a ventral commissure of the ventral root (vcvr, Figures 1a4-a6, c, e, 2a5, a6, c, e, Table 3). Dorsally, an anterior (acdr) and a posterior (pcdr) commissure of the dorsal root are present in *D. gyrociliatus* (Figure 1a5, a6, d, e, Table 3). An additional median (mcdr) commissure of the dorsal root is found in *D. taeniatus* (Figure 2a1-a3, d, e, Table 3), and a dorsal commissure (dcdr) is found in *T. axi*, Figure 3a1-a4, d, e, Table 3). Three major longitudinal nerve bundles extend from the anterior to the posterior dorsal commissures in all three species (apdr, Figures 1a1, a2, b1, c, 2a1, a2, c, 3a2, b3, c, Table 3) and subsequently give rise to the dorsal and dorso-lateral longitudinal nerve(s) (dln, dlln Figures 1a1, b3-b5, b6, c, e, 2a2, c, 5a1, a2, b5-b8, c, 3a, e, i). Dorsoventral bundles (dvb, Figures 1a3, b1, b2, 2a3, 5a4, a5, b2, not

included in the schematic drawings in Figures 1-3) extend from the anterior commissure of the ventral root dorsally to the anterior commissure of the dorsal root, where some fibers seem to fuse with the commissure, while some others extend posteriorly as part of the longitudinal nerve bundles. Nerves extending from the nuchal organs connect to the dorsal root of the circumesophageal connectives medioposterior to where the root branches into several condensed fiber bundles (nno, Figures 1a1, a3, c, e, 2a2, c, e, 3a1-a3, c, e). The ciliary bands of the prostomium (pcb) seem to be innervated by a series of nerve fibers rather than one confined nerve ring (npc, Figures 1a2, 2a2, 3a4, a5). Nerves extend from the prostomial compound cilia (pcc, Figures 1a6, 3a2) to the neuropil, where they seem to connect to the dorsal root of the circumesophageal connective in all three species (ncc, Figure 3a3). In general, the dorsal root shows more condensed (transverse and anterior-posterior) fiber bundles than the ventral root. Both the dorsal and the ventral root fuse at approximately the middle of the mouth opening and extend as one pair of circumesophageal connectives (cec, Figures 1a4-a6, b6, c, e, 2c, e, 3c, e, 4b, f, j), which join the ventral nerve cords.

The fibrous mass of the central neuropil (cnp, Figures 1-3) is surrounded by 600-750 (in *Dinophilus gyrociliatus*, Figure 5b), 650-750 (in *Trilobodrilus axi*, Figure 5f) and 700-900 somata (in *D. taeniatus*, Figure 5d), which in the former two are arranged in a dumbbell shape, but in *D. taeniatus* in a more antero-posteriorly compressed cell mass with lobe-like protrusions in the posterior region (Figures 4, 5). The somata are densely packed on the anterior, lateral, posterior and dorsal sides of the neuropil, but only scarcely covering its ventral side (Figures 4, 5).

3.1.2. Ventral nervous system

One pair of circumesophageal connectives extends into the paired ventrolateral nerve cords (vlnc) and the (later-on fused) paired ventromedian nerve cords (mvn, Figure 4). The latter branch off from the ventrolateral cords at the level of the anteriormost commissure and fuse to form one ventromedian nerve at the level of the second main commissure (mcom2, Figure 4a-c, e-g, i-k) in all three species. One (in *D.* taeniatus, Figure 4e, g, h, and *T. axi*, Figure 4i-l) or two (in *D. gyrociliatus*, Figure 4a-d) pairs of paramedian nerves (pmvn, Figure 4, Table 3) emerge from the ventrolateral nerve cords slightly more posterior and extend parallel to the ventromedian nerve. As far as we could determine, all ventral longitudinal nerve bundles join the terminal commissure (tcom, Figure 4a, e, i, j). The largest discrepancy in the nervous systems of the three investigated species is in the number and distribution of transverse nerve bundles (commissures): *D. gyrociliatus* displays the highest number with three (in the anterior four segments) and thereafter two commissures in an superficially irregular pattern only vaguely associated to individual segments (anterior commissure - acom, median commissure - mcom, posterior commissure - pcom, Figure 4a-d, Table 3). *D. taeniatus* exemplifies a more condensed pattern, with only one prominent transverse nerve bundle per segment (com, Figure 4e-h, Table 3). *T. axi* seems to exhibit a mixed pattern with one prominent commissure per segment, but an altering number of transverse nerve bundles anterior and posterior to it (acom, mcom, pcom, Figure 4i-l, Table 3).

3.1.3. Stomatogastric nerves

Nerves of the stomatogastric nervous system (stns, stnr - stomatogastric nerve ring around the pharynx) are not well represented by acetylated alpha-tubulin-like immunoreactivity (LIR, Figures 1a3-a5, b5, b6, e, 2e, 5b1-b3, e), but better visible with several neuropeptide markers (e.g. FVRIamide, RNamide/sCAP, vasotocin, DLamide, FLamide, FVamide, Excitatory peptide (EP), MLD/pedal peptide, Myoinhibitory peptide (MIP), FMRFamide, serotonin,

Figures 10-17, 19, 21) in one, two or all three dinophilid species. One dense ring of nerve fibers is formed around the esophagus (stnr, Figures 1a3-a5, b5, b6, e, 2e, 3a6-a8, b8, e, Tables 3, 4), another can be detected embracing the midgut-hindgut transition (mht, Figure 13d, Tables 3, 4). Only few neuropeptides can be detected by specific neuropeptide-LIR in the weak mesh of nerve fibers of the gut epithelium.

3.1.4. Additional nerves

Seven longitudinal nerves extend throughout the body as paired ventrolateral, lateral, dorsolateral and an unpaired dorsal longitudinal nerve (Figure 4a1, a5, b3, Table 3). They are remarkably thinner than the nerve bundles of the ventral nervous system (often only consisting of individual to few nerve fibers) and their origin could not be successfully traced in all cases. Especially the dorsal nerves, however, seem to emerge from the neuropil in the brain (Figures 1a1, b3-b6, c, e, 2a2, c, e, 3a1, a2, b5-b8, c, e, 4a, e, i). These longitudinal nerves are supplemented by three (in *D. taeniatus*), four (in *D. gyrociliatus*) or six (in *T. axi*) transverse nerves per segment (segments are inferred from external ciliary bands and commissural sets in the ventral nervous system), which emerge from the ventrolateral nerve cords and extending along the body circumference (Figure 4, Table 3).

3.2. Neuropeptide- and serotonin-immunoreactive patterns within the nervous systems and brains of three dinophilid species

To further characterize nervous system anatomy using cell-specific markers, we decided to also use neuropeptide antibodies. Several antibodies recognizing annelid neuropeptides have been developed for the nereid annelid *Platynereis dumerilii* (Conzelmann et al., 2011; Conzelmann and Jekely, 2012; Shahidi et al., 2015; Williams et al., 2015; Williams et al., 2017). To check the conservation of the *Platynereis* peptides in the three species we searched

in the available transcriptomes of *D. gyrociliatus* (SRX2030658, Kerbl et al., (2016b)), *D. taeniatus* (SRX1025580, Andrade et al. (2015)) and *T. axi* (SRR2014693, Struck et al. 2015)), where we identified homologs for several *Platynereis* proneuropeptides in at least one of the species (Table 1). We selected 14 neuropeptides for further studies, including the commercial antibody directed against FMRFamide, and the antibodies based on Platynereis-sequences against allatotropin (AT), calcitonin (CT), DLamide (DL), excitatory peptide (EP), FLamide (FL), FVamide (FV), FVRIamide (FVRI), myoinhibitory peptide (MIP), MLD/pedal peptide (MLD), RGWamide (RGW), RNamide/sCAP (sCAP), SIFamide (SIF), and vasotocin (VT) (Figure 6, Table 1).

Since the predicted mature peptides for the respective neuropeptide are similar between the species, and can be aligned to the sequences of *P. dumerilii* (Figure 6), we expect that also the antibodies will likely recognize these peptides in the three dinophilid species tested here. As discussed below, the quality of the transcriptomes used here might not have been sufficient to detect all neuropeptides, which is why we could detect immunoreactivity of some antibodies, though their underlying peptide sequence was not detected in the transcriptome of the respective species.

Since the antibodies used in this study have been designed based on sequences of *P. dumerilii* rather than on any of the investigated dinophilid species, the neurotransmitter-like immunoreacitivity is referred to as –LIR in the following.

All neurotransmitter-immunoreactivity patterns indicated that the labeled cells are uni- or bipolar, with very few (often weakly labeled) dendrites and unbranched, continuous axons with stable diameter (Figures 7-21).

3.2.1. Serotonin (Figure 7)

Serotonin is not a neuropeptide, but a monoamine neurotransmitter, which is commonly used in the description of nervous system architecture due to its presence in the major parts of the nervous system (e.g. nerve fibers and somata in the brain, ventral nervous system, peripheral and stomatogastric nerves, (Hay-Schmidt, 2000). Besides the data of the previously described acetylated a-tubulin staining serotonin is therefore used to describe the neural structures in the three dinophilid species.

Serotonin-LIR is well-represented in the three dinophilid species in this study, where it labels nerve fibers in the neuropil and all bundles of the ventral nervous system (ventrolateral longitudinal nerve cords, paramedian longitudinal nerves, medioventral longitudinal nerve and commissures), some longitudinal and transverse nerves and somata associated to mainly the brain and the commissures in the ventral nervous system (Figure 7, Table 4). The immunoreactivity pattern is similar among all tested Dinophilidae-species and in accordance with previous findings (Müller and Westheide, 2002; Kerbl et al., 2016a). Different to the other neuropeptides presented in this study, the number (three pairs) and the location (dorsoposterior of the neuropil) of somata seems to be conserved in Dinophilidae (Figures 5, 7a, c, e, g, i, k, Table 4). All somata are clearly demarcated cells, with low numbers of projections (Figure 7b, g, k). These cells project their axons into all parts of the neuropil, where the mostly uniform neurites form a dense network, which could not be further resolved. As demonstrated by previous developmental studies (Kerbl et al., 2016a), several axons extend through the pair of circumesophageal commissures from the ventral nerve cords into the neuropil, too. The labeled neurites in the paramedioventral nerves and the medioventral nerve most likely originate from few associated somata, which are present lateral to the anterior commissures of segments 1-3 (Figure 7b, d, h, l), and only scarcely spread along the

posterior ventral nervous system (Figure 7d, j).

3.2.2. Allatotropin (AT, Figure 8)

Allatotropin-like immunoreactive cells are present in all three species in the brain, the ventral nervous system and in additional nerves (irc, Figure 8, Table 4), yet no obvious similarity could be detected between the distribution of immunoreactive cells of the three species. The arrangement of somata in the brain differs between the cells being arranged posteriorly (*D. taeniatus*, Figures 5, 8e, g), anteroventrally (*D. gyrociliatus*, Figures 5, 8a-c) and both dorsoposteriorly and ventroanteriorly (*T. axi*, Figures 5, 8i, k). While none of these cells seems to have connections to either the sensory or locomotory cilia of the prostomium in any of the investigated species, their axons extend into the neuropil in a similar pattern to the one observed with serotonin-LIR. The distribution of neural elements in the ventral nervous system varies between *D. gyrociliatus* (two pairs of thin nerve fiber bundles in the ventrolateral nerve cords and one pair of fibers in the median nerve as well as additional somata in the middle of the segments between the commissures, maybe affecting ventrolateral longitudinal muscles of the body wall, Figure 8d, Table 4), *D. taeniatus* (nerve fibers only within the ventral longitudinal nerve cords, Figure 8f, Table 4), and *T. axi* (one thin fiber bundle in each ventrolateral nerve cord and one pair of somata lateral to the ventrolateral nerve cord in each segment, Figure 8l, Table 4). *D. taeniatus* also shows neural innervation with allatotropin-like immunoreactive cells in the male reproductive system (Figure 8f, h), suggesting a role in regulating sexual behavior. In *D. gyrociliatus*, elements of the stomatogastric nerve ring and additional nerves are also labeled (Table 4, data not shown).

3.2.3. Calcitonin (CT, Figure 9)

Calcitonin-LIR is detected in four medio- to ventroposterior somata in the brain in *D. gyrociliatus* (irc, in close proximity to prostomial dorsal glands and eyes, Figures 5, 9a, d, Table 4) and in two dorsoposterior somata dorsal in the brain in *D. taeniatus* (Figures 5, 9e, g, h, Table 4). Only few nerve fibers in the neuropil could be traced in the neuropil of *D. gyrociliatus* (Figure 9b, c), while the labeled fibres in the neuropil of *D. taeniatus* show strong calcitonin-LIR in especially the dorsal root (Figure 9f-h). Their further path or their final connection points could however not be traced. We therefore suggest the few posterior immunoreactive cells in the brain to be related to similar functions in the two *Dinophilus* species. Although the staining is very faint, three additional pairs of calcitonin-like immunoreactive somata are found in the stomatogastric nerve ring (stnr, Figure 9c, Table 4) in *D. gyrociliatus* and *D. taeniatus*. *T. axi* does not have any calcitonin-like immunoreactive elements.

3.2.4. DLamide (DL, Figure 10)

Despite the presence of DLamide precursor sequence in the transcriptome of *D. gyrociliatus* (Table 1), DLamide-LIR is only found in *D. taeniatus* and *T. axi* (Figures 5, 10, Table 4). While this neuropeptide seems to be present in the brain as well as in the ventral, peripheral and stomatogastric nervous system of *D. taeniatus* (Figures 5, 10, Table 4), only the brain and the stomatogastric nervous system in *T. axi* display this immunoreactivity (Figure 10e-h, Table 4). Immunoreactive somata are found adjacent to the base of the dorsal and ventral roots in both *D. taeniatus* and *T. axi*, and also close to the prostomial compound cilia in the latter (Figure 10a-c, e-h). Regardless of the overall dissimilarity of the immunoreactive cells in the brain, the posterior cells are located in similar positions with regards to major neural architectural landmarks (dorsal and ventral roots of the circumesophageal connectives) in the two species.

3.2.5. Excitatory peptide (EP, Figure 11)

Excitatory peptide (EP) shows a broad distribution with many immunoreactive somata in the brain, the ventral and the stomatogastric nervous system in the two *Dinophilus*-species (Figures 5, 11a-h, Table 4). Immunoreactivity patterns in the ventral nervous system are largely congruent between these two species with several fibers in the ventrolateral nerve cords, fewer fibers in the median and paramedian nerves and in the commissures (Figure 11b, d, f, h). These species also show a high amount of immunoreactive elements in the stomatogastric nerve ring around the pharynx (Figure 11c, f, g). The number of the EP-like immunoreactive cells in the brain in lowest in *T. axi* with only two posteromedian cells (Figures 5, 11i-l, Table 4), with the lateral, bipolar cells extending seemingly transmitting the information from sensory cells of the prostomial ciliary bands to the central region of the central neuropil (Figure 11l). *Dinophilus taeniatus* (Figures 5, 11e-g, Table 4) and *D. gyrociliatus* (Figures 5, 11a-c, Table 4) – regardless of the different number of cells –show a scattered distribution of immunoreactive cells throughout the entire brain, with a strong concentration of immunoreactive fibres in the entire neuropil. Several somata are in proximity to where the nerves from the nuchal organs connect to the neuropil and to the nerves extending towards the ciliary bands (data not shown). The scattered distribution pattern of the high number of labeled somata does not allow for functional assumptions between the investigated species.

3.2.6. FLamide (FL, Figure 12)

Dinophilus gyrociliatus has three pairs of somata ventroposteriorly in the brain (Figures 5, 12a, c, d). *Dinophilus taeniatus* has one pair of weakly labeled somata showing FLamide-LIR in the dorsoposterior region of the brain in the mediolateral lobes (Figures 5, 12e, g, h).

Trilobodrilus axi has two pairs of somata anteromedian and dorsolateral to the central neuropil (Figures 5, 12i-k). It is impossible to trace the neurites in all species due to the weak labeling of these structures. All species show posterolateral cells in the brain, which might indicate their involvement in similar functions, which have to be further investigated. While the immunoreactivity patterns are found only in the brains of *D. gyrociliatus* (Figures 5, 12a, c, d, Table 4) and *D. taeniatus* (Figures 5, 12e, h, Table 4), *T. axi* has an additional pair of FLamide-like immunoreactive somata lateral to the ventral nerve cords approximately in the middle of the body (Figures 5, 12i-l, Table 4).

3.2.7. FMRFamide (FMRF, Figure 13)

FMRFamide is the most broadly distributed neuropeptide in the entire nervous system, with up to 56 somata in the brain (Figures 5, 13a-c, e-k, Table 4), and was therefore also used in previous studies of the studied species (Müller and Westheide, 2002; Kerbl et al., 2016a). The majority of labeled somata are located dorsal to the central neuropil of the brain (Figures 5, 13a-c, e-i, k, Table 4), and project their neurites into the ventral nerve cords and the medioventral nerve (in *D. gyrociliatus* also the medial paramedian nerve (pmvn)) of the ventral nervous system through the circumesophageal connectives (Figure 13b, d, f, l, m, Table 4). Commissures are only weakly labeled (Figure 13b, d, f, l, m), and in contrast to serotonin-LIR, their origin are not easily traced due to their somata being dispositioned further along the ventrolateral nerve cord (Figure 13d, f, l). A nerve ring around the pharynx as well as one to two nerve rings around the midgut-hindgut-transition can be revealed in the stomatogastric nervous system (Table 4, data not shown).

3.2.8. FVamide (FV, Figure 14)

FVamide-like immunoreactive neurites are strictly associated with the commissures of the ventral root of the circumesophageal connectives in *T. axi* (brc, only weakly labeled, Figures 5, 14h-k, Table 4), and the associated, equally weakly labeled somata are also restricted to the ventral side. In both *D. gyrociliatus* and *D. taeniatus*, however, both immunoreactive somata and nerve fibres seem to be randomly distributed throughout the brain (Figures 5, 14a-g), with their detailed tracing obstructed by the weak labeling of the respective structures (in *D. gyrociliatus* and *T. axi*, Figure 14b-d, i-k) or the dense packing of immunoreactive elements (in *D. taeniatus*, Figure 14f, g). The number of immunoreactive somata associated with the brain complicates the identification of possibly similar patterns. The two *Dinophilus*-species also show FVamide-LIR in the stomatogastric nerve ring around the pharynx (Figures 5, 14b, f, g, Table 4), though only within a limited number of somata and fibers (Figure 14b, g).

3.2.9. FVRIamide (FVRI, Figure 15)

FVRIamide-LIR is detected in *D. gyrociliatus* and *T. axi* in a superficially similar pattern to FMRFamide-LIR in the brain, the ventral- as well as stomatogastric nervous system (Figure 15, Table 4), but additional, more peripheral nerves are only weakly labeled (Figure 15d, g, m, Table 4). Although the distribution pattern characterized by a higher density of somata in the brain on the dorsal side is similar to FMRFamide (compare to Figures 5, 13), the number of FVRIamide-like immunoreactive somata is remarkably lower in all three dinophilid species (Figures 5, 15a, e, l, Table 4) and does not seem to overlap with FMRFamide-like immunoreactive somata (Figure 5), yet their neurites can be found in the entire neuropil. The many immunoreactive cells in the brain complicate the assessment of possible similarities between the three species. Especially remarkable is the accumulation of immunoreactive cells at the midgut-hindgut transition of the digestive system (most obvious in *D. gyrociliatus* and *T. axi*, less distinct in *D. taeniatus*, Figure 15b, m), while the remaining part of the

stomatogastric nervous system (with the exception of the nerve bundle forming the stomatogastric nerve ring around the esophagus, stnr, Figure 15b, c, f) consists mainly of individual fibers forming an irregular net around pharynx, stomach and gut (Figure 15m).

3.2.10. Myoinhibitory peptide (MIP, Figure 16)

Myoinhibitory peptide (MIP)-LIR is present in all species investigated in this study, although only in small numbers of somata and weakly labeled fibers (Figures 5, 16, Table 4). While four somata exhibit immunoreactivity in the brain in *D. gyrociliatus* (Figures 5, 16a-d, Table 4), the same number of cells is only weakly visible in the other two species (Figure 16e, g, i-l). Labeled nerve fibers in the brain, stomatogastric and ventral nervous system are most prominently found in *D. taeniatus* (Figure 16g, h, Table 4), while *D. gyrociliatus* only has MIP-like immunoreactive elements in the brain and stomatogastric nervous system (Figure 16a-d, Table 4), and *T. axi* only has four somata and two nerve fibers labeled centrally in the neuropil (Figure 16i-l, Table 4). No similarity could be detected between the distribution patterns of immunoreactive cells of the three species.

3.2.11. MLD/pedal peptide (MLD, Figure 17)

MLD/pedal peptide-LIR is detected in *D. gyrociliatus* and *T. axi* (Figures 5, 17, Table 4), *Dinophilus taeniatus* does not show immunoreactive elements (Table 4). The distribution of the cells exhibiting MLD/pedal peptide-LIR in the brain is roughly similar in the two former species, although the immunoreactive somata are located more dorsal in *T. axi* (Figures 5, 17f-j) than in *D. gyrociliatus* (Figures 5, 17a-d). The somata are arranged in a semicircle in close proximity to the prostomial muscle fibres in both species and project fibers into the neuropil, which are weakly labeled, but seemingly present in both the dorsal and the ventral roots of the circumesophageal connectives (Figure 17b-d, h). Additionally, the ventral

nervous system shows individual, weakly labeled fibers in *D. gyrociliatus* (Table 4), and the median commissures are flanked by one pair of MLD/pedal peptide-like immunoreactive somata (data not shown).

3.2.12. RGWamide (RGW, Figure 18)

Four RGWamide-like immunoreactive somata are located anteriorly in the brain in *D. gyrociliatus* (Figure 5, 18, Table 4). Similar to MIP-LIR (see Figure 16a-d), these somata are located strictly dorsal in the brain, two of them being in close proximity to the prostomial compound cilia (Figure 18a, c). Due to the overall weak labeling of the neurons, only parts of the neurites extending into the dorsal commissure of the dorsal root of the circumesophageal connectives could be detected, and no other projections are traceable (Figure 16d). Neither *D. taeniatus* nor *T. axi* displays cells labeled with this antibody.

3.2.13. RNamide/sCAP (sCAP, Figure 19)

RNamide/small CardioActive Peptide (sCAP)-like immunoreactive elements are mainly found in the brains of the investigated species (Figures 5, 19a-c, e-k, Table 4). *Trilobodrilus axi* and *D. gyrociliatus* also show immunoreactivity in the stomatogastric and additional nerves (Figure 19d, Table 4), though only with few labeled fibers. In the brain, *D. gyrociliatus* (Figures 5, 19a-c) and *D. taeniatus* (Figures 5, 19e-g) demonstrate a similar, dorsal- to dorsoanterior distribution pattern, while RNamide-like immunoreactive somata in *T. axi* are more randomly distributed dorsally and ventrally (Figures 5, 19h-k). Again, the neurites extend into the neuropil, yet they could not be traced any further. The overall distribution patterns of immunoreactive cells in the brain is dissimilar between the three species, yet the anterior immunoreactive cells in *D. taeniatus* and *T. axi* indicate a probable conservation of these cells.

3.2.14. SIFamide (SIF, Figure 20)

SIFamide-LIR labels more somata in *D. taeniatus* than in *D. gyrociliatus* and *T. axi* (Figure 5, 20a, c-e, g-i, k-m, Table 4). The localization of the few immunoreactive somata in the brain differs in all three species, with one pair of anterodorsal cells in *D. gyrociliatus* (Figure 20a, c, d), two pairs of lateromedial and posteriomedial cells in *D. taeniatus* (Figure 20e, g, h), and one pair of ventroanterior cells in *T. axi* (Figure 20i, k-m). The latter, however, are in close proximity to the ciliated sensory organs (co, Figure 20k), but no neural projections could be detected in this region of the prostomium. We therefore assume that the distribution pattern of the posterior cells is similar between the investigated species. No immunoreactivity was detected in the ventral or stomatogastric nervous system or in additional nerves, though some epidermal glands in *T. axi* seemed to have retained the signal (Figure 20f).

3.2.15. Vasotocin (VT, Figure 21)

Vasotocin-LIR is only found in *D. gyrociliatus* and present in four somata approximately at the median level of the brain (Figures 5, 21, Table 4). One pair of immunoreactive somata is found in the posterior part of the brain close to an anterior branch of the dorsolateral prostomial longitudinal muscle bundle (Figure 21e). A second, slightly more dorsal pair is located in the anterior region close to the contralateral anterior branch of the dorsolateral longitudinal muscle bundle (prm, Figure 12e). The labeling was too weak to trace any neural projections.

4. Discussion

4.1. Numbers of transverse commissures differ, while gross nervous system architecture is conserved

Supplementing the information from previous studies (Beniash et al., 1992; Müller and Westheide, 2002; Fofanova et al., 2014), we found the overall organization of the neuropil in all three investigated species to be similar: The pair of circumesophageal connectives branch into a dorsal and a more prominent ventral root giving rise to several commissures (Figures 1-3, Table 3), which can be depicted in the otherwise unstructured neuropil. *Trilobodrilus axi* showed the highest number of commissures (Figure 3, Table 3), while *Dinophilus gyrociliatus* has the fewest (Figure 1, Table 3). Interestingly, *D. taeniatus* – which has the largest brain among the three species, and also differs in the arrangement of its somata (see below) – does not show a remarkably different layout of commissures (Figure 2, Table 3). Regardless of the differences in some of the bundles among the tested species, the overall architecture of at least one anterior and one posterior commissure branching off at each root indicates the conservation of these probably most essential elements. Variation in the number of commissures of the dorsal and ventral roots of the circumesophageal commissures as well as the location of the respective transverse nerve bundles has been previously shown to vary between groups (Müller and Westheide, 2002; Müller and Henning, 2004; Orrhage and Müller, 2005; Fischer et al., 2010; Helm et al., 2014; Meyer et al., 2015), yet it has not been shown to differ between closely related groups, such as established in this study.

The previously mentioned lobular appearance of the brain of *D. taeniatus* does not seem to be correlated with the formation of separated neuropil-compartments such as seen in the brains of macroscopic annelids such as *Nereis viridens* (Heuer and Loesel, 2007; Kulakova et al.,

2007), *Platynereis dumerilii* (Fischer et al., 2010; Heuer et al., 2010a) or *Capitella teleta* (Meyer and Seaver, 2009a). The different configuration of the brain in Dinophilidae might be a result of the size difference between the species, since *T. axi* and *D. gyrociliatus* are approximately similar in size and body shape, while *D. taeniatus* is at least three times larger, though not containing a proportionally higher amount of brain cells (700-900 cells as compared to 650-750 cells in *D. gyrociliatus* and 650-750 cells in *T. axi*, Figures 1-3, 5).

Similar to previous findings in dinophilids (Müller and Westheide, 2002; Fofanova et al., 2014; Kerbl et al., 2016a; b) and e.g. *C. teleta* (which also shows a uniform, yet macroscopic brain (Fröbius and Seaver, 2006; Meyer and Seaver, 2009a; b; Meyer et al., 2015), the seemingly homogeneous architecture of the brain does not negate the presence of clearly demarcated regions as indicated by expression patterns of different genes (Fröbius and Seaver, 2006; Meyer et al., 2015; Kerbl et al., 2016b), as well as the immunoreactive patterns of some neuropeptides, which could be shown in this study to be localized in specific regions of the brain (e.g. Figures 5, 9, 12, 16, 18, 20).

All dinophilid ventral nervous systems studied so far have a similar number of longitudinal elements (Figure 4, Table 3, Kotikova, 1973; Müller and Westheide, 2002; Fofanova and Voronezhskaya, 2012; Fofanova et al., 2014; Kerbl et al., 2016a), but differ vastly in the number and arrangement of transverse commissures (Figure 4, Table 3, Müller and Westheide, 2002; Kerbl et al., 2016a). Previous studies already pointed out the difference between the seemingly organized pattern in the ventral nervous system of adult *D. taeniatus* and also in some representatives of *Trilobodrilus* (Müller and Westheide, 2002; Kerbl et al., 2016a) as compared to the irregular distribution of numerous commissures in the ventral nervous system of *D. gyrociliatus* (Fofanova and Voronezhskaya, 2012; Fofanova et al.,

2014). The detailed analysis in this study indicates that one commissure is most prominent in each segment in all of the investigated species and additional transverse bundles (added during development) probably either remain individual, thinner nerve fiber bundles, or fuse with the main commissure. Developmental additions and probable fusions of these commissures have been shown by studying the development in *D. gyrociliatus* and *D. taeniatus* previously (Kerbl et al., 2016a), yet studies including embryonic and juvenile stages of *T. axi* are missing.

4.2. High quality of transcriptomes is vital when searching for proneuropeptide sequences

While a previous study used five antibodies against neuropeptide precursors and tested them on a broad range of animals without analyzing their transcriptomes (including cnidarians, annelids, molluscs, a bryozoan and crustaceans, (Conzelmann and Jekely, 2012), all neuropeptides tested here have been found in the transcriptome of mixed stages and sexes of *D. gyrociliatus* (Figure 6, Table 1), and nine and eight sequences could also be detected in the transcriptomes of *T. axi* (SRR2014693, Struck et al., 2015) and *D. taeniatus* (SRX1025580, Andrade et al., 2015), respectively (Table 1). However, several of the neuropeptides not found in the transcriptome also showed immunoreactivity in the nervous systems of one to all of the tested species. We therefore assume that the antibodies in these cases bind to similar neuropeptide sequences, which have not been identified in the transcriptome, yet potentially could be revealed in transcriptomes generated for the purpose of these searches rather than phylogenetic reconstructions. We however think, that the recently confirmed close relationship between the dinophilid species in this study (Worsaae, unpubl., Kajihara et al., 2015) allows us to suggest that the specific antibodies most likely label similar structures in the three species, regardless of whether they have been detected in the respective

transcriptomes by the here employed blast searches.

4.3. Plastic arrangement of neuropeptide somata in the three species

The here employed set of specific neuropeptides complement previous studies using the common neural markers FMRFamide and serotonin (the former being represented in numerous somata, the latter being limited to three pairs of somata in the posterior dorsal region of the brain (this study, Müller and Westheide, 2002; Fofanova et al., 2014; Kerbl et al., 2016a; b).

Hereby we established, that most of the tested neuropeptides show immunoreactivites in *D. gyrocililatus* (13/14) as compared to the lower numbers in *D. taeniatus* and *T. axi* (11/14), respectively (Table 4). Furthermore, there are approximately twice as many immunoreactive somata in the brain of *D. gyrociliatus* (210) than in *D. taeniatus* (98) and *T. axi* (101, Figure 2, Table 4), while the total number of brain somata does not differ remarkably (600-750 somata in *D. gyrociliatus*, 650-750 somata in *T. axi*, and 700-900 somata in *D. taeniatus*, respectively). The differences in specific neuropeptide patterns among the tested species is not only found in the brains, but also seen in the remaining portions of the nervous system (Figures 7-21, Table 4). This contrasts the seemingly conserved immunoreactivity in our three investigated species of e.g. serotonin, a monoamine neurotransmitter, which labels the same number of somata and proportion of nerve fibers in the nervous system. However, elements labeled by serotonin-LIR are mainly mototneurons and therefore not strongly involved in the neuromodulatory pathways between sensory cells and interneurons (Figure 7, Table 4, Müller and Westheide, 2002; Fofanova and Voronezhskaya, 2012; Kerbl et al., 2016a).

Given the previous statements of conservation of neuropeptidergic elements in the larval nervous system of distantly related species such as crustaceans, molluscs and annelids

(Conzelmann and Jekely, 2012), the finding of vast differences in arrangements between the adults of three closely related dinophilid species was unexpected (Figures 7-21, Table 4). Myoinhibitory peptide (MIP)-LIR for example was present only in the brain in *T. axi* and in the brain and the stomatogastric nervous system in *D. gyrociliatus*, while it also labeled portions of the ventral nervous system in *D. taeniatus* (Figure 16, Table 4). These differences were most apparent in the brain, where immunoreactive cells did not only differ in their number, but also in the localization of labeled somata. Again using MIP-LIR as an example, the four labeled somata in *T. axi* are strictly located mediodorsally in the posterior region of the brain, while the four somata in *D. taeniatus* are located more laterodorsal in the median and posterior region of the brain, and in *D. gyrociliatus* the somata are strictly lateral in the anterior- to medial region of the brain, in a slightly ventral location (Figures 6, 16, Table 4). These dramatic shifts in position indicate a change in connectivity/neural network and may even reflect a different outcome in functionality. It is possible that these changes correspond to a different employment of existing neural networks, which was already reported from established model systems such as *C. elegans*, crustaceans, *Drosophila* and the vertebrate retina (Bargmann, 2012; Bargmann and Marder, 2013). In that case these difference also indicate an unexpectedly dynamic evolution of the location of neuropeptide secretion among three closely related species. However, the present study and undifferentiated brains of the microscopic dinopjhilids did not allow for testing whether these differences reflect a reorganization of the somata themselves or of the peptides employed.

This reconstruction of immunoreactive somata arrangements still only provides an approximation of their position relative to the major neural commissures, but not relative to specific compartments of brain which is not existing in these microscopic worm (see below). The staining of these small and single cells generally did allow for detailed reconstruction of

the axons and dendrites of the somata, which would have helped to specify their connection to sensory structures or effector cells. Without these connection mapped it is not possible to finally test the functional homology of the specific immunoreactivity found in the somata. However, somata being the most prominent immunoreactive elements can assist in the primary characterization of the nervous system, and here provide provides insight into the neuropeptide landscape in previously neglected meiofaunal Spiralians, which is indicated to show more variation in the neuropeptide-distribution than in e.g. nematodes (Li and Kim, 2008; Henne et al., 2017a; b) .

4.4. Regionalization of microscopic brains may be accomplished by limiting functional areas to one or few cells rather than adding multifunctionality to cell clusters

Macroscopic brains have been shown across different animals groups to develop lobes or ganglia, in which clusters of cells have similar functions and often also similar cellular profiles (Heuer and Loesel, 2007; Farris, 2008; Loesel and Heuer, 2010; Richter et al., 2010; Heuer et al., 2010b; Conzelmann and Jekely, 2012; Helm et al., 2014; Farris, 2015). However, small and often uniform brains are found in some macroscopic annelids (e.g. *C. teleta,* (Meyer and Seaver, 2009a; b; Meyer et al., 2010; 2015) and in the majority of microscopic animals (such as *D. gyrociliatus,* but also the established model organism *C. elegans,* White et al., 1986; Varshney et al., 2011). Detecting regionalization in these brains and in case of the herein presented *D. gyrociliatus* – putatively reflecting different functionality of specific brain areas – is not easily accomplished based on e.g. immunohistochemistry and CLSM (Müller and Westheide, 2002; Fofanova et al., 2014; Kerbl et al., 2016a; b) or previous light microscopic studies (Nelson, 1904). However, a recent study on the molecular patterning of the compact *D. gyrociliatus* brain revealed clearly demarcated expression areas of a set of 11 genes commonly related to (early) neural patterning, which do suggest a functional

differentiation of the brain (Kerbl et al., 2016b). Although the distribution of immunoreactive cells of this study could not be correlated with the exact expression patterns of these genes, both studies lead us to suggest that - rather than undifferentiated cell groups achieving multifunctionality in the microscopic brains of dinophilids – specific functionality is limited to few or individual cells. This finer-scaled functional patterning of the brain is suggested based on present morphological investigations, but has to be tested functionally in future studies, using co-localization experiments with both immunohistochemistry and whole mount in situ hybridization using the present as well as a more extended set of neurotransmitters. Until then, we cannot ascertain whether the high degree of colocalization of neuropeptides in *C. elegans* (Li and Kim, 2008) will be also become obvious in dinophilid annelids, or whether the seemingly higher specificity of the neurons in dinophilids for the respective neurotransmitters is a result of evolution in the Spiralian lineage of invertebrates. This study thereby not only presents new findings on neurotransmitter distribution and variability, but also provides vital information on potential future research organisms for cellular profiling using ultrastructural and molecular analyses.

Conclusion

The brains of microscopic Dinophilidae, although lacking specialised morphological brain compartments or lobes, show several condensed nerve fiber bundles within the loose nerve fiber network constituting the central neuropil. While the longitudinal elements in the ventral nervous system are similar in the three dinophilids, the arrangement and number of transverse commissures linking these elements differs, as was also pointed out in previous studies (Müller and Westheide, 2002; Kerbl et al., 2016a). A suite of 14 neuropeptide markers tested on these brains did likewise not clearly demarcate compartments or larger regions, but did reveal an unexpected variation among the three dinophilids tested here. The highest

abundance in most neuropeptides as well as the highest number of different neuropeptides is found in *D. gyrociliatus*, while *D. taeniatus* and *T. axi* show only half the number of labeled cells, by similar number of nerve cells forming the brain. Based on findings in previous studies (Kerbl et al., 2016a), this could indicate that the neuropeptides have a broader distribution in juvenile and progenetic brains.

The disparate localization of cells with immunoreactivity to one of the 14 tested neuropeptides within each brain suggests that each cell is specific to a single neuropeptide and function rather than employing several at once. This finding may imply fascinating consequences to the question on how microscopic animals are able to cope with small, compact brains with low cell number suggesting that - rather than acquiring undifferentiated multifunctional brain cells, or loosing functionality - microscopic brains reduce the size of the functional regions within the brains by reducing the number of involved cells. Studies of meiofaunal species might therefore advance our understanding about how plastic the patterns in the nervous system are and subsequently reveal information about the evolution of nervous systems.

Declarations

Acknowledgements

The authors want to thank Áki Vang, Nicolas Bekkouche, Brett Gonzalez and Ludwik Gasiorowski for help with acquiring specimens of *Dinophilus taeniatus* from the Faroe Islands and *Trilobodrilus axi* from Sylt, Germany. We are grateful to Drs. Sonia Andrade and Thorsten Struck for providing access to the assembled transcriptomes of *Dinophius taeniatus* and *Trilobodrilus axi*, as well as to two anonymous reviewers for their comments on an earlier version of this manuscript.

Conflict of interests

The authors declare that they do not have a conflict of interest.

Author's contribution

AK prepared and fixed all specimens, conducted all staining experiments and set up the illustrations, tables and figure plates. GJ analyzed the transcriptome of *D. gyrociliatus* and – together with MC - provided the non-commercial antibodies designed against neuropeptides found in *Platynereis dumerilii*. AK and KW analyzed the acquired data, and drafted the manuscript. All authors corrected and approved the final version of the manuscript.

Data accessibility

The majority of datasets generated and analysed during the current study are included in this published article. Magenta-green converted copies of all figures are available in the supplementary materials of this article. Additional datasets are available from the corresponding authors on reasonable request.

References

Andrade SCS, Novo M, Kawauchi GY, Worsaae K, Pleijel F, Giribet G, Rouse GW. 2015. Articulating "Archiannelids": Phylogenomics and annelid relationships, with emphasis on meiofaunal taxa. Mol Biol Evol 32:2860–2875.

Argiolas A. 1999. Neuropeptides and sexual behaviour. Neurosci Biobehav Rev 23:1127–1142.

Asadulina A, Panzera A, Verasztó C, Liebig C, Jekely G. 2012. Whole-body gene expression pattern registration in *Platynereis* larvae. Evodevo 3:27.

Aso Y, Hattori D, Yu Y, Johnston RM, Iyer NA, Ngo T-TB, Dionne H, Abbott LF, Axel R, Tanimoto H, Rubin GM. 2014. The neuronal architecture of the mushroom body provides a logic for associative learning. Elife 3:e04577.

Bargmann CI, Marder E. 2013. From the connectome to brain function. Nature Methods

10:483–490.

Bargmann CI. 2012. Beyond the connectome: How neuromodulators shape neural circuits. Bioessays 34:458–465.

Barlow LA, Truman JW. 1992. Patterns of serotonin and sCP immunoreactivity during metamorphosis of the nervous system of the red abalone, *Haliotis rufescens*. Journal of Neurobiology 23:829–844.

Bekkouche N, Worsaae K. 2016a. Nervous system and ciliary structures of Micrognathozoa (Gnathifera): evolutionary insight from an early branch in Spiralia. Royal Society Open Science 3:160289.

Bekkouche N, Worsaae K. 2016b. Neuromuscular study of early branching *Diuronotus aspetos* (Paucitubulatina) yields insights into the evolution of organs systems in Gastrotricha. Zoological Lett 2:21.

Beniash EA, Yerlikova NN, Yevdonin LA. 1992. Some characteristics of the *Dinophilus vorticoides* anatomy of the nervous system. In: Bushinskaya GN, editor. Explorations of the Fauna of the Seas. Vol. Volume 43. St. Petersburg: Russian Academy of Sciences. p 5–9.

Cannon JT, Vellutini BC, Smith J, Ronquist F, Jondelius U, Hejnol A. 2016. Xenacoelomorpha is the sister group to Nephrozoa. Nature 530:89-93.

Cardona A, Saalfeld S, Preibisch S, Schmid B, Cheng A, Pulokas J, Tomancak P, Hartenstein V. 2010. An integrated micro- and macroarchitectural analysis of the *Drosophila* brain by computer-assisted serial section electron microscopy. PLoS Biol 8:e1000502.

Conzelmann M, Jekely G. 2012. Antibodies against conserved amidated neuropeptide epitopes enrich the comparative neurobiology toolbox. Evodevo 3:1–12.

Conzelmann M, Offenburger S-L, Asadulina A, Keller T, Münch TA, Jekely G. 2011. Neuropeptides regulate swimming depth of *Platynereis* larvae. Proc Natl Acad Sci USA 108:E1174–83.

Conzelmann M, Williams EA, Krug K, Franz-Wachtel M, Macek B, Jekely G. 2013a. The neuropeptide complement of the marine annelid *Platynereis dumerilii*. 14:1–15.

Conzelmann M, Williams EA, Tunaru S, Randel N, Shahidi R, Asadulina A, Berger J, Offermanns S, Jekely G. 2013b. Conserved MIP receptor–ligand pair regulates *Platynereis* larval settlement. PNAS 110:8224–8229.

Diaz-Miranda L, de Motta GE, García-Arrarás JE. 1991. Localization of neuropeptides in the nervous system of the marine annelid *Sabellastarte magnifica*. Cell Tiss Res 266:209–217.

Donworth PJ. 1985. A reappraisal and validation of the species *Dinophilus taeniatus* Harmer 1889 and of taxonomically significant features in monomorphic dinophilids (Annelida: Polychaeta). Zool Anz 216:32–38.

Farris SM. 2008. Structural, functional and developmental convergence of the insect

mushroom bodies with higher brain centers of vertebrates. Brain Behav Evol 72:1–15.

Farris SM. 2015. Evolution of brain elaboration. Philos Trans R Soc Biol 370:20150054–20150054.

Fischer AHL, Henrich T, Arendt D. 2010. The normal development of *Platynereis dumerilii* (Nereididae, Annelida). Front Zool 7.

Fofanova EG, Nezlin LP, Voronezhskaya EE. 2014. Ciliary and nervous structures in juvenile females of the annelid *Dinophilus gyrociliatus* (O. Schmidt, 1848) (Annelida: Polychaeta). Russ J Mar Biol 40:43–52.

Fofanova EG, Voronezhskaya EE. 2012. The structure of archiannelid *Dinophilus gyrociliatus* ventral nerve cords. Acta Biol Hung 63:88–90.

Fröbius AC, Seaver EC. 2006. *Capitella* sp. I *homeobrain-like*, the first lophotrochozoan member of a novel paired-like homeobox gene family. Gene Expr Patterns 6:985–991.

Gasiorowski L, Bekkouche N, Worsaae K. 2017. Morphology and evolution of the nervous system in Gnathostomulida (Gnathifera, Spiralia). Org Divers Evol doi:10.1007/s13127-017-0324-8.

Giulianini PG, Edomi P. 2016. Neuropeptides controlling reproduction and growth in Crustacea: A molecular approach. In: Satake H, editor. Invertebrate Neuropeptides and Hormones. Kerala, India: Transworld Reserach Network. p 225–252.

Harmer SF. 1889. Notes on the anatomy of *Dinophilus*. Proc Cambridge Philos Soc 6:119–143.

Hay-Schmidt A. 1992. Ultrastructure and immunocytochemistry of the nervous system of the larvae of *Lingula anatina* and *Glottidia* sp. (Brachiopoda). Zoomorphology 112:189–205.

Hay-Schmidt A. 2000. The evolution of the serotonergic nervous system. Proc R Soc B 267:1071–1079.

Helm C, Adamo H, Hourdez S, Bleidorn C. 2014. An immunocytochemical window into the development of Platynereis massiliensis (Annelida, Nereididae). Int J Dev Biol 58:613–622.

Henne S, Friedrich F, Hammel JU, Sombke A, Schmidt-Rhaesa A. 2017a. Reconstructing the anterior part of the nervous system of *Gordius aquaticus* (Nematomorpha, Cycloneuralia) by a multimethodological approach. J Morph 278:106–118.

Henne S, Sombke A, Schmidt-Rhaesa A. 2017b. Immunohistochemical analysis of the anterior nervous system of the free-living nematode *Plectus* spp. (Nematoda, Plectidae). Zoomorphology 136:175–190.

Heuer CM, Loesel R. 2007. Immunofluorescence analysis of the internal brain anatomy of *Nereis diversicolor* (Polychaeta, Annelida). Cell Tiss Res 331:713–724.

Heuer CM, Müller CH, Todt C, Loesel R. 2010a. Comparative neuroanatomy suggests

repeated reduction of neuroarchitectural complexity in Annelida. Front Zool 7:21.

Heuer CM, Müller CHG, Todt C, Loesel R. 2010b. Comparative neuroanatomy suggests repeated reduction of neuroarchitectural complexity in Annelida. Front Zool 7:1–21.

Jägersten G. 1951. Life cycle of *Dinophilus*, with special reference to the encystment and its dependence on temperature. Oikos 3:143–165.

Jekely G. 2013. Global view of the evolution and diversity of metazoan neuropeptide signaling. Proc Natl Acad Sci USA 110:8702–8707.

Johnston MJG, McVeigh P, McMaster S, Fleming CC, Maule AG. 2010. FMRFamide-like peptides in root knot nematodes and their potential role in nematode physiology. J Helminthol 84:253–265.

Kajihara H, Ikoma M, Yamasaki H, Hiruta SF. 2015. *Trilobodrilus itoi* sp. nov., with a re-description of *T. nipponicus* (Annelida: Dinophilidae) and a molecular phylogeny of the genus. Zool Sci 32:405–417.

Kerbl A, Bekkouche N, Sterrer W, Worsaae K. 2015. Detailed reconstruction of the nervous and muscular system of Lobatocerebridae with an evaluation of its annelid affinity. BMC Evol Biol 15:277.

Kerbl A, Fofanova EG, Mayorova TD, Voronezhskaya EE, Worsaae K. 2016a. Comparison of neuromuscular development in two dinophilid species (Annelida) suggests progenetic origin of *Dinophilus gyrociliatus*. Front Zool 13:49.

Kerbl A, Martin-Durán JM, Worsaae K, Hejnol A. 2016b. Molecular regionalization in the compact brain of the meiofaunal annelid *Dinophilus gyrociliatus* (Dinophilidae). Evodevo 7:20.

Korschelt E. 1887. Die Gattung *Dinophilus* und der bei ihr auftretende Geschlechtsdimorphismus. Zool Jahrb, Abt allg Zool Physiol Tiere 2:955–967.

Kotikova EA. 1973. New data concerning the nervous system of Archiannelida. Zool Jahrb, Abt allg Zool Physiol Tiere 52:1611–1615.

Kristan WB Jr., Calabrese RL, Friesen WO. 2005. Neuronal control of leech behavior. Progress in Neurobiology 76:279–327.

Kulakova M, Bakalenko N, Novikova E, Cook CE, Eliseeva E, Steinmetz PRH, Kostyuchenko RP, Dondua A, Arendt D, Akam M, Andreeva T. 2007. Hox gene expression in larval development of the polychaetes Nereis virens and *Platynereis dumerilii* (Annelida, Lophotrochozoa). Dev Genes Evol 217:39–54.

Lam SCB, Ruan Z, Zhao T, Long F, Jenett A, Simpson J, Myers EW, Peng H. 2010. Segmentation of center brains and optic lobes in 3D confocal images of adult fruit fly brains. Methods 50:63–69.

Laumer CE, Bekkouche N, Kerbl A, Goetz F, Neves RC, Sørensen MV, Kristensen RM, Hejnol A, Dunn CW, Giribet G, Worsaae K. 2015. Spiralian phylogeny informs the evolution of microscopic lineages. Curr Biol 25:2000–2006.

Li C, Kim K 2008. Neuropeptides (April 7, 2008). WormBook, ed. The *C. elegans* Research Community, WormBook, doi/10.1895/wormbook.1.142.1, http://www.wormbook.org.

Lloyd PE, Kupfermann I, Weiss KR. 1984. Evidence for Parallel Actions of a Molluscan Neuropeptide and Serotonin in Mediating Arousal in *Aplysia*. Proc Natl Acad Sci USA 81:2934–2937.

Loesel R, Heuer CM. 2010. The mushroom bodies – prominent brain centres of arthropods and annelids with enigmatic evolutionary origin. Acta Zool (Stockholm) 91:29–34.

McDougall C, Chen W-C, Shimeld SM, Ferrier DEK. 2006. The development of the larval nervous system, musculature and ciliary bands of *Pomatoceros lamarckii* (Annelida): heterochrony in polychaetes. Front Zool 3:16.

Meyer NP, Boyle MJ, Martindale MQ, Seaver EC. 2010. A comprehensive fate map by intracellular injection of identified blastomeres in the marine polychaete *Capitella teleta*. Evodevo 1:27.

Meyer NP, Carrillo-Baltodano A, Moore RE, Seaver EC. 2015. Nervous system development in lecithotrophic larval and juvenile stages of the annelid *Capitella teleta*. Front Zool:1–27.

Meyer NP, Seaver EC. 2009a. Neurogenesis in an annelid: Characterization of brain neural precursors in the polychaete *Capitella* sp. I. Dev Biol 335:237–252.

Meyer NP, Seaver EC. 2009b. Brain development in the annelid *Capitella* sp. I: Insights into nervous system evolution. Dev Biol 331:463–464.

Miron M-J, Anctil M. 1988. Serotoninlike immunoreactivity in the central and peripheral nervous system of the scale worm *Harmothoe imbricata* (Polychaeta). J Comp Neurol 275:429–440.

Müller MC, Henning L. 2004. Ground plan of the polychaete brain - I. Patterns of nerve development during regeneration in *Dorvillea bermudensis* (Dorvilleidae). J Comp Neurol 471:49–58.

Müller MCM, Sterrer W. 2004. Musculature and nervous system of *Gnathostomula peregrina* (Gnathostomulida) shown by phalloidin labeling, immunohistochemistry, and cLSM, and their phylogenetic significance. Zoomorphology 123:169–177.

Müller MCM, Westheide W. 1997. Das Nervensystem parapodienloser Polychaeten: Orthogonale Strukturen des Nervensystems juveniler Stadien und progenetischer Arten. Verhandlungen der Deutschen Zoologischen Gesellschaft 90:209.

Müller MCM, Westheide W. 2002. Comparative analysis of the nervous systems in presumptive progenetic dinophilid and dorvilleid polychaetes (Annelida) by immunohistochemistry and cLSM. Acta Zoologica 83:33–48.

Nelson JA. 1904. The early development of *Dinophilus*: A study in cell-lineage. Proc Acad Nat Sci Phil 56:687–737.

Nielsen C, Worsaae K. 2010. Structure and occurrence of cyphonautes larvae (bryozoa,

ectoprocta). J Morph 271:1094–1109.

Nylander I, Roman E. 2012. Neuropeptides as mediators of the early-life impact on the brain; implications for alcohol use disorders. Front Mol Neurosci 5:1–19.

Orchard I, Lange AB. 2013. FMRFamide-Like Peptides (FLPs). In: Handbook of Biologically Active Peptides. Elsevier. p 237–246.

Orrhage L, Müller MCM. 2005. Morphology of the nervous system of Polychaeta (Annelida). Hydrobiologia 535/536:79–111.

Pape H-C, Juengling K, Seidenbecher T, Lesting J, Reinscheid RK. 2010. Neuropeptide S: A transmitter system in the brain regulating fear and anxiety. Neuropharmacology 58:29–34.

Purschke G. 1993. Structure of the prostomial appendages and the central nervous system in the Protodrilida (Polychaeta). Zoomorphology 113:1–20.

Randel N, Asadulina A, Bezares-Calderón LA, Verasztó C, Williams EA, Conzelmann M, Shahidi R, Jekely G. 2014. Neuronal connectome of a sensory-motor circuit for visual navigation. Elife 3:868.

Randel N, Shahidi R, Verasztó C, Bezares-Calderón LA, Schmidt S, Jekely G. 2015. Inter-individual stereotypy of the *Platynereis* larval visual connectome. Elife 4:27.

Richter S, Loesel R, Purschke G, Schmidt-Rhaesa A, Scholtz G, Stach T, Vogt L, Wanninger A, Brenneis G, Döring C, Faller S, Fritsch M, Grobe P, Heuer CM, Kaul S, Møller OS, Müller CH, Rieger V, Rothe BH, Stegner ME, Harzsch S. 2010. Invertebrate neurophylogeny: suggested terms and definitions for a neuroanatomical glossary. Front Zool 7:49.

Rimskaya-Korsakova NN, Kristof A, Malakhov VV, Wanninger A. 2016. Neural architecture of *Galathowenia oculata* Zach, 1923 (Oweniidae, Annelida). Front Zool 13:5.

Schmidt O. 1858. Die rhabdocoelen Strudelwürmer aus der Umgebung von Krakau. Denkschriften der königlichen Akademie der Wissenschaften, mathematische naturwissenschaftliche Classe CLXV:20–46.

Schmidt-Rhaesa A, Harzsch S, Purschke G. 2015. Structure and Evolution of Invertebrate Nervous Systems. Oxford University Press.

Schoofs L, Beets I. 2016. Neuropeptides control life-phase transitions. Proc Natl Acad Sci USA:1–2.

Schwaha T, Wanninger A. 2012. Myoanatomy and serotonergic nervous system of plumatellid and fredericellid phylactolaemata (lophotrochozoa, ectoprocta). J Morph 273:57–67.

Schwaha TF, Wanninger A. 2015. The serotonin-lir nervous system of the Bryozoa (Lophotrochozoa): a general pattern in the Gymnolaemata and implications for lophophore evolution of the phylum. BMC Evol Biol 15.

Stent GS, Thompson WJ, Calabrese RL. 1979. Neural control of heartbeat in the leech and in some other invertebrates. Physiological Reviews 59:101–136.

Struck TH, Golombek A, Weigert A, Franke FA, Westheide W, Purschke G, Bleidorn C, Halanych KM. 2015. The evolution of annelids reveals two adaptive routes to the interstitial realm. Curr Bio 25:1993–1999.

Suska A, Miguel-Aliaga I, Thor S. 2011. Segment-specific generation of *Drosophila* Capability neuropeptide neurons by multi-faceted Hox cues. Dev Biol 353:72–80.

Sweedler JV, Li L, Rubakhin SS, Alexeeva V, Dembrow NC, Dowling O, Jing J, Weiss KR, Vilim FS. 2002. Identification and characterization of the feeding circuit-activating peptides, a novel neuropeptide family of *Aplysia*. J Neurosci 22:7797–7808.

Uyeno TA, Kier WM. 2005. Functional morphology of the cephalopod buccal mass: a novel joint type. J Morph 264:211–222.

Varshney LR, Chen BL, Paniagua E, Hall DH, Chklovskii DB. 2011. Structural properties of the *Caenorhabditis elegans* neuronal network. PLoS Comput Biol 7:e1001066–21.

Verleyen P, Huybrechts J, Baggerman G, Van Lommel A, De Loof A, Schoofs L. 2004. SIFamide is a highly conserved neuropeptide: a comparative study in different insect species. Biochemical and Biophysical Research Communications 320:334–341.

Wanninger A, Koop D, Bromham L, Noonan E, Degnan BM. 2005. Nervous and muscle system development in *Phascolion strombus* (Sipuncula). Dev Genes Evol 215:509–518.

Waterhouse AM, Procter JB, Martin DMA, Clamp M, Barton GJ. 2009. Jalview Version 2 - a multiple sequence alignment editor and analysis workbench. Bioinformatics 25(9): 1189-1191.

Westheide W. 1967. Die Gattung *Trilobodrilus* (Archiannelida, Polychaeta) von der deutschen Nordseeküste. Helgolander Meeresunters:207–215.

Westheide W. 1985. The systematic position of the Dinophilidae and the archiannelid problem. In: Conway Morris S, George JD, Gibson R, Platt HM, editors. The origins and relationships of lower invertebrates. Vol. Special volume 28. Oxford: Systematic Association. p 310–326.

Westheide W. 2008. Polychaetes: Interstitial Families. 2nd ed. (Crothers JH, editor.). London: The Linnean Society of London (Field Studies Council Shrewsbury).

White JG, Southgate E, Thomson JN, Brenner S. 1986. The structure of the nervous system of the nematode *Caenorhabditis elegans*. Philos Trans R Soc Biol 314:1–340.

Wilgren M, Reuter M, Gustafsson M. 1986. Neuropeptides in free-living and parasitic flatworms (Platyhelminthes). An immunocytochemical study. Hydrobiologia 132:93–99.

Williams EA, Conzelmann M, Jekely G. 2015. Myoinhibitory peptide regulates feeding in the marine annelid *Platynereis*. Front Zool 12:15.

Williams EA, Verasztó C, Jasek S, Conzelmann M, Shahidi R, Bauknecht P, Jekely G. 2017.

Synaptic and peptidergic connectome of a neurosecretory centre in the annelid brain. bioRxiv:115204.

Williamson R, Chrachri A. 2007. A model biological neural network: the cephalopod vestibular system. Philos Trans R Soc Biol 362:473–481.

Windoffer R, Westheide W. 1988a. The nervous system of the male *Dinophilus gyrociliatus* (Polychaeta, Dinophilidae): II. Electron microscopical reconstruction of nervous anatomy and effector cells. J Comp Neurol 272:475–488.

Windoffer R, Westheide W. 1988b. The nervous system of the male *Dinophilus gyrociliatus* (Annelida: Polychaeta). I. Number, types and distribution pattern of sensory cells. Acta Zool (Stockholm) 69:55–64.

Wollesen T, Loesel R, Wanninger A. 2009. Pygmy squids and giant brains: mapping the complex cephalopod CNS by phalloidin staining of vibratome sections and whole-mount preparations. Journal of Neuroscience Methods 179:63–67.

Worsaae K, Rimskaya-Korsakova NN, Rouse GW. 2016. Neural reconstruction of bone-eating *Osedax* spp. (Annelida) and evolution of the siboglinid nervous system. BMC Evol Biol 16:83–23.

Worsaae K, Rouse GW. 2008. Is *Diurodrilus* an annelid? J Morph 269:1426–1455.

Worsaae K, Rouse GW. 2010. The simplicity of males: dwarf males of four species of *Osedax* (Siboglinidae; Annelida) investigated by confocal laser scanning microscopy. J Morph 271:127–142.

Worsaae K, Sterrer W, Kaul-Strehlow S, Hay-Schmidt A, Giribet G. 2012. An anatomical description of a miniaturized acorn worm (Hemichordata, Enteropneusta) with asexual reproduction by paratomy. PLoS ONE 7.

Young JZ. 1971. The anatomy of the nervous system of *Octopus vulgaris*. Oxford University Press.

Zhen M, Samuel AD. 2015. *C. elegans* locomotion: small circuits, complex functions. Current Opinion in Neurobiology 33:117–126.

FIGURES

Figure 1. The neuropil of female *Dinophilus gyrociliatus*.

The neuropil is visualized by acetylated α-tubulin-LIR (a, b), which was used to obtain the data for the reconstruction of the neuropil (c-e). a1-a6) sections through the brain in dorso-ventral direction (a1 being the dorsalmost, a6 the ventralmost section, anterior end of the

animal directed upwards, scale bar is 10µm), b1-b6) cross-section through the brain in antero-posterior direction (b1 being the anteriormost, b6 the posteriormost section, dorsal side of the animal directed upwards, scale bar is 10µm), c-e) reconstruction of the neuropil in *D. gyrociliatus* females, focussing on the dorsal root (c, omitting the ventral root), the ventral root (d, omitting the dorsal root) and the entire brain (e). A magenta-green converted copy of this figure is provided as supplementary material to this article. Abbreviations: acdr – anterior commissure of the dorsal root of the circumesophageal connective, acvr – anterior commissure of the ventral root of the circumesophageal connective, apdr – anterior-posterior nerve bundle of the dorsal root of the circumesophageal connective, br – brain, cec – circumesophageal connective, cnp – central neuropil, dcdr – dorsal commissure of the dorsal root of the circumesophageal connective, dfg – ducts of the frontal gland, dlln – dorsolateral longitudinal nerve, dln – dorsal longitudinal nerve, drcc – dorsal root of the circumesophageal connective, dvb – dorsoventral nerve bundle, mcvr – median commissure of the ventral root of the circumesophageal connective, mo – mouth opening, nno – nerves between the nuchal organs and the central neuropil, no – nuchal organ, npc – nerves between cells of the prostomial ciliary bands and the central neuropil, pbdr – posterior bundle of the dorsal root of the circumesophageal connective, pcb1, 2 – prostomial ciliary band 1, 2, pcc – prostomial compound cilia, pcdr – posterior commissure of the dorsal root of the circumesophageal connective, pcvr – posterior commissure of the ventral root of the circumesophageal connective, stnr – stomatogastric nerve ring, vcvr – ventral commissure of the ventral root of the circumesophageal connective, vrcc – ventral root of the circumesophageal connective.

Figure 2. The neuropil of *Dinophilus taeniatus*.

The neuropil is visualized by acetylated α-tubulin-LIR (a, b), which was used to obtain the data for the reconstruction of the neuropil (c-e). a1-a6) sections through the brain in dorso-ventral direction (a1 being the dorsalmost, a6 the ventralmost section, anterior end of the animal directed upwards, scale bar is 10µm), b1-b6) cross-section through the brain in antero-posterior direction (b1 being the anteriormost, b6 the posteriormost section, dorsal side of the animal directed upwards, scale bar is 10µm), c-e) reconstruction of the neuropil in *D. taeniatus*, with focus on the dorsal root (c, omitting the ventral root), the ventral root (d, omitting the dorsal root) and the entire brain (e). Additional condensed bundles, which have not been detected in *D. gyrociliatus* are highlighted in orange, green and blue. A magenta-green converted copy of this figure is provided as supplementary material to this article. Abbreviations: acdr – anterior commissure of the dorsal root of the circumesophageal connective, acvr – anterior commissure of the ventral root of the circumesophageal connective, apdr – anterior-posterior nerve bundle of the dorsal root of the circumesophageal connective, br – brain, cec – circumesophageal connective, cnp – central neuropil, dlln – dorsolateral longitudinal nerve, dln – dorsal longitudinal nerve, drcc – dorsal root of the circumesophageal connective, dvb – dorsoventral nerve bundle, lnp – lacuna in the central neuropil, mcdr – median commissure of the dorsal root of the circumesophageal connective, mcvr – median commissure of the ventral root of the circumesophageal connective, mo – mouth opening, nno – nerves between the nuchal organs and the central neuropil, no – nuchal organ, npc – nerves between cells of the prostomial ciliary bands and the central neuropil, pcb1 – prostomial ciliary band 1, pcdr – posterior commissure of the dorsal root of the circumesophageal connective, pcvr – posterior commissure of the ventral root of the circumesophageal connective, stnr – stomatogastric nerve ring, vcvr – ventral commissure of the ventral root of the circumesophageal connective, vrcc – ventral root of the circumesophageal connective.

Figure 3. The neuropil of *Trilobodrilus axi*.

The neuropil is visualized by acetylated α-tubulin-LIR (a, b), which was used to obtain the data for the reconstruction of the neuropil (c-e). a1-a8) sections through the brain in dorso-ventral direction (a1 being the dorsalmost, a8 the ventralmost section, anterior end of the animal directed upwards, scale bar is 10µm), b1-b8) cross-section through the brain in antero-posterior direction (b1 being the anteriormost, b8 the posteriormost section, dorsal side of the animal directed upwards, scale bar is 10µm), c-e) reconstruction of the neuropil in *T. axi* with focus on the dorsal root (c, omitting the ventral root), the ventral root (d, omitting the dorsal root) and the entire brain (e). Additional condensed bundles, which have not been detected in *D. gyrociliatus* are highlighted in yellow, orange, red green and blue, in accordance with the neuropil reconstruction in *D. taeniatus*. A magenta-green converted copy of this figure is provided as supplementary material to this article. Abbreviations: acdr – anterior commissure of the dorsal root of the circumesophageal connective, acvr – anterior commissure of the ventral root of the circumesophageal connective, apdr – anterior-posterior nerve bundle of the dorsal root of the circumesophageal connective, br – brain, cec – circumesophageal connective, co – ciliated organ = eye, cnp – central neuropil, dcdr – dorsal commissure of the dorsal root of the circumesophageal connective, dlln – dorsolateral longitudinal nerve, dln – dorsal longitudinal nerve, drcc – dorsal root of the circumesophageal connective, dvb – dorsoventral nerve bundle, lln – lateral longitudinal nerve, lnp – lacuna in the central neuropil, mcdr – median commissure of the dorsal root of the circumesophageal connective, mcvr – median commissure of the ventral root of the circumesophageal connective, mo – mouth opening, ncc – nerves of the prostomial compound cilia, nno – nerves between the nuchal organs and the central neuropil, no – nuchal organ, npc – nerves between cells of the prostomial ciliary bands and the central neuropil,

pcb1, 2 – prostomial ciliary band 1, 2, pcc – prostomial compound cilia, pcdr – posterior commissure of the dorsal root of the circumesophageal connective, pcvr – posterior commissure of the ventral root of the circumesophageal connective, stnr – stomatogastric nerve ring, vcf – ventral ciliary field, vcvr – ventral commissure of the ventral root of the circumesophageal connective, vlln – ventrolateral longitudinal nerve, vrcc – ventral root of the circumesophageal connective.

Figure 4. The nervous system in three dinophilids (with focus on the ventral nervous system).

The nervous system is visualized by acetylated α-tubulin-LIR (b-d, f-h, j-l), which was used to obtain the data for the reconstruction of the nervous system (focussing on the ventral nervous system, a, e, i). a, e, i) reconstruction of the nervous system in *Dinophilus gyrociliatus*, *D. taeniatus* and *Trilobodrilus axi*. The animals are shown from the ventral side. b) ventral nervous system of a female *D. gyrociliatus*, with focus on the anterior region with condensed first commissural sets (c) and on a segment in the middle region of the body with anterior, median and posterior commissure (d), f) ventral nervous system of *D. taeniatus*, with focus on the anterior region (g) and on a segment in the middle region of the body with one thick commissure (h), j) ventral nervous system of *T. axi*, with focus on the anterior region with condensed commissural sets (k) and on a segment in the middle region of the body with one prominent and additional thin commissures (l). A magenta-green converted copy of this figure is provided as supplementary material to this article. Abbreviations: acom – anterior commissures, ans – angled segmental nerve, br – brain, cb – ciliary band, cec – circumesophageal connective, com – commissure, dlln – dorsolateral longitudinal nerve, dln – dorsal longitudinal nerve, drcc – dorsal root of the circumesophageal connective, lln – lateral longitudinal nerve, mcom – median commissure, mvn – medioventral nerve, nacb –

nerve anterior to the ciliary band, ncb – nerve of the ciliary band, nis – intersegmental nerve, no – nuchal organ, npcb – nerve posterior to the ciliary band, ns – segmental nerve, pcb – prostomial ciliary band, pcc – prostomial compound cilia, pcom – posterior commissure, pmvn – paramedian nerve(s), tcom – terminal commissure, vlln – ventrolateral longitudinal nerve, vlnc – ventrolateral nerve cord, vrcc – ventral root of the circumesophageal connective.

Figure 5. Overview pictures of the three dinophilid species (*Dinophilus gyrociliatus, D. taeniatus* and *Trilobodrilus axi*) including the interactive 3D-brain templates with mapped neurotransmitters.

The entire specimens are shown as scanning electron microscopic images (a in dorsolateral view, c in ventrolateral view, e in dorsal view) with the anterior end up next to the respective brain templates (b, d, f), which are all initially displayed in dorsal view. The interactive 3D-templates can be activated in conventional Adobe Acrobat Reader by clicking on the pictures next to the SEM-images for a more detailed analysis of the individual patterns. The nerve cells are based on the DAPI-labeling of one adult specimen (representing the respective species) and each manually mapped immunoreactive cell is based on three (in *D. gyrociliatus* and *T. axi*) or one to two (in *D. taeniatus*) specimens. Spheres indicate the designated nucleus of an immunoreactive cell as assigned by manual registration of the data to the template (see Materials and Methods-sections for more details of the mapping-process).

Once the interactive mode is activated, the model can be moved either between previously set dorsal, lateral and ventral view or moved freely. Furthermore, the individual neurotransmitter-immunoreactivity patterns can be activated and deactivated (clicked on or off) to allow for a better spatial orientation, by activating the extending menu (the tree-icon in the activity-bar above the model). Next to the model hierarchy, the colors are also explained in the bottom of the plate. Abbreviations: ag – adhesive gland, cb – ciliary band, mo – mouth

opening, no – nuchal organ, pcb – prostomial ciliary band, pcc – prostomial compound cilia, pyg – pygidium, vcf – ventral ciliary field.

Figure 6. Sequence alignment of proneuropeptide sequences found in *Dinophilus gyrociliatus*.

Sequences of the identified peptides in the transcriptome of *D. gyrociliatus* (SRX2030658), *D. taeniatus* (SRX1025580) and *T. axi* (SRR2014693) were identified by BLAST-searches using proneuropeptide-sequences of *P. dumerilii* as a query (Table 1). Protein sequences of the four species were then aligned using Clustalw in Jalview 2 (Waterhouse et al., 2009). Only the predicted mature peptides are shown (indicated by the boxes), flanked by the cleavage sites (commonly KR). the C-term Gly is predicted to be converted to an amide group. The alignments are color-labeled according to the similarity between the sequences, the darker colors indicating a higher similarity than the lighter ones. Species abbreviations: Dgy – *Dinophilus gyrociliatus*, Dta – *Dinophilus taeniatus*, Pdu – *Platynereis dumerilii*, Tax – *Trilobodrilus axi*. Neuropeptide precursor abbreviations: AKH – adipokinetic hormone, AS-A – allatostatin A, AS-C – allatostatin C, AT – allatotropin, BUR-A – bursicon A, BUR-B – bursicon B, CCW – CCWamide, DL – DLamide, CT – calcitonin, EFLG – EFLGamide, FL – FLamide, EP – excitatory peptide, FMRF – FMRFamide, FV – FVamide, FVRI – FVRIamide, GnRH – gonadotropin releasing hormone, IRP – insulin-related peptide, LKI – leucokinin, MIP – myoinhibitory peptide/allatostatin B, MM – myomodulin, NPY – neuropeptide Y, PEP1 – pedal peptide 1, PEP2 – pedal peptide 2, VT – vasotocin-neurophysin, PH3 – prohormone 3, RGW – RGWamide, RY – RYamide, sCAP – small cardioactive peptide/RNamide, SIF – SIFamide, WI – WIamide, W/I – whitnin.

Figure 7. Serotonin-LIR in the nervous system of *Dinophilus gyrociliatus*, *D. taeniatus* and *Trilobodrilus axi*.

a, e, i) template of the brain cells with the cells labeled with the respective neurotransmitter-LIR in dorsal (uppermost), lateral (middle, dorsal side up) and ventral (lowest) view, all with the anterior to the left. b-d, f-h, j-l) maximum intensity projections of specimens labeled with serotonin-LIR. Scale bar is 10µm, little icons next to the image caption indicate the orientation of the specimens and the location of detailed scans by pink rectangles, some of the immunoreactive cells are indicated by the abbreviation "irc". Acetylated α-tubulin-LIR shown in green, serotonin-LIR in pink, DAPI in cyan, and phalloidin in yellow. a) distribution of serotonin-like immunoreactive cells in the brain of *D. gyrociliatus*, b) ventrolateral view of the entire female *D. gyrociliatus*, with a dorsal detail of the brain (c) and a ventral view of the ventral nervous system (d), e) distribution of serotonin-like immunoreactive cells in the brain of *D. taeniatus*, f) ventral view of the entire female *D. taeniatus*, with a dorsal detail of the prostomium (g) and the ventral nervous system (h), i) distribution of serotonin-like immunoreactive cells in the brain of *T. axi*, j) lateral view of the entire *T. axi*, with a detail of the prostomium (k) and a ventral view of the ventral nervous system (l). A magenta-green converted copy of this figure is provided as supplementary material to this article. Abbreviations: br – brain, cec – circumesophageal connective, cm – circular muscle, cnp – central neuropil, com – commissure, dlln – dorsolateral longitudinal nerve, dln – dorsal longitudinal nerve, drcc – dorsal root of the circumesophageal connective, irc – immunoreactive cell, lm – longitudinal muscle, mo – mouth opening, mvn – medioventral nerve, nacb – nerve anterior to the ciliary band, ncb – ciliary band nerve, nis – intersegmental nerve, nno – nerve between the nuchal organs and the central neuropil, no – nuchal organ, npcb – nerve posterior to the ciliary band, npl – nerve plexus of the ventral

nervous system, pmvn – paramedioventral nerve, stnr – stomatogastric nerve ring, vlnc – ventrolateral nerve cord, vrcc – ventral root of the circumesophageal connective.

Figure 8. Allatotropin-LIR in the nervous system of *Dinophilus gyrociliatus, D. taeniatus* and *Trilobodrilus axi*.

a, e, i) template of the brain cells with the cells labeled with the respective neuropeptide-LIR in dorsal (uppermost), lateral (middle, dorsal side up) and ventral (lowest) view, all with the anterior to the left. b-d, f-h, j-l) maximum intensity projections of specimens labeled with allatotropin-LIR. Scale bar is 10µm, little icons next to the image caption indicate the orientation of the specimens and the location of detailed scans by pink rectangles, some of the immunoreactive cells are indicated by the abbreviation "irc". Acetylated α-tubulin-LIR shown in green, DAPI in cyan, phalloidin in yellow, and the respective cells immunoreactive for the neuropeptide antibody in pink. a) distribution of allatotropin-like immunoreactive cells in the brain of *D. gyrociliatus*, b) ventral view of the entire female *D. gyrociliatus*, with a dorsal detail of the anterior body region (c) and a detail of the ventral nerve cord (d), e) distribution of allatotropin-like immunoreactive cells in the brain of *D. taeniatus*, f) dorsal view of the entire *D. taeniatus*, with a detail of the prostomium (g) and a detail of the copulatory organ (h), i) distribution of allatotropin-like immunoreactive cells in the brain of *T. axi*, j) ventral view of the entire *T. axi*, with a dorsal detail of the prostomium (k) and a ventral close-up of the ventral nervous system (l). A magenta-green converted copy of this figure is provided as supplementary material to this article. Abbreviations: br – brain, cnp – central neuropil, com – commissure, cop – copulatory organ, hg – hindgut, irc – immunoreactive cell, mo – mouth opening, mvn – medioventral nerve, n – nephridium, nis – intersegmental nerve, ns – segmental nerve, phb – pharyngeal bulb, prm – prostomial musculature, pyg – pygidium, sm – sigmoid muscle, sto – stomach, vllm – ventrolateral

longitudinal muscle, vlm – ventral longitudinal muscle, vlnc – ventrolateral nerve cord, vrcc – ventral root of the circumesophageal connective.

Figure 9. Calcitonin-LIR in the nervous system of *Dinophilus gyrociliatus* and *D. taeniatus*.

a, e) template of the brain cells with the cells labeled with the respective neuropeptide-LIR in dorsal (uppermost), lateral (middle, dorsal side up) and ventral (lowest) view, all with the anterior to the left. b-d, f-h) maximum intensity projections of specimens with calcitonin-LIR. Scale bar is 10µm, little icons next to the image caption indicate the orientation of the specimens and the location of detailed scans by pink rectangles, some of the immunoreactive cells are indicated by the abbreviation "irc". Acetylated α-tubulin-LIR shown in green, DAPI in cyan, phalloidin in yellow, and the respective cells immunoreactive for the neuropeptide antibody in pink. a) distribution of calctitonin-like immunoreactive cells in the brain of *D. gyrociliatus*, b) dorsal view of the entire female *D. gyrociliatus*, with a dorsal detail of the anterior prostomium (c) and the labeled cells (d), e) distribution of calcitonin-like immunoreactive cells in the brain of *D. taeniatus*, f) dorsal view of the entire *D. taeniatus*, with details of the anterior body region (g) and the labeled cells and axons (h). A magenta-green converted copy of this figure is provided as supplementary material to this article. Abbreviations: br – brain, cnp – central neuropil, dllm – dorsolateral longitudinal muscle, dm – diagonal muscle, irc – immunoreactive cell, pcb1 – prostomial ciliary band 1, phb – pharyngeal bulb, phm – pharyngeal musculature, pr – prostomium, prm – prostomial musculature, stnr – stomatogastric nerve ring, vllm – ventrolateral longitudinal muscle.

Figure 10. DLamide-LIR in the nervous system of *Dinophilus taeniatus* and *Trilobodrilus axi*.

a, e) template of the brain cells with the cells labeled with the respective neuropeptide-LIR in dorsal (uppermost), lateral (middle, dorsal side up) and ventral (lowest) view, all with the anterior to the left. b-d, f-h) maximum intensity projections of specimens labeled with DLamide-LIR. Scale bar is 10µm, little icons next to the image caption indicate the orientation of the specimens and the location of detailed scans by pink rectangles, some of the immunoreactive cells are indicated by the abbreviation "irc". Acetylated α-tubulin-LIR shown in green, DAPI in cyan, phalloidin in yellow, and the respective cells immunoreactive for the neuropeptide antibody in pink. a) distribution of DLamide-like immunoreactive cells in the brain of *D. taeniatus*, b) ventral view of the entire *D. taeniatus*, with a detail of the prostomium (c) and a detail of the anterior part of the ventral nerve cord (d), e) distribution of DLamide-like immunoreactive cells in the brain of *T. axi*, f) ventral view of the entire *T. axi*, with a lateral detail of the prostomium (g) and a ventral view of the labeled stomatogastric nervous system (h). A magenta-green converted copy of this figure is provided as supplementary material to this article. Abbreviations: cec – circumesophageal connective, cnp – central neuropil, com1-5 – commissure 1-5, drcc – dorsal root of the circumesophageal connective, hg – hindgut, irc – immunoreactive cell, mo – mouth opening, mvn – medioventral nerve, n – nephridium, pmvn – paramedioventral nerve, stnr – stomatogastric nerve ring, stns – stomatogastric nervous system, sto – stomach, vlnc – ventrolateral nerve cord, vrcc – ventral root of the circumesophageal connective.

Figure 11. EP-LIR in the nervous system of *Dinophilus gyrociliatus*, *D. taeniatus* and *Trilobodrilus axi*.

a, e, i) template of the brain cells with the cells labeled with the respective neuropeptide-LIR in dorsal (uppermost), lateral (middle, dorsal side up) and ventral (lowest) view, all with the anterior to the left. b-d, f-h, j-l) maximum intensity projections of specimens labeled with EP-

LIR. Scale bar is 10µm, little icons next to the image caption indicate the orientation of the specimens and the location of detailed scans by pink rectangles, some of the immunoreactive cells are indicated by the abbreviation "irc". Acetylated α-tubulin-LIR shown in green, DAPI in cyan, phalloidin in yellow, and the respective cells immunoreactive for the neuropeptide antibody in pink. a) distribution of EP-like immunoreactive cells in the brain of *D. gyrociliatus*, b) dorsal view of the entire female *D. gyrociliatus*, with a detail of the brain and stomatogastric nervous system (c) and the ventral nervous system (d), e) distribution of EP-like immunoreactive cells in the brain of *D. taeniatus*, f) ventral view of the entire female *D. taeniatus*, with a dorsal detail of the prostomium, brain and stomatogastric nervous system (g) and the ventral nervous system (h), i) distribution of EP-like immunoreactive cells in the brain of *T. axi*, j) ventral view of the entire *T. axi*, with a detail of the prostomium (k) and a close-up of the labeled cells in the brain (l). A magenta-green converted copy of this figure is provided as supplementary material to this article. Abbreviations: br – brain, cb – ciliary band, cec – circumesophageal connective, cm – circular muscle, cnp – central neuropil, co – ciliated organ = eye, com – commissure, drcc – dorsal root of the circumesophageal connective, egg – egg(s), hg – hindgut, irc – immunoreactive cell, mvn – medioventral nerve, ph – pharynx, phb – pharyngeal bulb, prm – prostomial musculature, pyg – pygidium, stnr – stomatogastric nerve ring, sto – stomach, vllm – ventrolateral longitudinal muscle, vlm – ventral longitudinal muscle, vlnc – ventrolateral nerve cord, vrcc – ventral root of the circumesophageal connective.

Figure 12. FLamide-LIR in the nervous system of *Dinophilus gyrociliatus*, *D. taeniatus* and *Trilobodrilus axi*.

a, e, i) template of the brain cells with the cells labeled with the respective neuropeptide-LIR in dorsal (uppermost), lateral (middle, dorsal side up) and ventral (lowest) view, all with the

anterior to the left. b-d, f-h, j-l) maximum intensity projections of specimens labeled with FLamide-LIR. Scale bar is 10µm, little icons next to the image caption indicate the orientation of the specimens and the location of detailed scans by pink rectangles, some of the immunoreactive cells are indicated by the abbreviation "irc". Acetylated α-tubulin-LIR shown in green, DAPI in cyan, phalloidin in yellow, and the respective cells immunoreactive for the neuropeptide antibody in pink. a) distribution of FLamide-like immunoreactive cells in the brain of *D. gyrociliatus*, b) dorsal view of the entire female *D. gyrociliatus*, with a dorsal detail of the prostomium and brain (c) and a detail of the labeled cells dorsal in the brain (d), e) distribution of FLamide-like immunoreactive cells in the brain of *D. taeniatus*, f) dorsal view of the entire female *D. taeniatus*, with a detail of the prostomium (g) and a detail of the labeled cell in the brain lateral to the mouth opening (h), i) distribution of FLamide-like immunoreactive cells in the brain of *T. axi*, j) ventral view of the entire *T. axi*, with a detail of the prostomium (k) and a close-up of the labeled cells in the ventral nervous system (l). A magenta-green converted copy of this figure is provided as supplementary material to this article. Abbreviations: br – brain, cec – circumesophageal connective, cnp – central neuropil, dllm – dorsolateral longitudinal muscle, dm – diagonal muscle, drcc – dorsal root of the circumesophageal connective, egg – egg(s), hg – hindgut, irc – immunoreactive cell, mo – mouth opening, n – nephridium, phb – pharyngeal bulb, prm – prostomial musculature, sm – sigmoid muscle, stnr – stomatogastric nerve ring, vllm – ventrolateral longitudinal muscle, vlnc – ventrolateral nerve cord, vrcc – ventral root of the circumesophageal connective.

Figure 13. FMRFamide-LIR in the nervous system of *Dinophilus gyrociliatus*, *D. taeniatus* and *Trilobodrilus axi*.

a, e, i) template of the brain cells with the cells labeled with the respective neuropeptide-LIR in dorsal (uppermost), lateral (middle, dorsal side up) and ventral (lowest) view, all with the

anterior to the left. b-d, f-h, j-l) maximum intensity projections of specimens labeled with FMRFamide-LIR. Scale bar is 10µm, little icons next to the image caption indicate the orientation of the specimens and the location of detailed scans by pink rectangles, some of the immunoreactive cells are indicated by the abbreviation "irc". Acetylated α-tubulin-LIR shown in green, DAPI in cyan, phalloidin in yellow, and the respective cells immunoreactive for the neuropeptide antibody in pink. a) distribution of FMRFamide-like immunoreactive cells in the brain of *D. gyrociliatus*, b) ventrolateral view of the entire female *D. gyrociliatus*, with a dorsal detail of the brain (c) and a detail of the ventral nervous system (d), e) distribution of FMRFamide-like immunoreactive cells in the brain of *D. taeniatus*, f) lateral view of the entire male *D. taeniatus*, with a dorsal view of the prostomium (g) and a ventral detail of the ventral nervous system (h), i) distribution of FMRFamide-like immunoreactive cells in the brain of *T. axi*, j) lateral view of the entire *T. axi*, with a dorsal detail of the prostomium (k), and ventral view of the anterior part of the ventral nervous system (l). A magenta-green converted copy of this figure is provided as supplementary material to this article. Abbreviations: br – brain, cnp – central neuropil, co – ciliated organ = eye, com – commissure, cop – copulatory organ, drcc – dorsal root of the circumesophageal connective, irc – immunoreactive cell, mo – mouth opening, mvn – medioventral nerve, n – nephridium, ncb – ciliary band nerve, pcc – prostomial compound cilia, phb – pharyngeal bulb, phm – pharyngeal musculature, pmvn – paramedioventral nerve, prm – prostomial musculature, stnr – stomatogastric nerve ring, sto – stomach, test – testis, vlm – ventral longitudinal muscle, vlnc – ventrolateral nerve cord, vrcc – ventral root of the circumesophageal connective.

Figure 14. FVamide-LIR in the nervous system of *Dinophilus gyrociliatus*, *D. taeniatus* and *Trilobodrilus axi*.

a, e, h) template of the brain cells with the cells labeled with the respective neuropeptide-LIR in dorsal (uppermost), lateral (middle, dorsal side up) and ventral (lowest) view, all with the anterior to the left. b-d, f, g, i-k) maximum intensity projections of specimens labeled with FVamide-LIR. Scale bar is 10µm, little icons next to the image caption indicate the orientation of the specimens and the location of detailed scans by pink rectangles, some of the immunoreactive cells are indicated by the abbreviation "irc". Acetylated α-tubulin-LIR shown in green, DAPI in cyan, phalloidin in yellow, and the respective cells immunoreactive for the neuropeptide antibody in pink. a) distribution of FVamide-like immunoreactive cells in the brain of *D. gyrociliatus*, b) dorsal view of the entire female *D. gyrociliatus*, with a detail of the brain (c) and a close-up of the labeled cells in the brain (d), e) distribution of FVamide-like immunoreactive cells in the brain of *D. taeniatus*, f) a lateral detail of the prostomium and brain, and g) a lateral view of the entire female *D. taeniatus*, h) distribution of FVamide-like immunoreactive cells in the brain of *T. axi*, i) ventral view of the entire *T. axi*, with a detail of the prostomium (j) and a close-up of the labeled cells in the neuropil (k). A magenta-green converted copy of this figure is provided as supplementary material to this article. Abbreviations: br – brain, cb – ciliary band, cec – circumesophageal connective, cm – circular muscle, cnp – central neuropil, co – ciliated organ = eye, dllm – dorsolateral longitudinal muscle, egg – egg(s), hg – hindgut, irc – immunoreactive cell, n – nephridium, phb – pharyngeal bulb, phm – pharyngeal muscles, prm – prostomial musculature, sm – sigmoid muscle, stnr – stomatogastric nerve ring, stns – stomatogastric nervous system, sto – stomach, vcf – ventral ciliary field, vllm – ventrolateral longitudinal muscle, vlnc – ventrolateral nerve cord.

Figure 15. FVRIamide-LIR in the nervous system of *Dinophilus gyrociliatus*, *D. taeniatus* and *Trilobodrilus axi*.

a, e, i) template of the brain cells with the cells labeled with the respective neuropeptide-LIR in dorsal (uppermost), lateral (middle, dorsal side up) and ventral (lowest) view, all with the anterior to the left. b-d, f-h, j-m) maximum intensity projections of specimens labeled with FVRIamide-LIR. Scale bar is 10µm, little icons next to the image caption indicate the orientation of the specimens and the location of detailed scans by pink rectangles, some of the immunoreactive cells are indicated by the abbreviation "irc". Acetylated α-tubulin-LIR shown in green, DAPI in cyan, phalloidin in yellow, and the respective cells immunoreactive for the neuropeptide antibody in pink. a) distribution of FVRIamide-like immunoreactive cells in the brain of *D. gyrociliatus*, b) lateral view of the entire female *D. gyrociliatus*, with a lateral view of a detail of the anterior body region (c) and a detail of the ventral nerve cord (d), e) distribution of FVRIamide-like immunoreactive cells in the brain of *D. taeniatus*, f) ventral view of the entire female *D. taeniatus*, with a detail of the prostomium (g) and a detail of the ventral nerve cord (h), i) distribution of FVRIamide-like immunoreactive cells in the brain of *T. axi*, j) ventral view of the entire *T. axi*, with a detail of the prostomium (k), a close-ups of the labeled cells in dorsal view (l) and a detail of the stomatogastric nervous system at the midgut-hindgut-transition (m). A magenta-green converted copy of this figure is provided as supplementary material to this article. Abbreviations: br – brain, co – ciliated organ = eye, com – commissure, cnp – central neuropil, dllm – dorsolateral longitudinal muscle, dm – diagonal muscle, drcc – dorsal root of the circumesophageal connective, egg – egg(s), irc – immunoreactive cell, mcom – medial commissure, mht – midgut-hindgut-transition, mo – mouth opening, mvn – medioventral nerve, n – nephridium, pcc – prostomial compound cilia, phb – pharyngeal bulb, pmvn – paramedioventral nerve, sm – sigmoid muscle, stnr – stomatogastric nerve ring, stns – stomatogastric nervous system, sto – stomach, tcom – terminal commissure, vllm – ventrolateral longitudinal muscle, vlnc – ventrolateral nerve cord, vrcc – ventral root of the circumesophageal connective.

Figure 16. MIP-LIR in the nervous system of *Dinophilus gyrociliatus*, *D. taeniatus* and *Trilobodrilus axi*.

a, e, i) template of the brain cells with the cells labeled with the respective neuropeptide-LIR in dorsal (uppermost), lateral (middle, dorsal side up) and ventral (lowest) view, all with the anterior to the left. b-d, f-h, j-l) maximum intensity projections of specimens labeled with MIP-LIR. Scale bar is 10µm, little icons next to the image caption indicate the orientation of the specimens and the location of detailed scans by pink rectangles, some of the immunoreactive cells are indicated by the abbreviation "irc". Acetylated α-tubulin-LIR shown in green, DAPI in cyan, phalloidin in yellow, and the respective cells immunoreactive for the neuropeptide antibody in pink. a) distribution of MIP-like immunoreactive cells in the brain of *D. gyrociliatus*, b) ventral view of the entire female *D. gyrociliatus*, with a lateral detail of the prostomial region with corresponding musculature (c) and with the labeled cells (d), e) distribution of MIP-like immunoreactive cells in the brain of *D. taeniatus*, f) dorsal view of the entire female *D. taeniatus*, with a detail of the prostomium (g) and the ventral nervous system (h), i) distribution of MIP-like immunoreactive cells in the brain of *T. axi*, j) lateral view of the entire *T. axi*, with a detail of the prostomium (k) and a close-up of the labeled cells (l). A magenta-green converted copy of this figure is provided as supplementary material to this article. Abbreviations: br – brain, cec – circumesophageal connective, cm – circular muscle, cnp – central neuropil, co – ciliated organ = eye, com – commissure, dllm – dorsolateral longitudinal muscle, dm – diagonal muscle, drcc – dorsolateral circumesophageal connective, egg – egg(s), hg – hindgut, irc – immunoreactive cell, mvn – medioventral nerve, n – nephridium, pcc – prostomial compound cilia, ph – pharynx, phb – pharyngeal bulb, prm – prostomial musculature, sm – sigmoid muscle, stnr – stomatogastric nerve ring, sto – stomach, vllm – ventrolateral longitudinal muscle, vlm – ventral longitudinal

muscle, vlnc – ventrolateral nerve cord, vrcc – ventral root of the circumesophageal connective.

Figure 17. MLD/pedal peptide-LIR in the nervous system of *Dinophilus gyrociliatus* and *Trilobodrilus axi*.

a, f) template of the brain cells with the cells labeled with the respective neuropeptide-LIR in dorsal (uppermost), lateral (middle, dorsal side up) and ventral (lowest) view, all with the anterior to the left. b-e, g-j) maximum intensity projections of specimens labeled with MLD/pedal peptide-LIR. Scale bar is 10µm, little icons next to the image caption indicate the orientation of the specimens and the location of detailed scans by pink rectangles, some of the immunoreactive cells are indicated by the abbreviation "irc". Acetylated α-tubulin-LIR shown in green, DAPI in cyan, phalloidin in yellow, and the respective cells immunoreactive for the neuropeptide antibody in pink. a) distribution of MLD/pedal peptide-like immunoreactive cells in the brain of *D. gyrociliatus*, b) ventral view of the entire female *D. gyrociliatus*, with a detail of the brain in lateral (c) and dorsal view (d) and a lateral view of the posterior region (e), f) distribution of MLD/pedal peptide-like immunoreactive cells in the brain of *T. axi*, g) ventral view of the entire *T. axi*, with a detail of the prostomium in ventral (h) and lateral view (i) and a close-up of the labeled cell in the brain (j). A magenta-green converted copy of this figure is provided as supplementary material to this article. Abbreviations: br – brain, cm – circular muscle, cnp – central neuropil, co – ciliated organ = eye, dm – diagonal muscle, drcc – dorsal root of the circumesophageal connective, hg – hindgut, irc – immunoreactive cell, mht – midgut-hindgut transition, mo – mouth opening, n – nephridium, phb – pharyngeal bulb, prm – prostomial musculature, pyg – pygidium, sm – sigmoid muscle, stnr – stomatogastric nerve ring, stns – stomatogastric nervous system, sto –

stomach, vllm – ventrolateral longitudinal muscle, vlm – ventral longitudinal muscle, vlnc – ventrolateral nerve cord, vrcc – ventral root of the circumesophageal connective.

Figure 18. RGWamide-LIR in the nervous system of *Dinophilus gyrociliatus*.

a) template of the brain cells with the cells labeled with the respective neuropeptide-LIR in dorsal (uppermost), lateral (middle, dorsal side up) and ventral (lowest) view, all with the anterior to the left. b-d) maximum intensity projections of specimens labeled with RGWamide-LIR. Scale bar is 10µm, little icons next to the image caption indicate the orientation of the specimens and the location of detailed scans by pink rectangles, some of the immunoreactive cells are indicated by the abbreviation "irc". Acetylated α-tubulin-LIR shown in green, DAPI in cyan, phalloidin in yellow, and the respective cells immunoreactive for the neuropeptide antibody in pink. a) distribution of RGWamide-like immunoreactive cells in the brain of *D. gyrociliatus*, b) dorsal view of the entire female *D. gyrociliatus*, with a lateral detail of the prostomium (c), and a dorsal close-up of the labeled cells in the brain (d). A magenta-green converted copy of this figure is provided as supplementary material to this article. Abbreviations: br – brain, dllm – dorsolateral longitudinal muscle, dm – diagonal muscle, irc – immunoreactive cell, mo – mouth opening, phb – pharyngeal bulb, prm – prostomial musculature, sm – sigmoid muscle, vllm – ventrolateral longitudinal muscle.

Figure 19. RNamide/sCAP-LIR in the nervous system of *Dinophilus gyrociliatus*, *D. taeniatus* and *Trilobodrilus axi*.

a, e, h) template of the brain cells with the cells labeled with the respective neuropeptide-LIR in dorsal (uppermost), lateral (middle, dorsal side up) and ventral (lowest) view, all with the anterior to the left. b-d, f-g, i-k) maximum intensity projections of specimens labeled with RNamide/sCAP-LIR. Scale bar is 10µm, little icons next to the image caption indicate the

orientation of the specimens and the location of detailed scans by pink rectangles, some of the immunoreactive cells are indicated by the abbreviation "irc". Acetylated α-tubulin-LIR shown in green, DAPI in cyan, phalloidin in yellow, and the respective cells immunoreactive for the neuropeptide antibody in pink. a) distribution of RNamide/sCAP-like immunoreactive cells in the brain of *D. gyrociliatus*, b) lateral view of the entire female *D. gyrociliatus*, with a detail of the brain (c) and a lateral detail of the posterior body region (d), e) distribution of RNamide/sCAP-like immunoreactive cells in the brain of *D. taeniatus*, f) dorsal view of the entire male *D. taeniatus*, with a detail of the prostomium and brain (g), h) distribution of RNamide/sCAP-like immunoreactive cells in the brain of *T. axi*, i) ventral view of the entire *T. axi*, with a detail of the prostomium (j) and a close-ups of the labeled cells in dorsal view (k). A magenta-green converted copy of this figure is provided as supplementary material to this article. Abbreviations: adh – adhesive glands, br – brain, cb – ciliary band, cnp – central neuropil, cop – copulator organ, drcc – dorsal root of the circumesophageal connective, irc – immunoreactive cell, mht – midgut-hindgut transition, mo – mouth opening, n – nephridium, ph – pharynx, pyg – pygidium, sm – sigmoid muscle, stns – stomatogastric nervous system, test – testis, vllm – ventrolateral longitudinal muscle, vlnc – ventrolateral nerve cord, vrcc – ventral root of the circumesophageal connective.

Figure 20. SIFamide-LIR in the nervous system of *Dinophilus gyrociliatus*, *D. taeniatus* and *Trilobodrilus axi*.

a, e, i) template of the brain cells with the cells labeled with the respective neuropeptide-LIR in dorsal (uppermost), lateral (middle, dorsal side up) and ventral (lowest) view, all with the anterior to the left. b-d, f-h, j-m) maximum intensity projections of specimens labeled with SIFamide-LIR. Scale bar is 10µm, little icons next to the image caption indicate the orientation of the specimens and the location of detailed scans by pink rectangles, some of

the immunoreactive cells are indicated by the abbreviation "irc". Acetylated α-tubulin-LIR shown in green, DAPI in cyan, phalloidin in yellow, and the respective cells immunoreactive for the neuropeptide antibody in pink. a) distribution of SIFamide-like immunoreactive cells in the brain of *D. gyrociliatus*, b) dorsal view of the entire female *D. gyrociliatus*, with a detail of the prostomium (c) and a close-up of the labeled cells (d), e) distribution of SIFamide-like immunoreactive cells in the brain of *D. taeniatus*, f) dorsal view of the entire female *D. taeniatus*, with a detail of the prostomium (g) and a close-up of the labeled cells (h), i) distribution of SIFamide-like immunoreactive cells in the brain of *T. axi*, j) dorsal view of the entire *T. axi*, with a detail of the prostomium (k) and close-ups of the labeled cells in dorsal view (l) and in cross-sections (m, v-d indicating the ventral-dorsal axis). A magenta-green converted copy of this figure is provided as supplementary material to this article. Abbreviations: br – brain, cnp – central neuropil, co – ciliated organ = eye, dllm – dorsolateral longitudinal muscle, drcc – dorsal root of the circumesophageal connective, egg – egg(s), hg – hindgut, irc – immunoreactive cell, mo – mouth opening, n – nephridium, pcb1,2 – prostomial ciliary band 1, 2, pcc – prostomial compound cilia, ph – pharynx, phb – pharyngeal bulb, pr – prostomium, prm – prostomial musculature, sm – sigmoid muscle, sto – stomach, vllm – ventrolateral longitudinal muscle, vrcc – ventral root of the circumesophageal connective.

Figure 21. Vasotocin-LIR in the nervous system of *Dinophilus gyrociliatus*.

a) template of the brain cells with the cells labeled with the respective neuropeptide-LIR in dorsal (uppermost), lateral (middle, dorsal side up) and ventral (lowest) view, all with the anterior to the left. b-e) maximum intensity projections of specimens labeled with vasotocin-LIR. Scale bar is 10µm, little icons next to the image caption indicate the orientation of the specimens and the location of detailed scans by pink rectangles, some of the immunoreactive

cells are indicated by the abbreviation "irc". Acetylated α-tubulin-LIR shown in green, DAPI in cyan, phalloidin in yellow, and the respective cells immunoreactive for the neuropeptide antibody in pink. a) distribution of vasotocin-like immunoreactive cells in the brain of *D. gyrociliatus*, b) lateral view of the entire female *D. gyrociliatus*, with a detail of the prostomium (c), a close-up of a cross-section through the brain (d) and the correlation of the immunoreactive cells to the prostomial muscles (e). A magenta-green converted copy of this figure is provided as supplementary material to this article. Abbreviations: br – brain, dllm – dorsolateral longitudinal muscle, irc – immunoreactive cell, phb – pharyngeal bulb, prm – prostomial musculature, stns – stomatogastric nervous system, vllm – ventrolateral longitudinal muscle, vlm – ventral longitudinal muscle.

TABLES

Table 1. Neuropeptides identified in the transcriptome of *Dinophilus gyrociliatus, D. taeniatus* and *T. axi*.

Sequences of the identified proneuropeptide sequences in the transcriptome of *D. gyrociliatus* (SRX2030658), *D. taeniatus* (SRX1025580) and *T. axi* (SRR2014693) were identified by BLAST-searches using proneuropeptide-sequences of *P. dumerilii* as a query, and evaluated by alignment using Clustalw. The specificity of these antibodies against SIFamide, FVRIamide, and allatotropin was tested by morpholino gene knockdown (MLGKD) in larvae of *P. dumerilii*, and the specificity of antibodies against calcitonin, RNamide/sCAP, vasotocin, RGWamide, DLamde, FLamide, FVamide, FVRIamide, EP, MLD/pedal peptide, and MIP was tested by whole mount in situ hybridization (WMISH) in larvae (Table 1, Jekely unpubl., (Conzelmann et al., 2011; Asadulina et al., 2012; Conzelmann and Jekely, 2012; Williams et al., 2017). Positive immunoreactivity to the antibodies is indicated by grey-shaded background of the table field. Neuropeptide precursor abbreviations: AKH –

adipokinetic hormone, AS-A – allatostatin A, AS-C – allatostatin C, AT – allatotropin, BUR-A – bursicon A, BUR-B – bursicon B, CCW – CCWamide, DL – DLamide, CT – calcitonin, EFLG – EFLGamide, FL – FLamide, EP – excitatory peptide, FMRF – FMRFamide, FV – FVamide, FVRI – FVRIamide, GnRH – gonadotropin releasing hormone, IRP – insulin-related peptide, LKI – leucokinin, MIP – myoinhibitory peptide/allatostatin B, MM – myomodulin, NPY – neuropeptide Y, PEP1 – pedal peptide 1, PEP2 – pedal peptide 2, VT – vasotocin-neurophysin, PH3 – prohormone 3, RGW – RGWamide, RY – RYamide, sCAP – small cardioactive peptide/RNamide, SIF – SIFamide, WI – WIamide, W/I – whitnin.

Table 2. Antibody characteristics and concentrations.

This table list the names, the structure, information about the company, animals the antibodies were raised in as well as specificity and concentrations of antibodies against neurotransmitters used in this study. The specificity of these antibodies against SIFamide, FVRIamide, and allatotropin was tested by morpholino gene knockdown (MLGKD) in larvae of *P. dumerilii*, and the specificity of antibodies against calcitonin, RNamide/sCAP, vasotocin, RGWamide, DLamde, FLamide, FVamide, FVRIamide, EP, MLD/pedal peptide, and MIP was tested by whole mount in situ hybridization (WMISH) in larvae (Table 1, Jekely unpubl., (Conzelmann et al., 2011; Asadulina et al., 2012; Conzelmann and Jekely, 2012; Williams et al., 2017). RRID-numbers are given for commercially available and registered antibodies.

Table 3. Main characteristics of the dinophilid nervous system.

Several traits described in the nervous system of these three species are noted here, following the characters used by (Worsaae et al., 2016) and supplement by additional information about the number of commissures in the dorsal and ventral root of the circumesophageal connective

as well as the distribution pattern of the commissures along the ventral nervous system. In character 11, additional nerves associated with the ciliary bands are marked in bold. Abbreviations: ans – angled segmental nerves, nacb – nerves anterior to the ciliary band, ncb – nerves associated with the ciliary bands, nis – intersegmental nerves, npcb – nerves posterior to the ciliary bands, ns – segmental nerves.

Table 4. Neuropeptides identified with the respective antibodies in adults of *Dinophilus gyrociliatus*, *D. taeniatus* and *Trilobodrilus axi.*

The presence of neural elements labeled by specific neuropeptide-like immunoreactivity (LIR) is shown as distributed between the brain (BR), the ventral nervous system (VNS), the stomatogastric nervous system (SNS), and additional nerves (AN). Grey shading of the respective fields indicates that the neuropeptide precursor sequence has been found in the transcriptomes of *D. gyrociliatus* (SRX2030658), *D. taeniatus* (SRX1025580) and *T. axi* (SRR2014693) (Figure 1, Table 1). The number of somata labeled by neuropeptide-LIR in the brain is based on three individuals investigated in *D. gyrociliatus* and *T. axi*, while only one or two specimens could be investigated in *D. taeniatus*. These numbers indicate that *D. gyrociliatus* has approximately twice as many immunoreactive cells in the brain than the other two dinophilid species. Besides elements labeled with DLamide (which are missing in *D. gyrociliatus*), this species also apparently uses the broadest repertoire of neuropeptides as compared to the other dinophilids. Abbreviations: com – commissure, copn – nerves of the copulatory organ, dlln – dorsolateral longitudinal nerve, dln – dorsal longitudinal nerve, lln – lateral longitudinal nerve, mvn – medioventral nerve, ns – segmental nerve, pmvn – paramedian nerve, tn – transverse nerves (ncb – nerve of the ciliary band, nacb – nerve anterior to the ciliary band, npcb – nerve posterior to the ciliary band, nis – intersegmental

nerve, ns – segmental nerve), vlln – ventrolateral longitudinal nerve, vlnc – ventrolateral nerve cord.

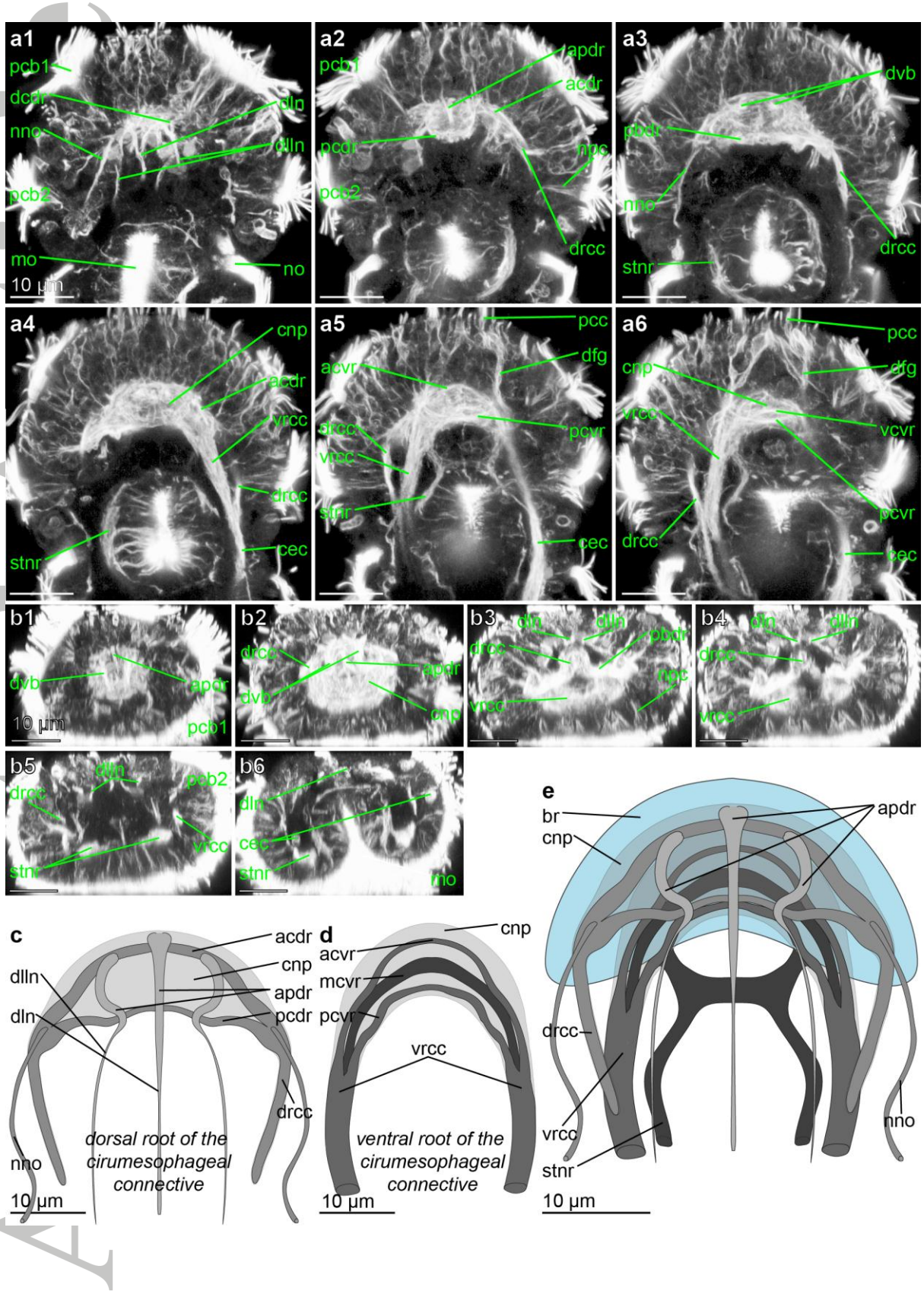

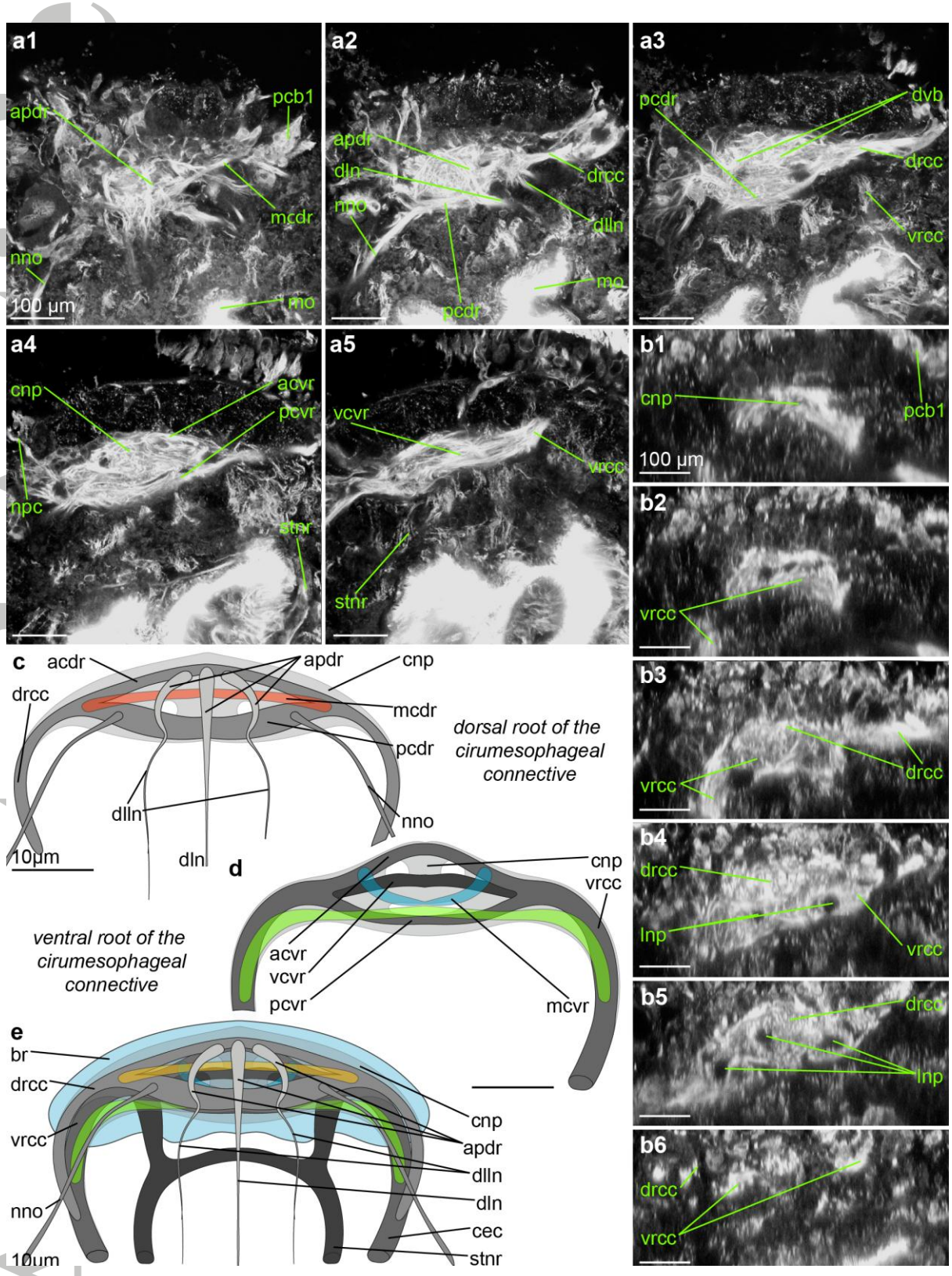

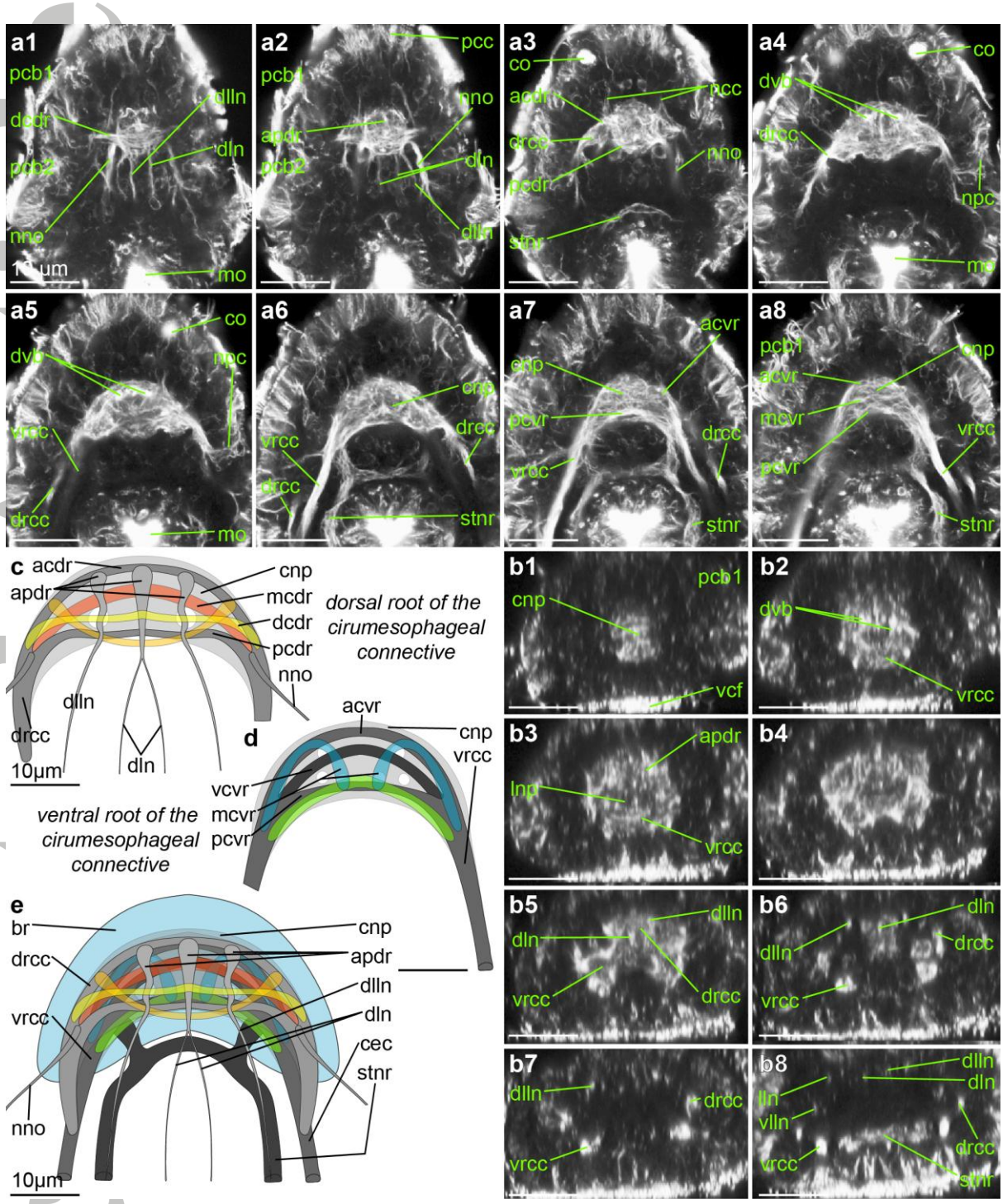

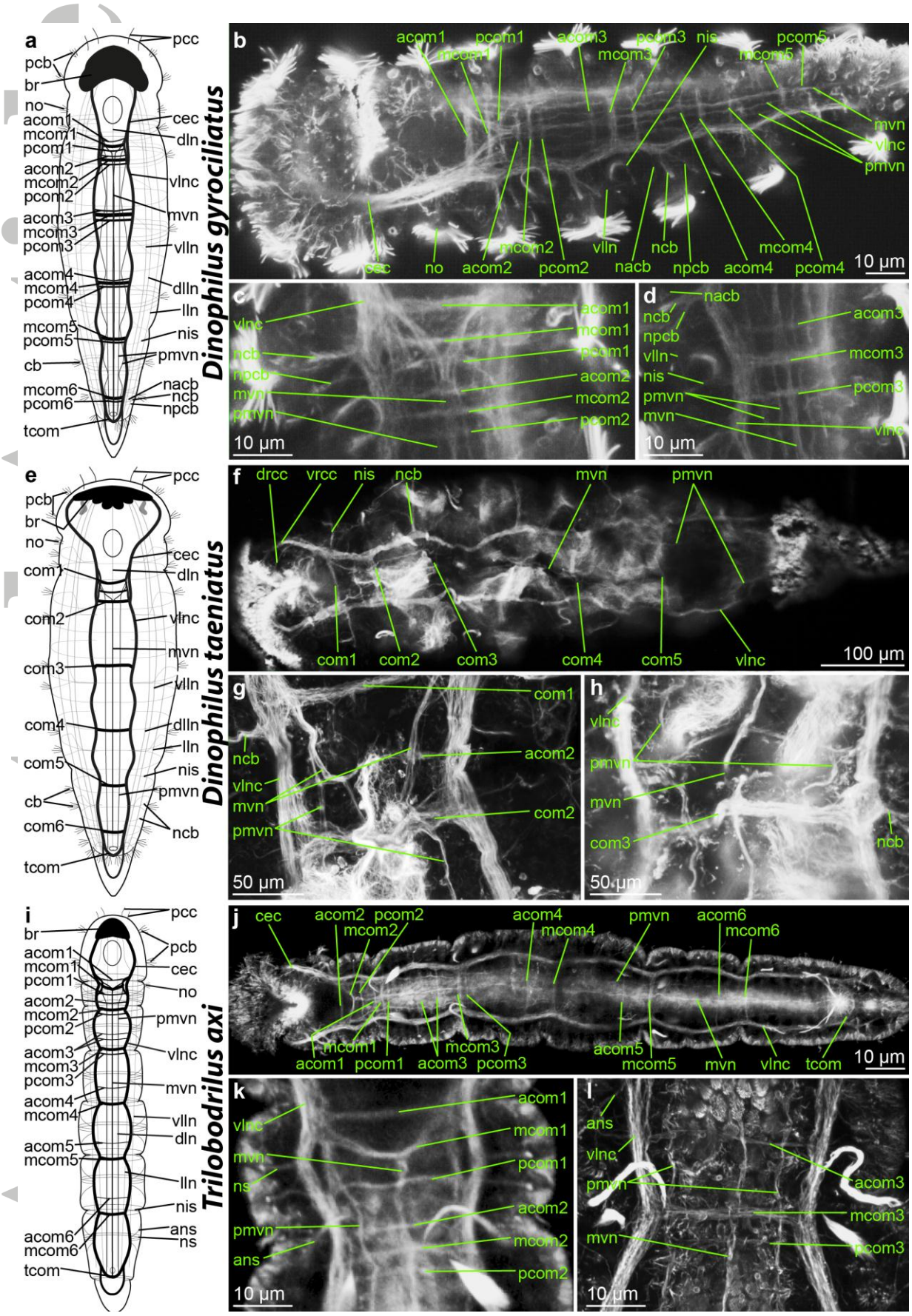

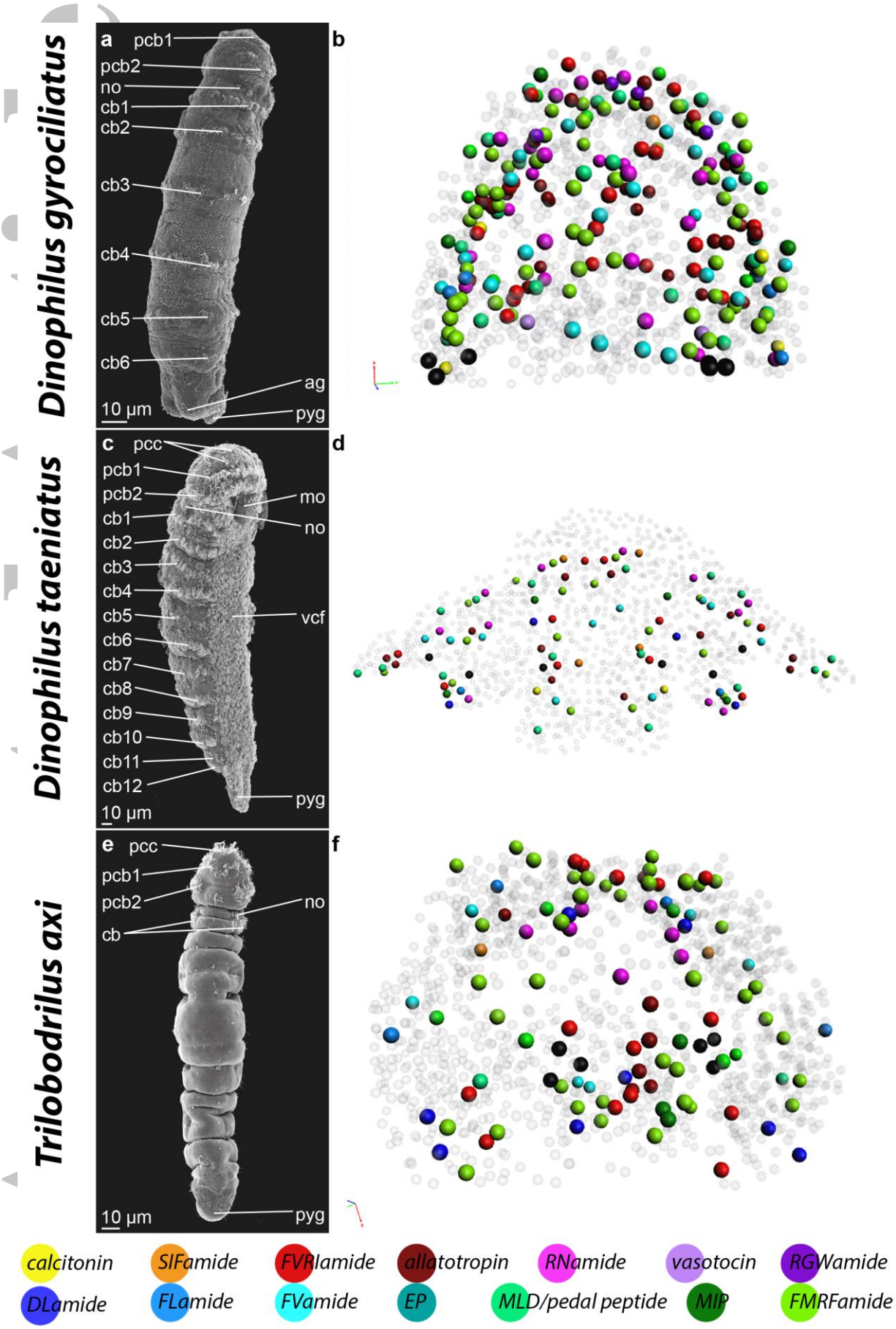

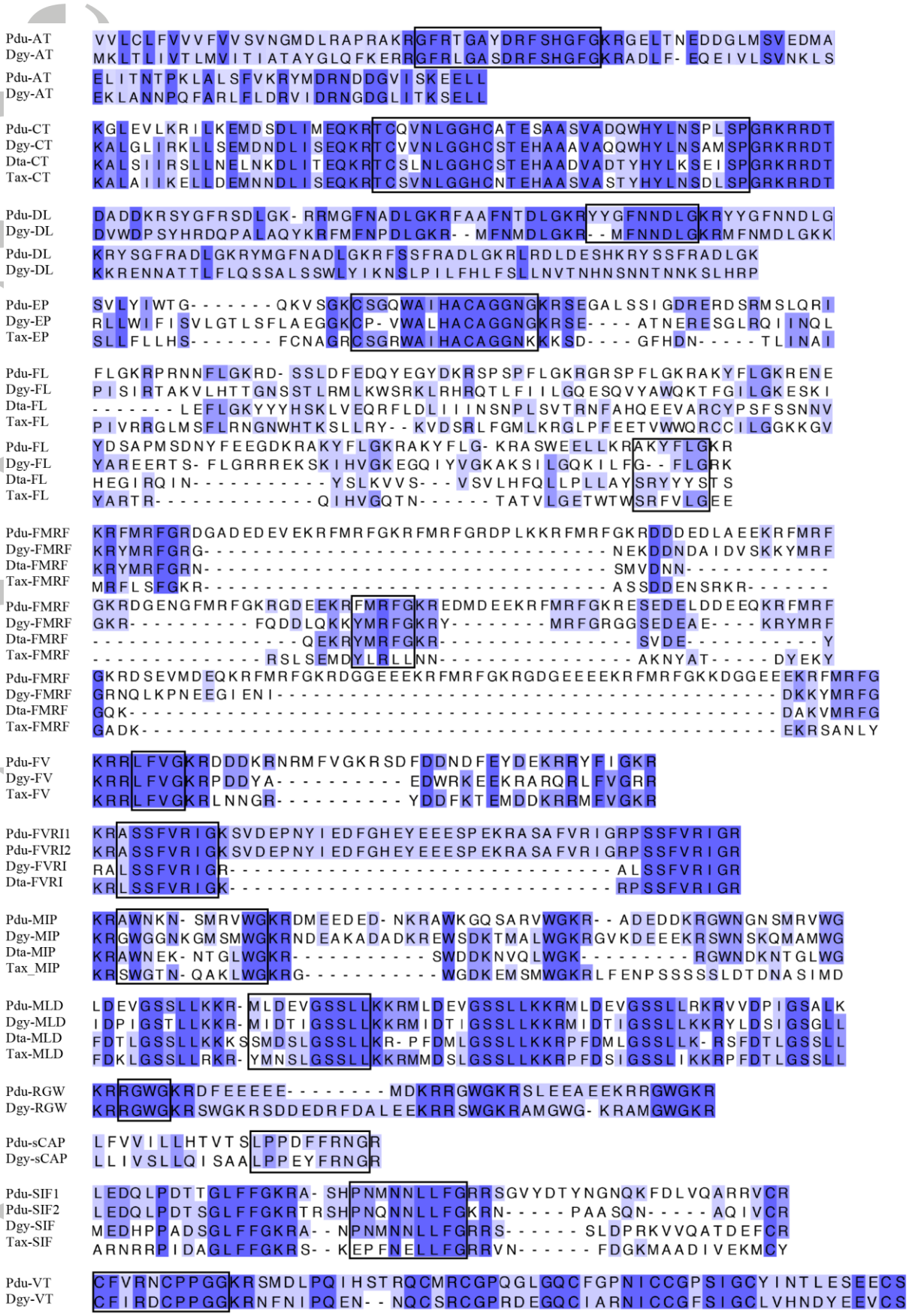

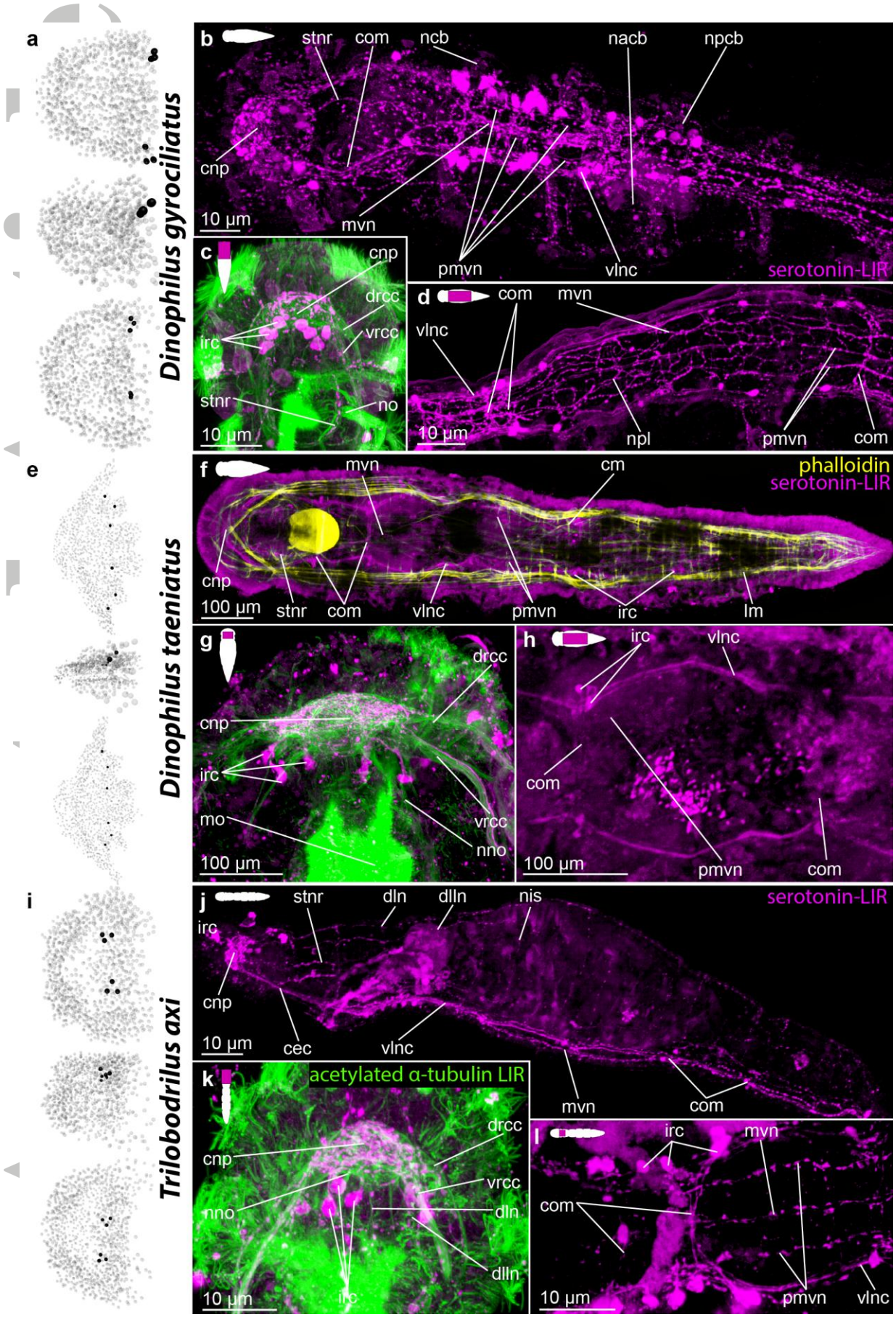

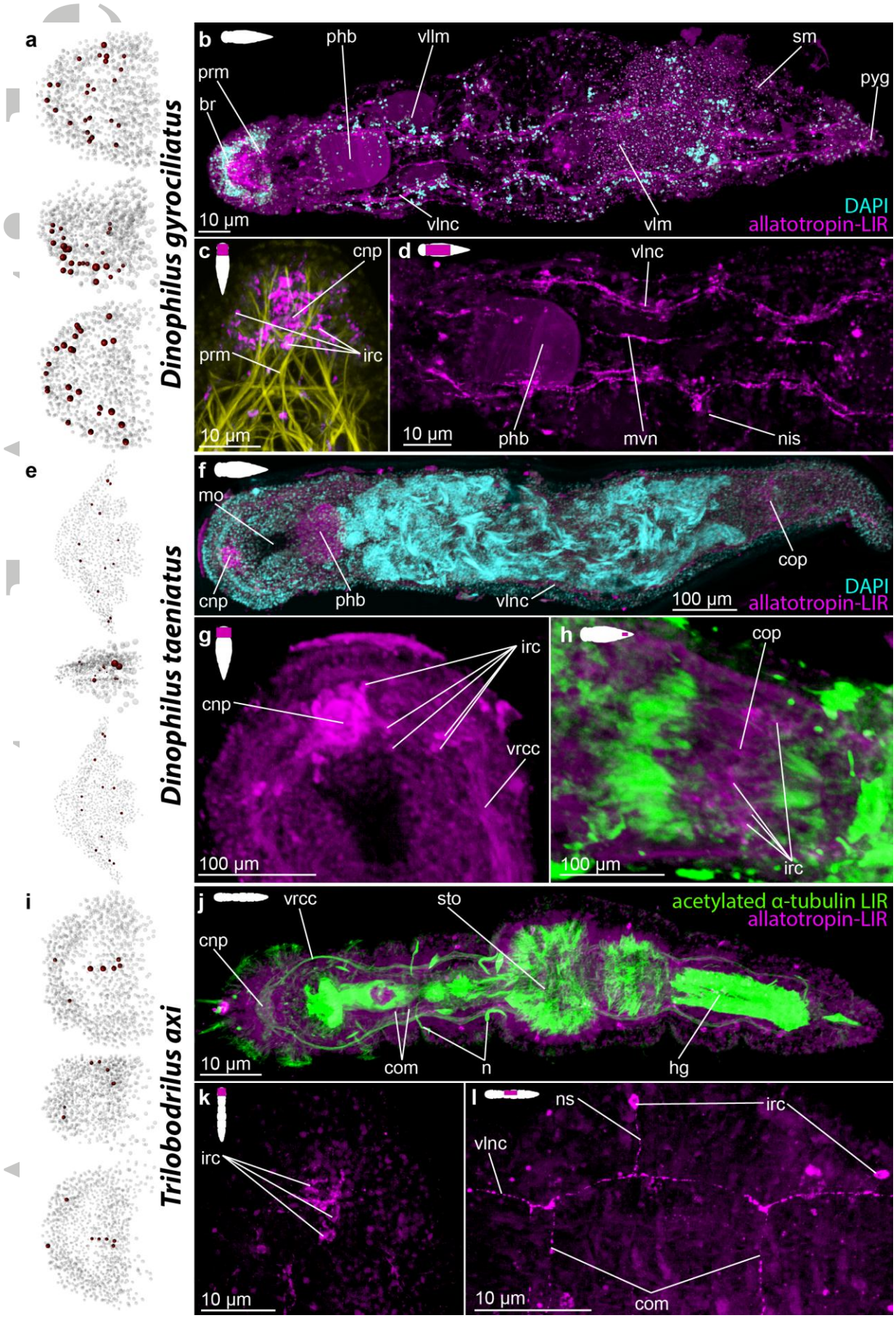

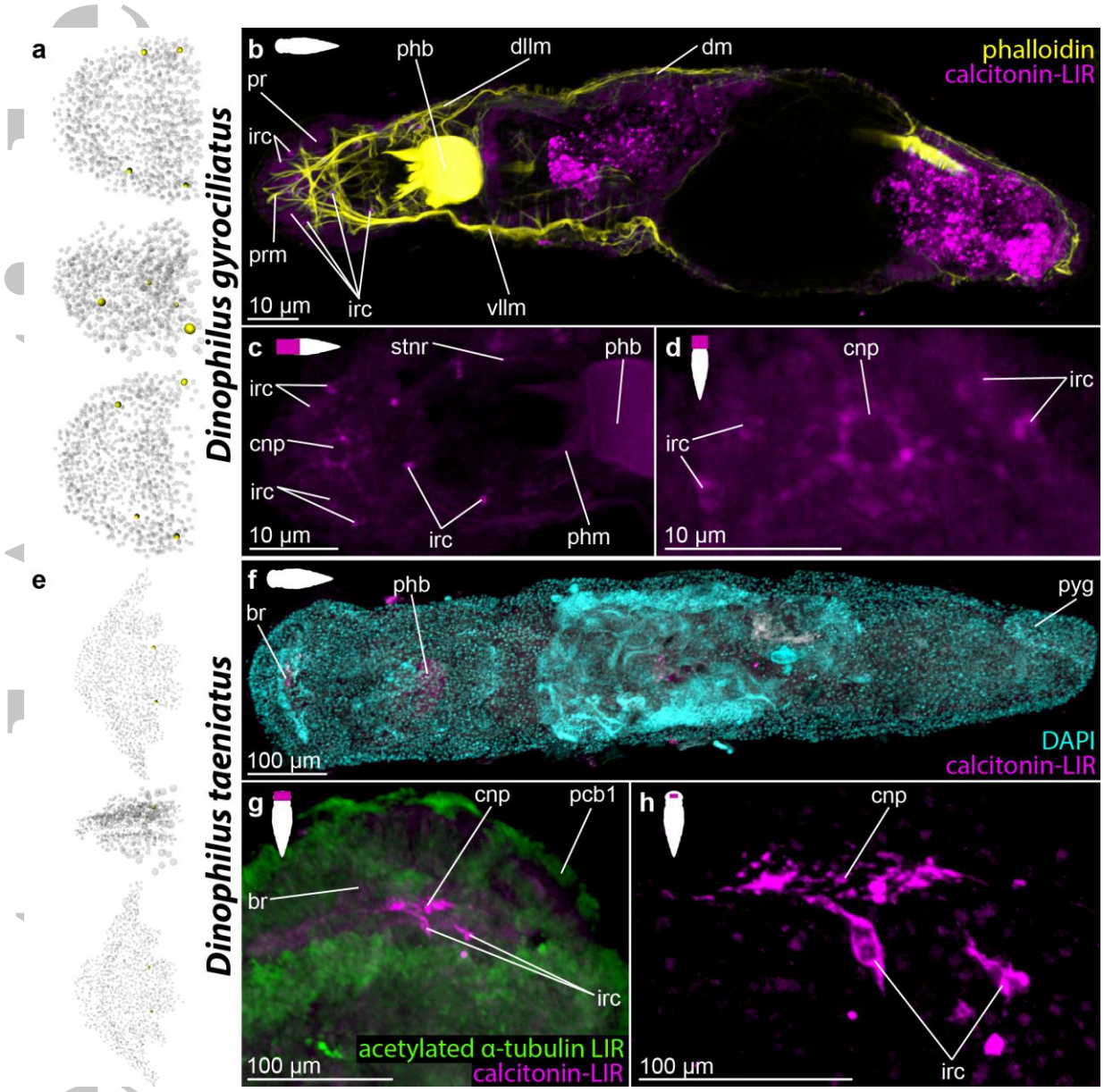

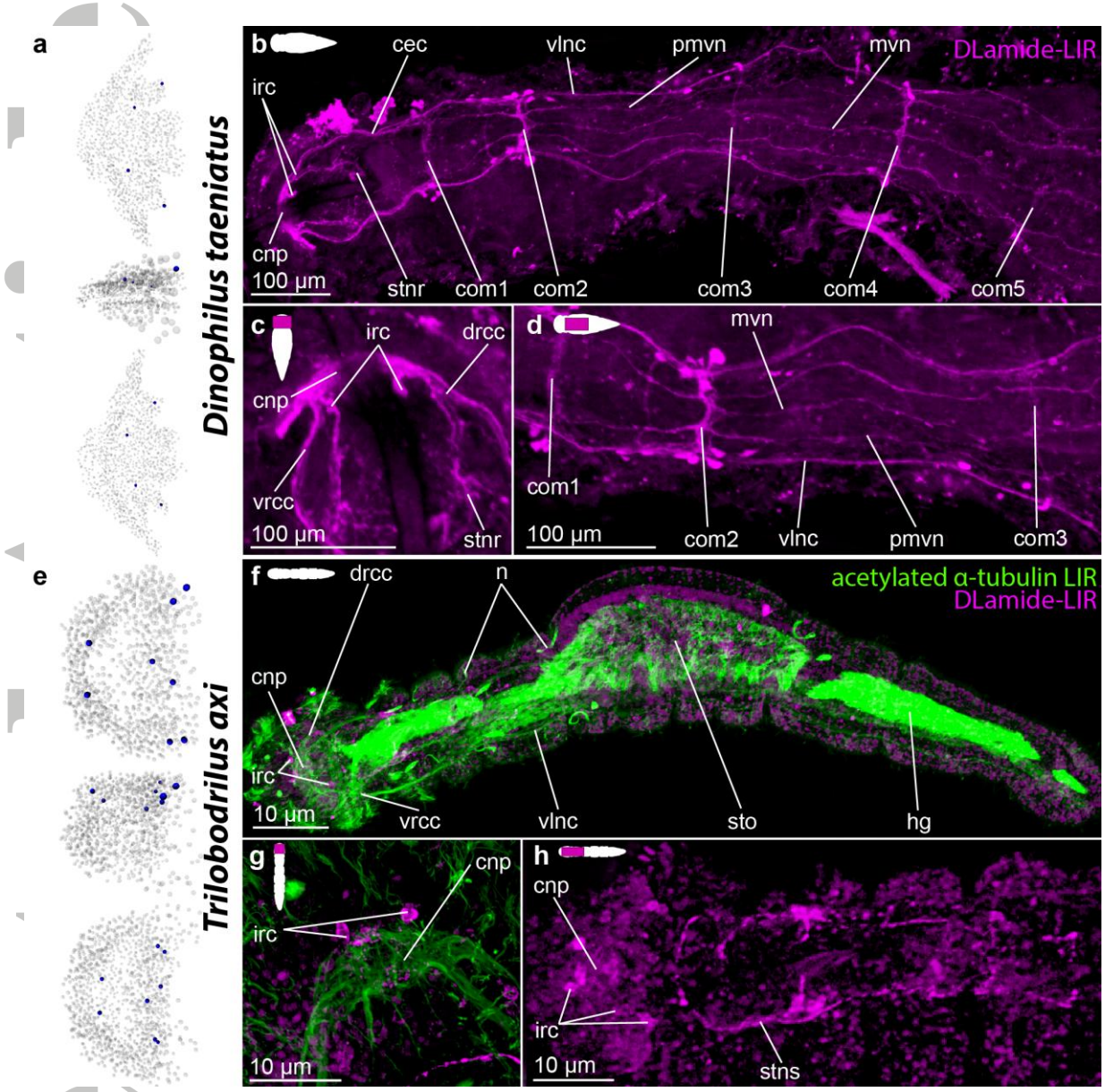

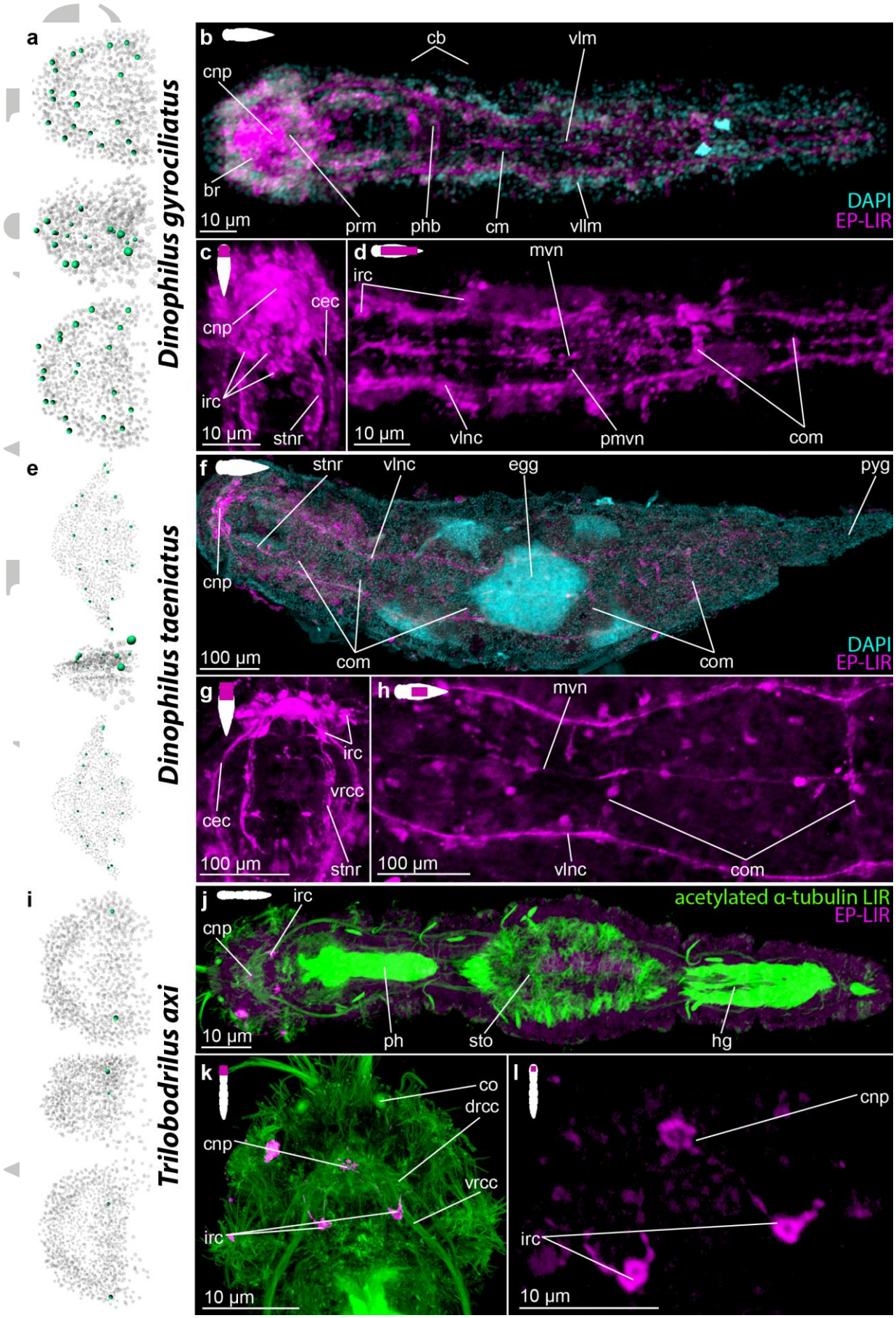

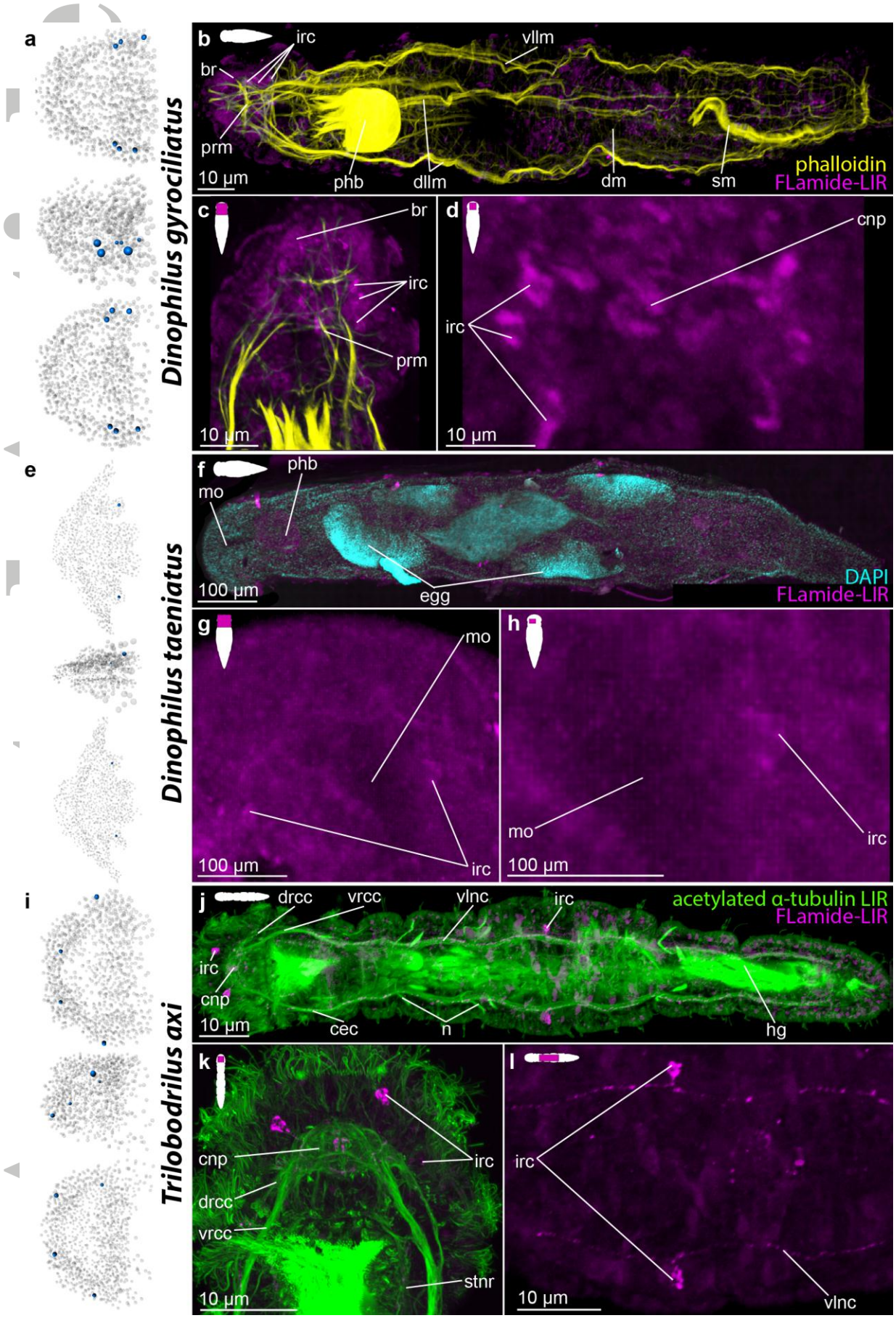

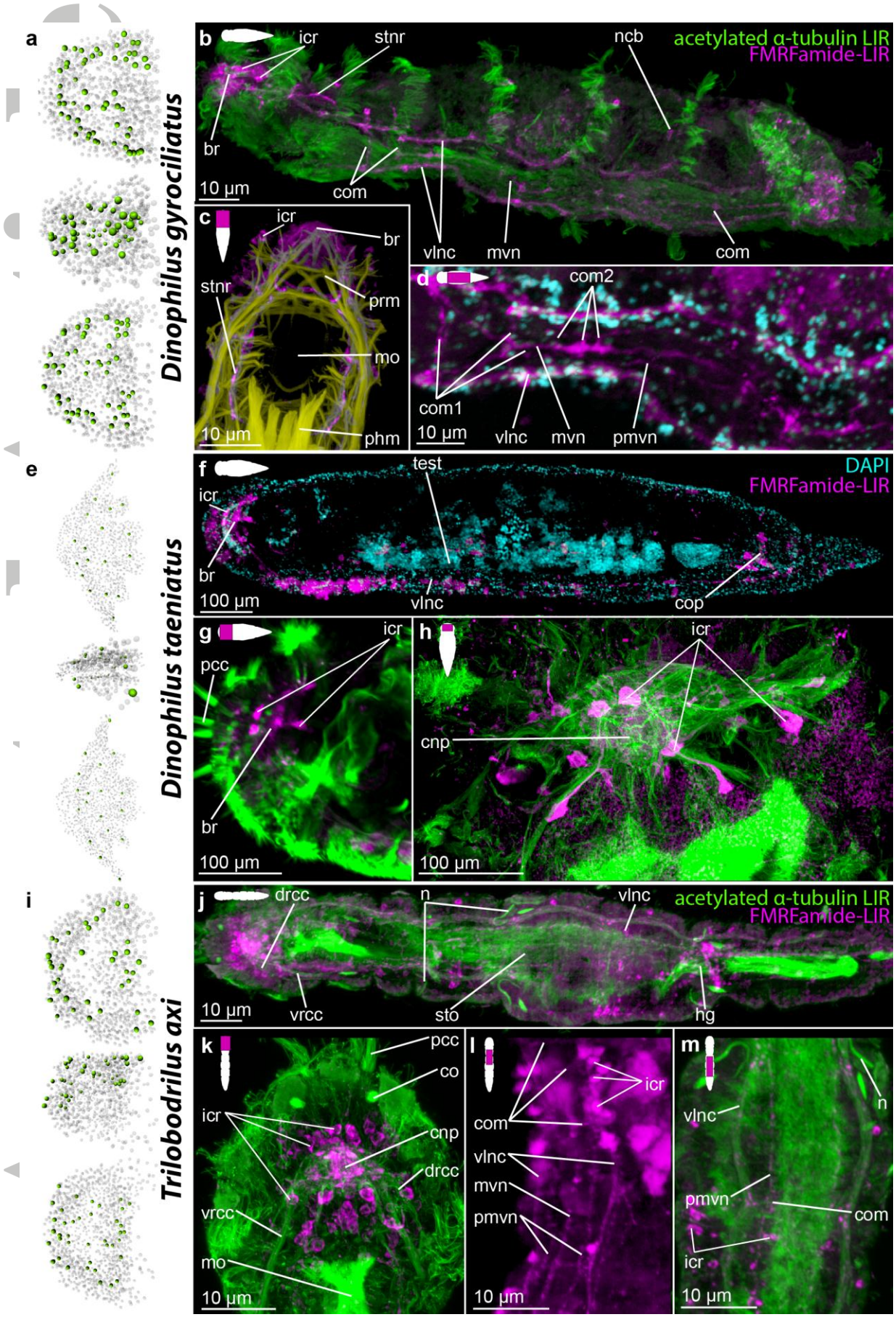

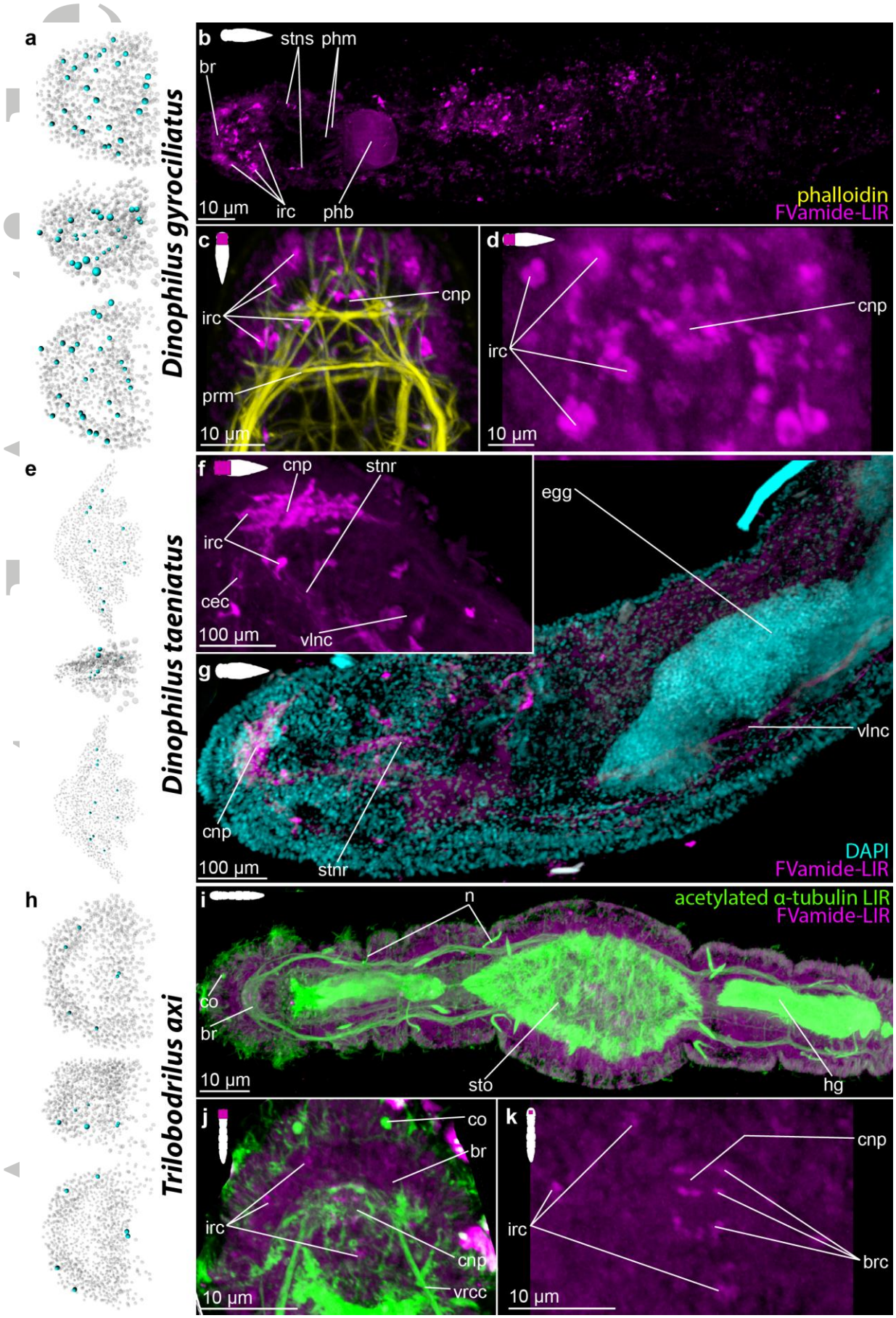

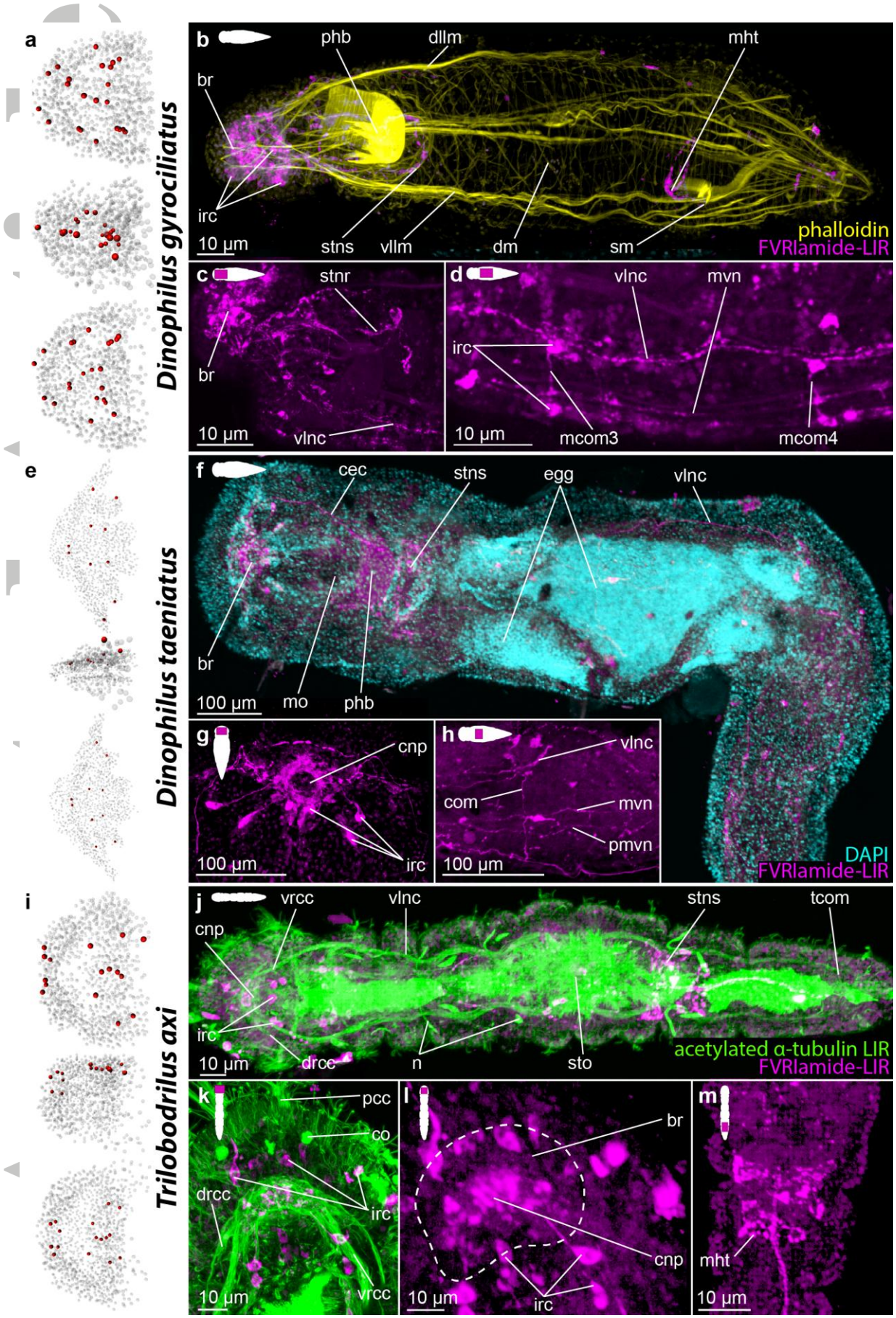

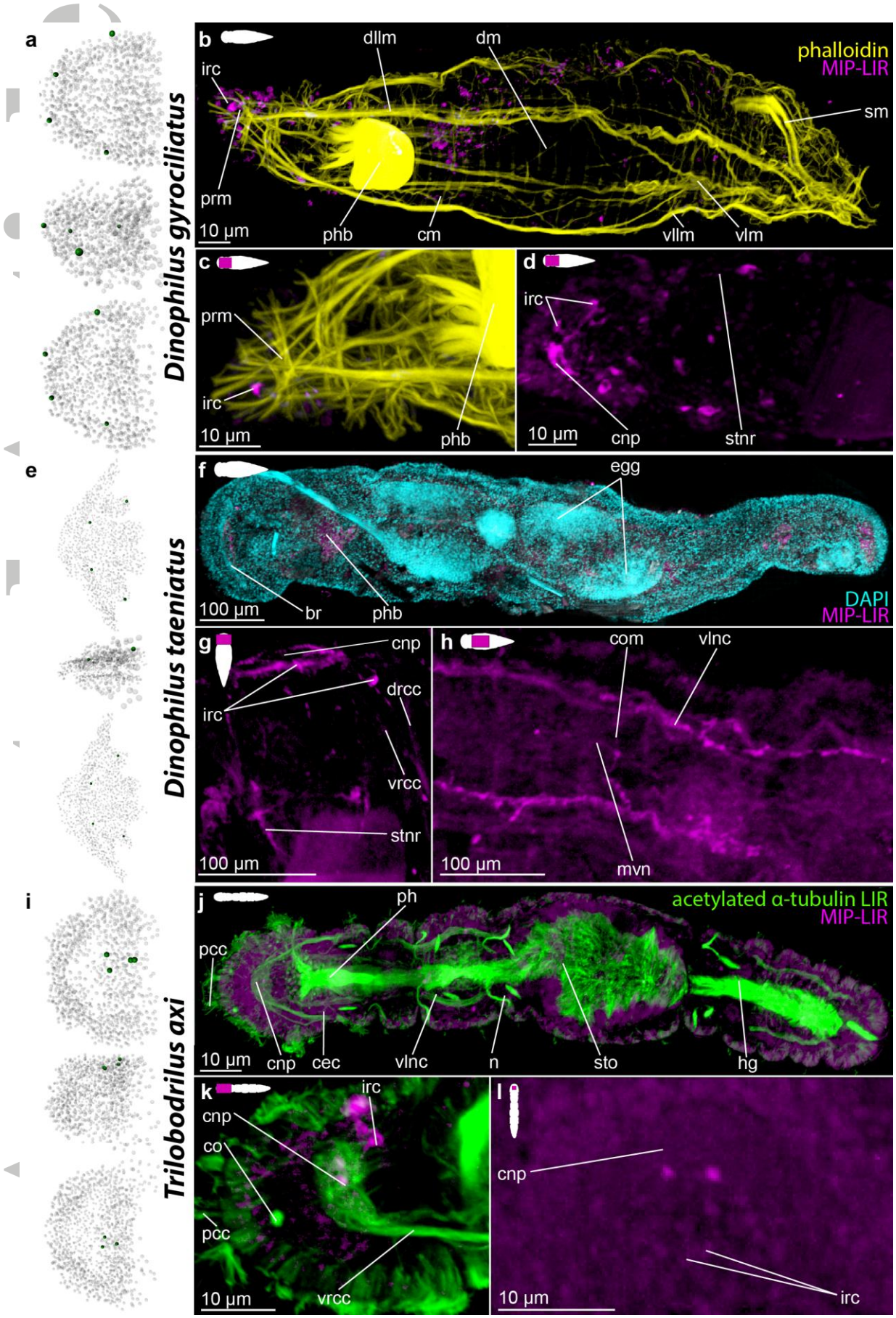

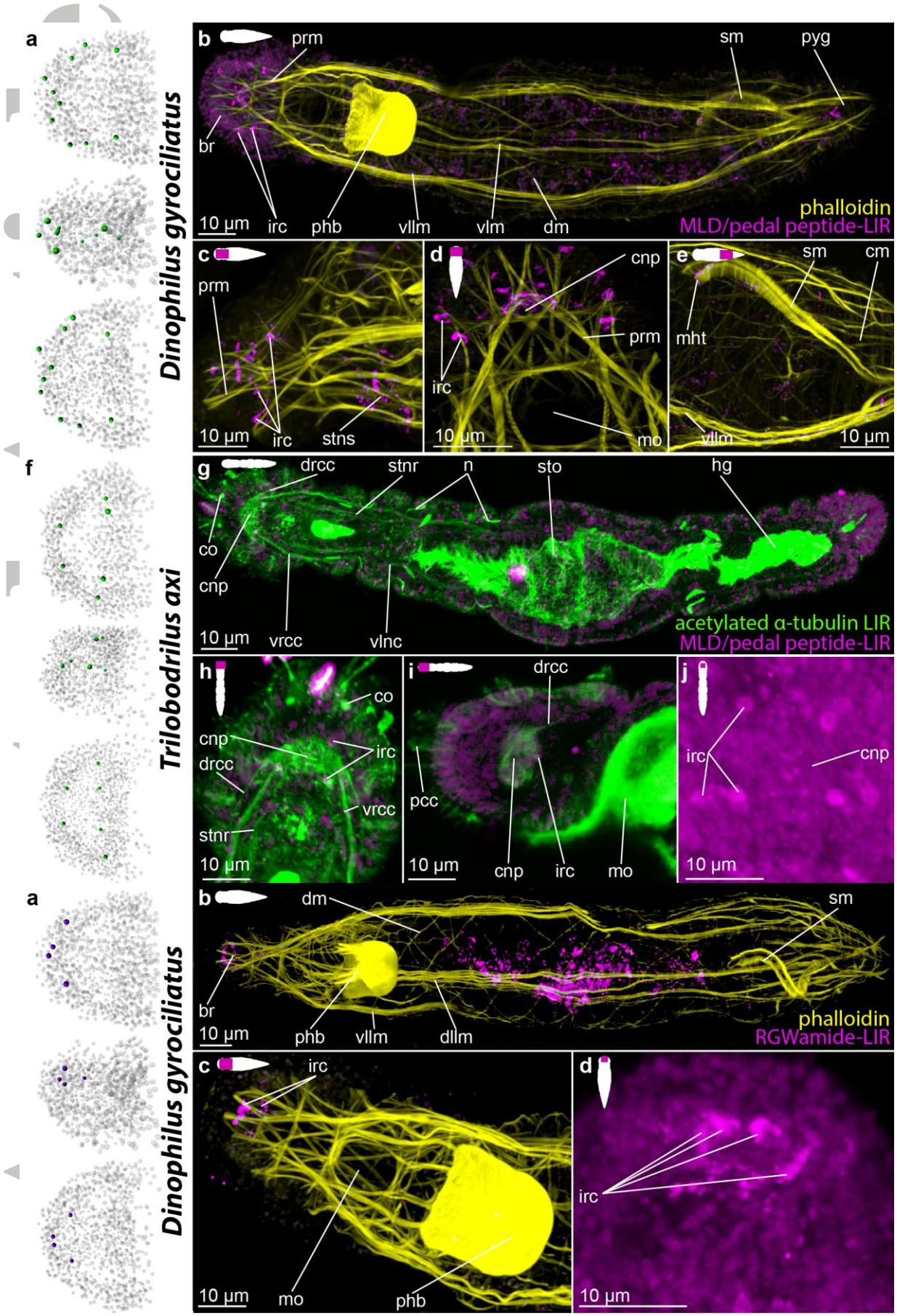

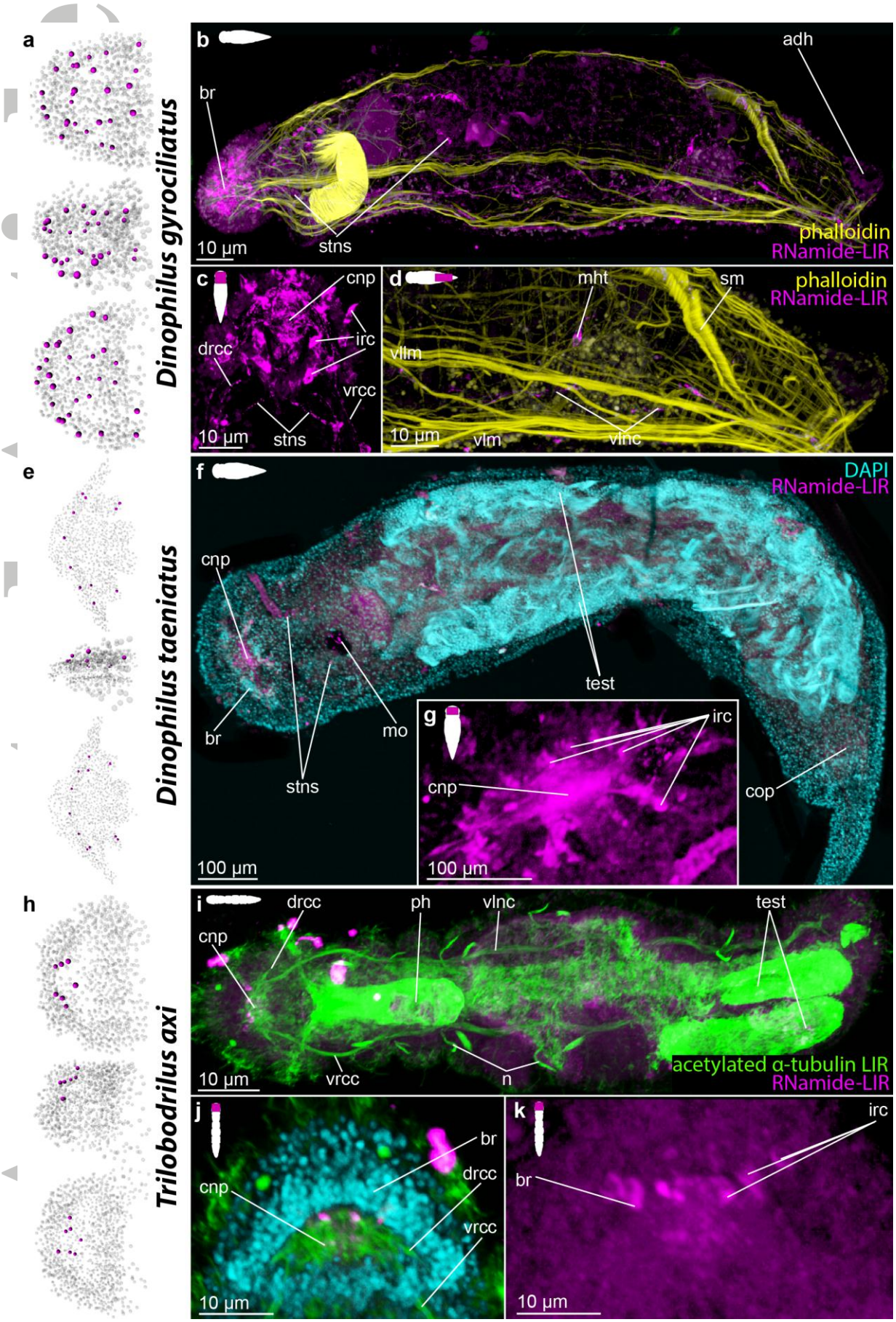

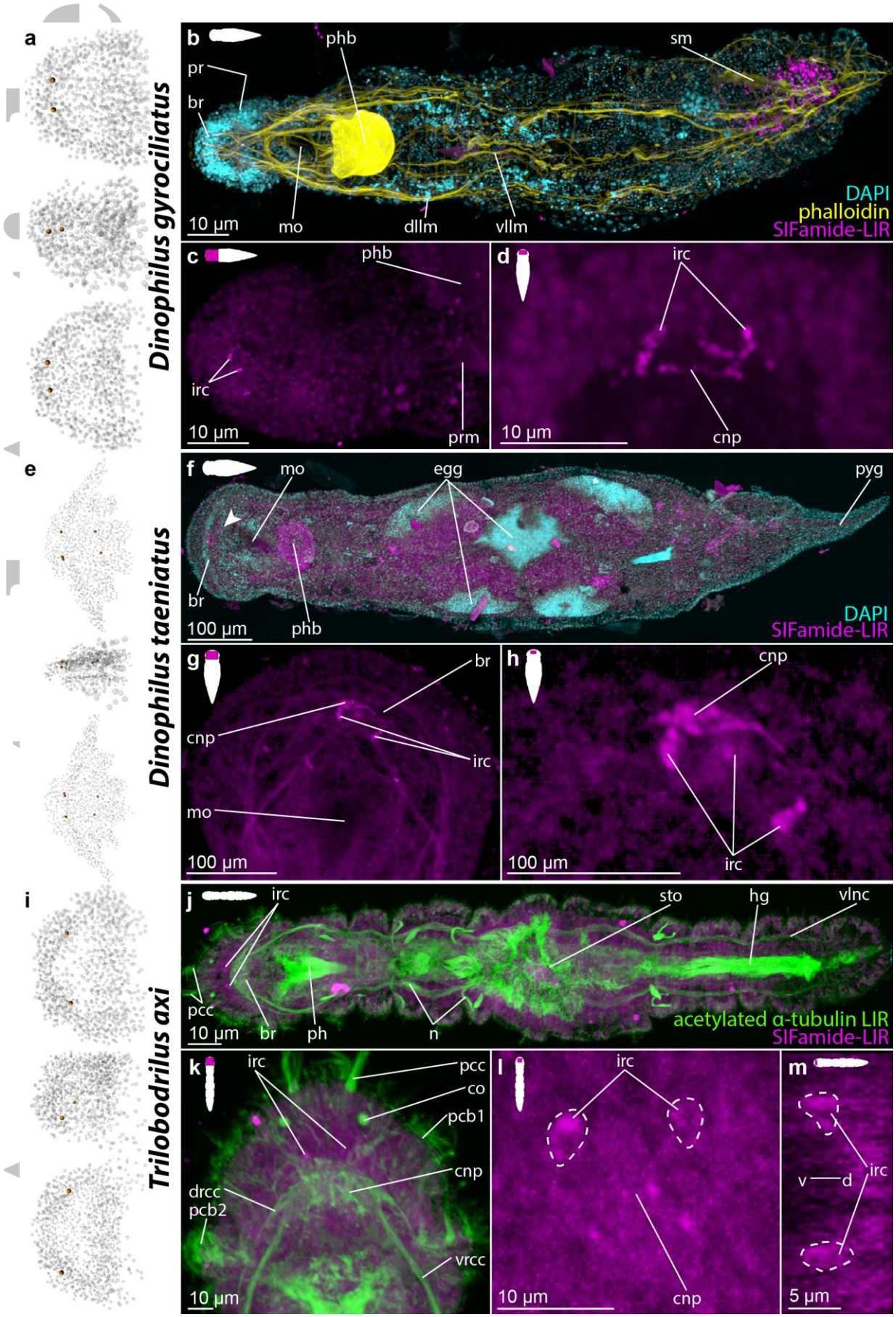

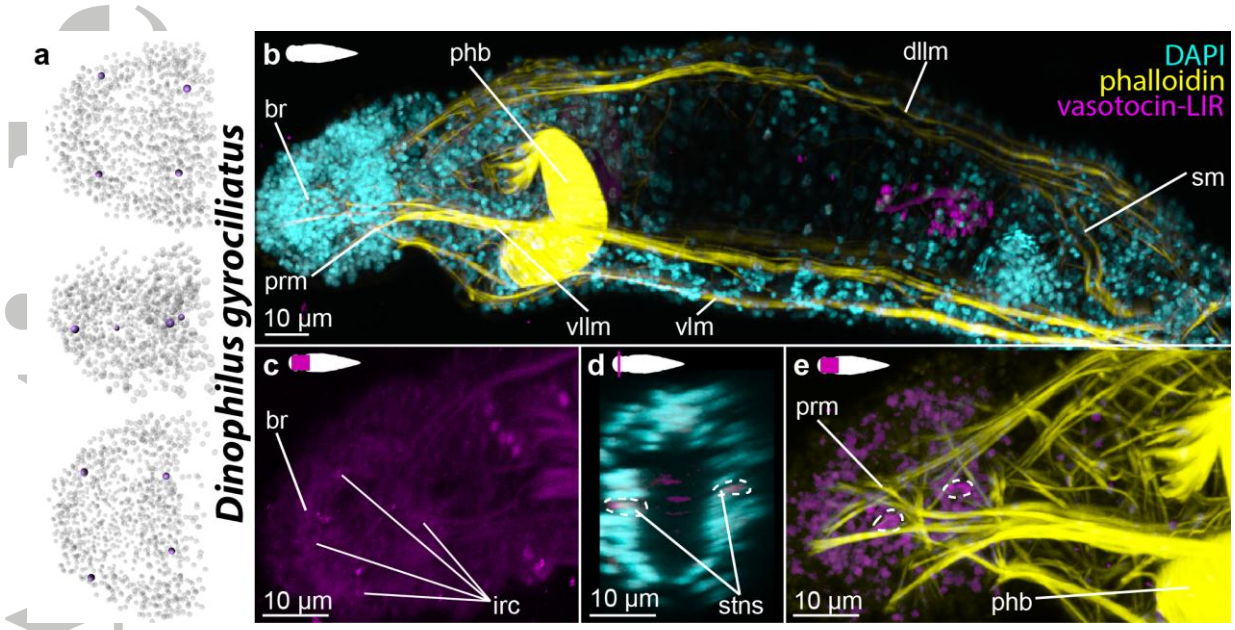

We describe and compare the immunoreactivity patterns of 14 neuropeptides among three closely related annelids (*Dinophilus gyrociliatus*, *D. taeniatus* and *Trilobodrilus axi*), which revealed unexpectedly high variation despite similar gross brain morphology. This suggests a faster adaptation of the neuropeptide landscapes than of the underlying morphology, as mechanism for the evolutionary divergence of life styles.

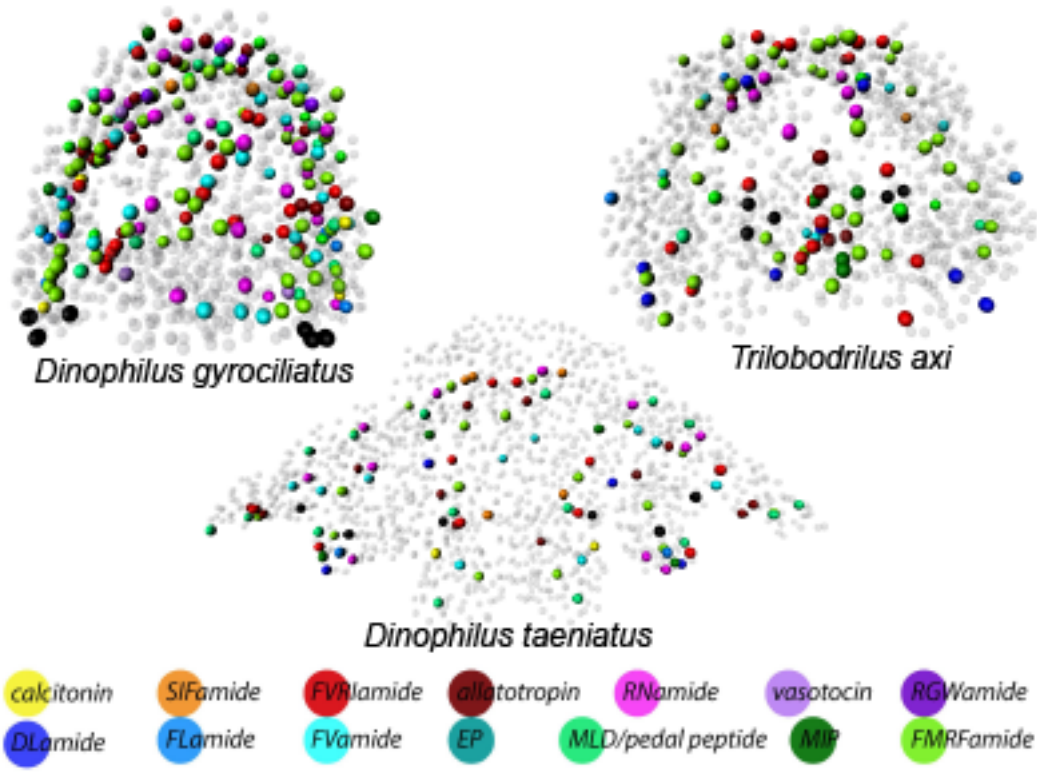

Neuro-peptide-precursor	ABs used	Location in *D. gyrociliatus* transcriptome	Location in *D. taeniatus* transcriptome	Location in *T. axi* transcriptome	Specificity tested in *P. dumerilii*
7B2	-	Locus_18214.4_Transcript_1	comp76302_c0_seq1len=272 path=[862:0-95 958:96-233 1096:234-271]	s_1_sequence.TS1_r1_(paired)_trimmed_(paired)_ contig_1684	WMISH
AKH	-	Locus_18773.0_Transcript_1	comp32120_c0_seq1len=323 path=[301:0-322]	s_1_sequence.TS1_r1_(paired)_trimmed_(paired)_ contig_3080	WMISH
AS-A	-	Locus_13673.0_Transcript_1	comp77072_c0_seq7l len=899 path=[2146:0-36 5815:37-48 5827:49-52 2335:53-254 2537:255-389 2672:390-790 3073:791-805 3088:806-807 3090:808-815 3098:816-863 3146:864-868 3151:869-898]	s_1_sequence.TS1_r1_(paired)_trimmed_(paired)_ contig_7759	-
AS-C	-	Locus_18845.0_Transcript_1	comp67244_c0_seq2len=344 path=[1:0-274 987:275-281 283:282-298 300:299-343]	s_1_sequence.TS1_r1_(paired)_trimmed_(paired)_ contig_5316	-
AT	X	Locus_19106.0_Transcript_1	-	-	MLGKD
BUR-A	-	Locus_15557.0_Transcript_2	-	-	WMISH
BUR-B	-	Locus_9061.0_Transcript_2	-	-	-
CCW	-	Locus_18800.0_Transcript_1	-	s_1_sequence.TS1_r1_(paired)_trimmed_(paired)_ contig_24950	WMISH
CT	X	Locus_9944.0_Transcript_1	comp67579_c1_seq1len=405 path=[351:0-43 1307:44-52 754:53-404]	s_1_sequence.TS1_r1_(paired)_trimmed_(paired)_ contig_22061	WMISH
DL	X	Locus_9360.0_Transcript_2	-	-	WMISH
EFLG	-	Locus_17328.3_Transcript_6	-	-	-
EP	X	Locus_19066.0_Transcript_1	comp69307_c0_seq1len=318 path=[1:0-118 120:119-239 241:240-285 287:286-317]	s_1_sequence.TS1_r1_(paired)_trimmed_(paired)_ contig_11986	WMISH
FL	X	Locus_15189.1_Transcript_1	comp76825_c0_seq4| len=511 path=[6431:0-84 7730:85-102 5645:103-510]	s_1_sequence.TS1_r1_(paired)_trimmed_(paired)_ contig_11190	WMISH
FMRF	X	Locus_5034.0_Transcript_1	comp69095_c0_seq1len=321 path=[1:0-221 223:222-320]	s_1_sequence.TS1_r1_(paired)_trimmed_(paired)_ contig_7101	-
FV	X	Locus_17328.3_Transcript_4	-	s_1_sequence.TS1_r1_(paired)_trimmed_(paired)_ contig_8665	WMISH
FVRI	X	Locus_4594.0_Transcript_1	comp75236_c0_seq1len=390 path=[1373:0-135 17:136-193 75:194-389]	-	MLGKD/ WMISH
IRP2/4	-	Locus_16843.0_Transcript_1	-	-	WMISH
IRP3/5	-	Locus_11072.0_Transcript_2	-	-	-
LKI	-	Locus_16399.0_Transcript_1	comp73719_c1_seq8| len=635 path=[971:0-9 981:10-29 5269:30-30 5270:31-33 1005:34-72 5312:73-75 1047:76-183 5358:184-186 1158:187-	s_1_sequence.TS1_r1_(paired)_trimmed_(paired)_ contig_5495	WMISH

			260 5394:261-266 1238:267-601 5513:602-605 2174:606-634]		
MIP	X	Locus_11964.0_Transcript_4	comp67269_c0_seq2| len=360 path=[80:0-100 180:101-155 235:156-233 313:234-359)	s_1_sequence.TS1_r1_(paired)_trimmed_(paired)_ contig_8026	WMISH
MM	-	Locus_9170.0_Transcript_2	comp69715_c0_seq1len=391 path=[1:0-351 1145:352-358 1152:359-364 1158:365-367 1161:368-390]	s_1_sequence.TS1_r1_(paired)_trimmed_(paired)_ contig_2482	WMISH
NPY-1	-	Locus_19137.0_Transcript_1	comp68849_c0_seq1len=212 path=[190:0-60 251:61-64 255:65-127 318:128-168 359:169-171 362:172-211]	-	-
NPY-2	-	Locus_3671.0_Transcript_1	-	-	-
NPY-3	-	Locus_11302.0_Transcript_1	-	-	-
PEP1	-	Locus_11404.0_Transcript_1	comp69093_c1_seq2len=357 path=[1233:0-38 1338:39-54 944:55-58 1357:59-103 511:104-356]	s_1_sequence.TS1_r1_(paired)_trimmed_(paired)_ contig_7342	-
PEP2	X (MLD)	Locus_18751.0_Transcript_1	comp74686_c0_seq3len=362 path=[1182:0-12 1693:13-17 1200:18-28 72:29-82 126:83-102 146:103-107 1459:108-126 167:127-128 169:129-135 176:136-143 184:144-297 338:298-321 362:322-361]	s_1_sequence.TS1_r1_(paired)_trimmed_(paired)_ contig_16591	WMISH
PH3	-	Locus_14783.1_Transcript_4	comp75253_c0_seq5len=448 path=[1:0-23 95:24-27 99:28-76 148:77-105 177:106-303 375:304-341 1947:342-379 976:380-423 2464:424-447]	s_1_sequence.TS1_r1_(paired)_trimmed_(paired)_ contig_1087	-
QERAS	-	Locus_18907.0_Transcript_1	comp64769_c0_seq1len=281 path=[1:0-14 16:15-188 190:189-280]	-	WMISH
RGW	X	Locus_18839.0_Transcript_1	-	-	WMISH
sCAP	X	Locus_4026.0_Transcript_2	comp65655_c0_seq1| len=592 path=[570:0-388 1282:389-395 966:396-591]	s_1_sequence.TS1_r1_(paired)_trimmed_(paired)_ contig_4117	WMISH
SIF	X	Locus_18810.0_Transcript_1	-	s_1_sequence.TS1_r1_(paired)_trimmed_(paired)_ contig_4690	MLGKD
VT	X	Locus_20304.0_Transcript_1	-	-	WMISH
W/I	-	Locus_18565.0_Transcript_1	comp71388_c0_seq1len=418 path=[712:0-231 944:232-249 962:250-360 1695:361-374 1709:375-378 1713:379-383 1096:384-417]	s_1_sequence.TS1_r1_(paired)_trimmed_(paired)_ contig_958	WMISH
WI	-	Locus_4056.0_Transcript_1	comp75766_c0_seq4len=519 path=[577:0-29 2669:30-47 2687:48-54 1328:55-72 1346:73-345 1619:346-465 1739:466-518]	s_1_sequence.TS1_r1_(paired)_trimmed_(paired)_ contig_9650	WMISH

Name	Structure/ details	Company	Raised in	Polyclonal/ monoclonal	Specificity tested in *P. dumerilii* by	Conc. [µg/ml]
α-acetylated α-tubulin	RRID:AB_477585	SIGMA T6793	Mouse	Monoclonal	- (commercial antibody)	1:200
α-acetylated α-tubulin	RRID:AB_10603594	SIGMA SAB3500023	Chicken	Polylclonal	- (commercial antibody)	1:200
α -serotonin	RRID:AB_477522	SIGMA S5545	Rabbit	Polyclonal	- (commercial antibody)	1:400
α -allatotropin	CGFRTGAYDRFSHGFa		Rabbit	Polyclonal	MLGKD (Shahidi et al., 2015)	1:1000
α -calcitonin	CATESAASVADQWHYLNSPLSPa		Rabbit	Polyclonal	WMISH (unpubl.)	1:1000
α -DLamide	CDLa		Rabbit	Polyclonal	WMISH (Conzelmann and Jekely, 2012)	1:1000
α -EP	CAGGNa		Rabbit	Polyclonal	WMISH (unpubl.)	1:1000
α -FLamide	CAKFMLa		Rabbit	Polyclonal	WMISH (Conzelmann et al., 2011; Conzelmann and Jekely, 2012)	1:1000
α -FMRFamide	RRID:AB_572232	IMMUNOSTAR 20091	Rabbit	Polyclonal	- (commercial antibody)	1:400
α -FVamide	CFVa		Rabbit	Polyclonal	MLGDK (Shahidi et al., 2015), WMISH (Conzelmann et al., 2011; Conzelmann and Jekely, 2012)	1:1000
α -FVRIamide	CFVRIa		Rabbit	Polyclonal	WMISH (Jekely et al., 2008)	1:1000
α -MIP	CEWSSNNMAMWa		Rabbit	Polyclonal	MLGDK (Williams et al., 2015)	1:1000
α -MLD/pedal peptide	CMLDEVGSSLLa		Rabbit	Polyclonal	WMISH (Williams et al., 2017)	1:1000
α -RGWamide	CRGWa		Rabbit	Polyclonal	WMISH (Conzelmann and Jekely, 2012)	1:1000
α -RNamide/sCAP	CLPPDFFRNa		Rabbit	Polyclonal	WMISH (unpubl.)	1:1000
α -SIFamide	CEPLEDQLPDTTGLFFa		Rabbit	Polyclonal	WMISH (unpubl.)	1:1000
α -vasotocin	CPPGa		Rabbit	Polyclonal	WMISH (unpubl.)	1:1000

	Character	*Dinophilus gyrociliatus*	*Dinophilus taeniatus*	*Trilobodrilus axi*
Brain	*1. Supraesophageal ganglion (brain)*	dorsal	dorsal	dorsal
	2. Subesophageal ganglion	present	present	present
	3. Circumesophageal connectives	1 pair	1 pair	1 pair
	4. Number of commissures in neuropil	6	6	6
	4a. Number of commissures in ventral root	3	3	2
	4b. Number of commissures in dorsal root	3	3	4
Ventral nervous system	*5. Number of ventral cords*	1 pair	1 pair	1 pair
	6. Median nerve (between ventral cords)	present (partly fused)	present (fused)	present (fused)
	7. Number of paramedian nerves	2 pairs	1 pair	1 pair
	8. Total number of commissures	18	9	15
	8a. Number of commissures in segments 1+2	6	3	6
	8b. Number of commissures in segment 3	3 (median bundle thickest)	2 (anterior bundle thicker than the posterior one)	4 (prominent median bundle w/ 2 anterior & 1 posterior)
	8c. Number of commissures in segment 4	3 (median bundle thickest)	2 (anterior one thicker than the posterior one)	2 (posterior one thicker than anterior one)
	8d. Number of commissures in segment 5	2	1	2 (anterior one thinner than posterior one)
	8e. Number of commissures in segment 6	1	1	2 (anterior one thinner than posterior one)
Additional nerves	*9. Dorsal longitudinal nerves*	present (1 pair)	present	present
	10. Lateral longitudinal nerves	8	8	8
	11. Transverse peripheral nerves per segment	4 (**ncb, nacb, npcb**, nis)	3 (2x **ncb**, nis)	4-6 (1-2 ns, 2 ans, 1-2 nis)
Stomato. nervous system	*12. Nerve ring around the esophagus*	present	present	present
	13. Nerve ring around the midgut-hindgut trans.	present	present	present
	14. Nerve net around digestive tract	present	present	present

Antibody	*Dinophilus gyrociliatus*				*Dinophilus taeniatus*				*Trilobodrilus axi*			
	BR	**VNS**	**SNS**	**AN**	**BR**	**VNS**	**SNS**	**AN**	**BR**	**VNS**	**SNS**	**AN**
Pattern of monoamine immunoreactivity												
Serotonin	X (6)	X (vlnc+pmvn+mvn+com)	X	X (dln+dlln+lln+vlln+tn)	X (6)	X (vlnc+pmvn+mvn+com)	X	X (dln+dlln+lln+vlln+tn)	X (6)	X (vlnc+pmvn+mvn+com)	X	X (dln+dlln+lln+vlln+tn)
Patterns of neuropeptide-like immunoreactivity												
Allatotropin (AT)	X (26)	X (vlnc+mvn)	X	X (lln+vlln)	X (12)	-	-	X (copn)	X (7)	X (vlnc+com)	-	X (ns)
Calcitonin (CT)	X (4)	-	X	X (dln+dlln+lln+vlln+tn)	X (2)	-	-	-	-	-	-	-
DLamide (DL)	-	-	-	-	X (4)	X (vlnc+pmvn+mvn+com)	X	X (dln+dlln+lln+vlln+com)	X (8)	-	X	-
Excitatory peptide (EP)	X (20)	X (vlnc+mvn+com)	X	-	X (14)	X (vlnc+mvn+com)	X	-	X (2)	-	-	-
FLamide (FL)	X (6)	-	-	-	X (2)	-	-	-	X (4)	X (vlnc)	X	-
FMRFamide (FMRF)	X (54)	X (vlnc+pmvn+mvn)	X	X (dln+dlln+lln+vlln+tn)	X (26)	X (vlnc+pmvn+mvn)	X	X (dln+dlln+lln+vlln)	X (39)	X (vlnc+pmvn+mvn)	X	X (dln+dlln+lln+vlln)
FVamide (FV)	X (26)	X (vlnc+mvn)	X	-	X (10)	X (vlnc)	X	-	X (6)	-	-	-
FVRIamide (FVRI)	X (22)	X (vlnc+mvn+com)	X	-	X (8)	X (vlnc+mvn+com)	-	X (dln+dlln+lln+vlln)	X (16)	X (vlnc+mvn+com)	X	-
Myoinhibitory peptide (MIP)	X (4)	-	X	-	X (4)	X (vlnc+mvn+com)	X	-	X (4)	-	-	-
MLD/pedal peptide (MLD)	X (10)	X (vlnc+pmvn+mvn)	-	X (dln+dlln+lln+vlln)	-	-	-	-	X (6)	-	-	-
RGWamide (RGW)	X (4)	-	-	-	-	-	-	-	-	-	-	-
RNamide/sCAP (sCAP)	X (28)	X (vlnc)	X	X (dln+dlln+lln+vlln	X (12)	-	-	-	X (7)	-	X	X (dln+dlln+lln+vlln)
SIFamide (SIF)	X (2)	-	-	-	X (4)	-	-	-	X (2)	-	-	-
Vasotocin (VT)	X (4)	-	-	-	-	-	-	-	-	-	-	-
Total number neuropeptide-like immunoreactivity-labelled perikarya in the brain	**210**				**98**				**101**			